WAVEFORM ANALYSIS OF GEOGRAPHIC PATTERNS RECORDED ON VISIBLE AND INFRARED IMAGERY

By
RICHARD EVERETT WITMER

A DISSERTATION PRESENTED TO THE GRADUATE COUNCIL OF
THE UNIVERSITY OF FLORIDA
IN PARTIAL FULFILLMENT OF THE REQUIREMENTS FOR THE
DEGREE OF DOCTOR OF PHILOSOPHY

UNIVERSITY OF FLORIDA
December, 1967

ACKNOWLEDGMENTS

Many persons have contributed their efforts to the organization and completion of this research project. Foremost among these is Dr. Clark I. Cross, Chairman of the author's Supervisory Committee. His professional example and intellectual stimulation have been major influences during this author's entire graduate career. Sincere appreciation is extended to Dr. Cross for this guidance and assistance. Dr. James R. Anderson, Chairman of the Department of Geography, not only contributed to the initial formulation of this study, but has assisted this author at all stages of his graduate career. Dr. Edmund E. Hegen has provided this author with intellectual and academic insights on innumerable occasions, and Dr. Richard A. Edwards has offered many helpful suggestions concerning the proper completion of this research. Gratitude is also extended to the many other faculty members of the University of Florida who have contributed to this author's academic and research pursuits.

This author is in the debt of many persons at Florida Atlantic University who have contributed to this

research effort. Dr. James P. Latham, Professor and Chairman of Geography, in his capacity as Principal Investigator of the Office of Naval Research contract under which this study was completed, provided financial assistance and helpful suggestions concerning the research methodology and instrumentation procedures. Mr. Herbert Evans, Technical Director of Learning Resources, and Mr. Curtis Norling, Chief Video Engineer, provided great assistance in the selection and operation of the various experimental components. Thanks are also extended to Mrs. Anita Becker, secretary of the Geography Department, for her typing assistance, and to Mr. Gerald Tapper, the author's student assistant, for his help with photographic and cartographic work.

Finally, the author's sincerest gratitude is extended to his wife, Judy, for her patience and assistance throughout the entire course of the research project.

TABLE OF CONTENTS

		Page
ACKNOWLEDGMENTS		ii
LIST OF TABLES		vi
LIST OF ILLUSTRATIONS		viii
CHAPTER		
I.	INTRODUCTION	1
	Research Objectives	3
	Electronic Analysis of Geographic Patterns	4
	Research Techniques and Methodology	8
II.	THE VISIBLE AND INFRARED IMAGERY	10
	General Characteristics of Visible Panchromatic Imagery	10
	General Characteristics of Infrared Imagery	16
	The Thermal Infrared Spectral Region	21
	Multispectral Remote Sensing Imagery	27
	Selection and Conventional Analysis of the Visible and Infrared Imagery	31
III.	WAVEFORM ANALYSIS METHODOLOGY	44
	Scan-Line Techniques	44
	Gray-Tone Level Recording	55
	Graphical Presentation of Waveforms	75
	Statistical Presentation of Gray-Tone Levels	77
IV.	EXPERIMENTAL RESULTS	96
	Waveform Analysis Results: Nine-Lens Multiband Camera Imagery	96
	Waveform Analysis Results: Panchromatic and Thermal Infrared Images	109
	Analysis of Scale and Resolution Differences	130

CHAPTER Page

V. CONCLUSION 132

Summary 132
Potential Utilization of Waveform Analysis in Geographic Research 136

APPENDICES 138

I. Primary Data: Nine-Lens Multiband Camera Imagery 139

II. Primary Data: Panchromatic and Thermal Infrared Images 146

III. Terrain-Type Compilations: Nine-Lens Multiband Camera Imagery 159

IV. Terrain-Type Compilations: Panchromatic and Thermal Infrared Images 166

V. Terrain-Type Compilations Corrected for Rise Time: Nine-Lens Multiband Camera Imagery 179

VI. Terrain-Type Compilations Corrected for Rise Time: Panchromatic and Thermal Infrared Images 186

SELECTED BIBLIOGRAPHY 199

BIOGRAPHICAL SKETCH 224

LIST OF TABLES

Table		Page
1.	Nine-Lens Multiband Camera Data	29
2.	Nine-Lens Multiband Camera Spectral Bands . . .	30
3.	Sensor Comparison Totals by Terrain Type: Nine-Lens Multiband Camera Imagery	104
4.	Sensor Comparison Totals by Terrain Type: Nine-Lens Multiband Camera Imagery (Corrected for Rise Time)	106
5.	Sensor Comparison Totals by Terrain Type: Panchromatic and Thermal Infrared Images (Paired Occurrences)	125
6.	Sensor Comparison Totals by Terrain Type: Panchromatic and Thermal Infrared Images (Paired Occurrences; Corrected for Rise Time)	128
7.	Primary Data: Frame 42, Lens 2, Lines 1 and 2	140
8.	Primary Data: Frame 42, Lens 4, Lines 1 and 2	142
9.	Primary Data: Frame 42, Lens 9, Lines 1 and 2	144
10.	Primary Data: Panchromatic Image, Line 1 . . .	147
11.	Primary Data: Panchromatic Image, Line 2 . . .	149
12.	Primary Data: Panchromatic Image, Line 3 . . .	151
13.	Primary Data: Thermal Infrared Image, Line 1	153

Table		Page

14. Primary Data: Thermal Infrared Image, Line 2 155

15. Primary Data: Thermal Infrared Image, Line 3 157

16. Terrain-Type Compilations: Frame 42, Lens 2, Lines 1 and 2 160

17. Terrain-Type Compilations: Frame 42, Lens 4, Lines 1 and 2 162

18. Terrain-Type Compilations: Frame 42, Lens 9, Lines 1 and 2 164

19. Terrain-Type Compilations: Panchromatic Image, All Lines 167

20. Terrain-Type Compilations: Thermal Infrared Image, All Lines 173

21. Terrain-Type Compilations Corrected for Rise Time: Frame 42, Lens 2, Lines 1 and 2 180

22. Terrain-Type Compilations Corrected for Rise Time: Frame 42, Lens 4, Lines 1 and 2 182

23. Terrain-Type Compilations Corrected for Rise Time: Frame 42, Lens 9, Lines 1 and 2 184

24. Terrain-Type Compilations Corrected for Rise Time: Panchromatic Image, All Lines 187

25. Terrain-Type Compilations Corrected for Rise Time: Thermal Infrared Image, All Lines 193

LIST OF ILLUSTRATIONS

Figure		Page
1.	The electromagnetic spectrum	11
2.	Spectral radiant emittance curves for blackbodies at several absolute temperatures	13
3.	Atmospheric spectral transmission	26
4.	Nine-lens multiband imagery, Frame 42, Lens 2	33
5.	Nine-lens multiband imagery, Frame 42, Lens 4	34
6.	Nine-lens multiband imagery, Frame 42, Lens 9	35
7.	Nine-lens multiband imagery map	37
8.	Panchromatic image, Stinchfield Woods and vicinity	39
9.	Thermal infrared image, Stinchfield Woods and vicinity	41
10.	Map of Stinchfield Woods and vicinity	43
11.	Monitor display of thermal infrared image and waveform	46
12.	Schematic illustration of video-tape-recording of multispectral imagery	56
13.	Schematic illustration of recording waveforms with oscilloscope camera	58
14.	Arrangement of components used in oscilloscope recording	59

Figure		Page

15. Recording waveforms produced by the Model 302 Video Analyzer 61

16. Monitor display of image and electronic sampling grid and scan line generated by the Model 302 Video Analyzer 62

17. Schematic illustration of photo-recording of real-time imagery and waveforms 63

18. Schematic illustration of photo-recording of video-taped imagery and waveforms 64

19. Photographing image, waveform, and scan line on monitor 65

20. Speed Graphic camera being used in exposure test 66

21. Oscilloscope camera being used to photograph waveform 68

22. Scan-line traverse of Lens 2, Line 2 70

23. Schematic illustration of strip-chart recording of real-time imagery and waveforms 73

24. Schematic illustration of strip-chart recording of video-taped imagery and waveforms 74

25. Graphical example of nomenclature of waveform parameters 76

26. Graphical presentation of waveform representing nine-lens multiband camera imagery, Frame 42, Lens 2, Line 1 78

27. Graphical presentation of waveform representing nine-lens multiband camera imagery, Frame 42, Lens 2, Line 2 79

Figure		Page
28.	Graphical presentation of waveform representing nine-lens multiband camera imagery, Frame 42, Lens 4, Line 1	80
29.	Graphical presentation of waveform representing nine-lens multiband camera imagery, Frame 42, Lens 4, Line 2	81
30.	Graphical presentation of waveform representing nine-lens multiband camera imagery, Frame 42, Lens 9, Line 1	82
31.	Graphical presentation of waveform representing nine-lens multiband camera imagery, Frame 42, Lens 9, Line 2	83
32.	Graphical presentation of waveform representing panchromatic image, Line 1	84
33.	Graphical presentation of waveform representing panchromatic image, Line 2	85
34.	Graphical presentation of waveform representing panchromatic image, Line 3	86
35.	Graphical presentation of waveform representing thermal infrared image, Line 1 . . .	87
36.	Graphical presentation of waveform representing thermal infrared image, Line 2 . . .	88
37.	Graphical presentation of waveform representing thermal infrared image, Line 3 . . .	89

CHAPTER I

INTRODUCTION

The earth sciences are experiencing a renaissance in their ability to utilize new methods which have been developed for perceiving various distributions of geographic phenomena. These methods include the development of new techniques for objective quantified analysis of geographic distributions, and also include the development of certain instrumented systems which record various aspects of distributed phenomena by sampling certain spectral regions of the electromagnetic spectrum. In general, these instrumented systems are called "remote sensors" and include such devices as thermal infrared scanners, radars, microwave scanners, and television systems, as well as the more conventional types of photographic equipment, such as those used for conventional aerial photography.

All of these remote sensing systems (with the exception of color photography) produce imagery which has form similar to conventional aerial photography, i.e., some assemblage of gray tones which is superimposed on a format

which indicates relative position. The superimposition of information coded by gray tone on a spatial framework is in reality a geographic distribution. The phenomena contained in the gray-tone information appearing in the distribution are not always of constant character, as might be expected of the most fundamental and most commonly used remote sensing system, the camera. The phenomena vary, not only with the spectral region being sampled, but with the design parameters of the sensing instrument itself. The choice of spectral region, for example, might indicate the general category or categories of geographic phenomena whose distribution and density were being recorded, while the design characteristics of the sensor might indicate the resolution or fidelity with which the system is recording the geographic information.

The recent declassification of some of the new remote sensing systems and their imagery has permitted large numbers of earth scientists to expand their research into avenues previously unknown or denied to them, and to use such data as is originated by these systems to permit more meaningful investigations into research already in progress.

Great quantities of remote-sensor imagery are available to the academic and scientific communities, and undoubt-

edly this storehouse will greatly expand as the proliferation of systems and available imagery continues, and as declassification proceeds. Unfortunately, the great bulk of this imagery lies unseen and uninterpreted for the simple reason that there are insufficient numbers of scientists able to consider adequately this great mass of information. In light of this problem, it is obvious that there is an urgent need to develop methodological frameworks capable of relieving the image interpreter of some of the more routine tasks of identification and integration of certain types of phenomena recorded on matched sets of multispectral imagery. Such methodological frameworks would also contribute to the objective analysis of certain aspects of geographic distributions.

Research Objectives

Electronic Scanning Technique

The first research objective is to apply a specific electronic scanning technique, namely television scan line waveform analysis, to matched sets of multispectral imagery recorded in the visible and infrared portions of the electromagnetic spectrum. This technique will provide an unbiased, objective method of sampling such imagery in order to measure

and discriminate between certain characteristics of geographic distributions.

Waveform Discrimination Methodology

A second objective of this research is to develop a methodology for discriminating between various basic geographic patterns sampled by parallel scan lines by analyzing the character of the waveforms generated as gray-tone graphs of the areas traversed by these scan lines. Such a methodology will allow similar transmitted signals containing geographic information coded in the form of gray-tone to be related to other geographic phenomena.

Other Research Objectives

Subsidiary objectives of this research include: (1) an evaluation of the quantitative and qualitative validity of such a methodology; (2) investigation of the utility and advantages of using such techniques in geographic research; and (3) continuation of a long-range program of investigating the potentials, methodologies, and results of applying certain electronic devices to geographic research.

Electronic Analysis of Geographic Patterns

Of particular interest to geographers interested in applying rigorous quantitative methodologies to spatial dis-

tributions of phenomena is the work done by various scientists who have directed their research toward electronic and automated analysis of such distributions. These investigations began by applying basic mathematical and geometric tools in order to simplify the complex analysis of information handled by electronic systems.

In the early 1950's, Klimm[1] and Latham[2] initiated research dealing with various quantitative measurements of the size, distance, and orientation aspects of cropland areas in Pennsylvania. During this research, the Rotated Parallel Traverse Method[3] was also developed and subsequently applied to the problem of quantifying cropland distributions.

In a 1959 report,[4] Latham reiterated research previously accomplished which established the following results:

---

[1] Lester E. Klimm, "Regional Description Based on Texture and Pattern of Unit Areas" (Abstract), Annals of the Association of American Geographers, September, 1956, p. 256.

[2] James P. Latham, "The Distance Relations of Cropland Areas in Pennsylvania" (Abstract), Annals of the Association of American Geographers, September, 1958, p. 277.

[3] James P. Latham, The Distance Relations and Some Other Characteristics of Cropland Areas in Pennsylvania; An Experiment in Methodology, Technical Report No. 4, NR 389-055 (Washington: Office of Naval Research, 1958).

[4] James P. Latham, A Study of the Application of Electronic Scanning and Computer Devices to the Analysis of Geographic Phenomena, Final Report, NR 387-023 (Washington: Office of Naval Research, 1959).

(1) that the sampling, by a cathode-ray tube flying-spot scanner, of mapped or photographed distributions, in order to differentiate phenomena by gray-tone, was technically feasible; (2) that scanning densitometers could measure intercept lengths having fixed gray-tone limits; and (3) that flying-spot scanners could identify and measure specific occurrences on a gray-tone background and scan large areas rapidly. Additional mention was also made of the possibility of applying electronic computers and data-handling systems to such problems.

In two 1962 articles,[5, 6] Rosenfeld demonstrated the applicability of Latham's theoretical investigation by video-scanning pre-selected portions of typical terrain types appearing on large-scale (1:5,500) aerial photographs. This work established that certain basic relationships exist between terrain types and video signals, and also demonstrated that gray-tone control is of utmost importance when identifications are to be made from gray-tone levels alone.

---

[5] Azriel Rosenfeld, "Automatic Recognition of Basic Terrain Types from Aerial Photographs," Photogrammetric Engineering, March, 1962, pp. 115-132.

[6] Azriel Rosenfeld, "An Approach to Automatic Photographic Interpretation," Photogrammetric Engineering, September, 1962, pp. 660-665.

In a 1962 paper[7] and a 1964 summary report,[8] Latham expanded on previous research and presented new concepts dealing with the potential geographic uses of quantified electronic analysis of spatial distributions. These included the development of new graphic methods and the processing of several statistical variables by computer methods.

The research of which this dissertation is a part has been in progress since 1965 and has been reported on at various intervals.[9]

---

[7]James P. Latham, "Role of Instrumentation in Geographic Research," paper presented to the Annual Meetings of the American Association for the Advancement of Science, Philadelphia, Pennsylvania, December 29, 1962.

[8]James P. Latham, Electronic Measurement and Analysis of Geographic Phenomena, Final Report, NR 387-023 (Washington: Office of Naval Research, 1964), pp. 2-3.

[9]James P. Latham, "Remote Sensing of Environment," Geographical Review, April, 1966, pp. 288-291; James P. Latham, "Resume of the Special Session on Remote Sensing Held at the 1965 AAAS Meeting," in Proceedings of the Fourth Symposium on Remote Sensing of Environment (Ann Arbor: University of Michigan, 1966), pp. 539-546; James P. Latham, "Machine Evaluation of Images for Regionalization Problems," paper presented to the Commission on the Interpretation of Aerial Photographs, International Geographical Union, Ottawa, Canada, March 16, 1967; James P. Latham and Richard E. Witmer, Comparative Waveform Analysis of Multisensor Imagery, Technical Report No. 3, NR 387-034 (Washington: Office of Naval Research, 1967).

Research Techniques and Methodology

Introductory Research

Before attempting any waveform experimentation and analysis, it is imperative that a review of previous investigations into the general characteristics of visible (panchromatic) and infrared imagery be accomplished, in order to ascertain the variables that must be considered in the experimental design and in the analysis of the resultant data and observations. A summary of this review is presented in Chapter II.

Imagery Selection

After the significant variables associated with multispectral sets of imagery have been isolated and evaluated, the actual imagery to be used will be selected. This imagery will first be analyzed by the more conventional visual interpretative and geographic methods before waveform analysis. The basic geographic patterns evident on the imagery will be analyzed and mapped in order to facilitate the interpretation and analysis of the subsequent recorded waveforms. This section is also presented in Chapter II.

Waveform Monitoring and Recording

Following the selection of the imagery to be used,

several different experimental designs will be tested and evaluated for waveform frequence response and recording fidelity. The most appropriate experimental procedure will then be applied to the multispectral sets of imagery. Several parts of each image will be sampled by parallel scan lines, and the resultant waveforms produced will be recorded. The recorded waveforms will then be enlarged and superimposed on a sampling grid in order to measure accurately gray-tone level and other waveform parameters. Chapter III is devoted to this topic.

Waveform Analysis

After completing the various measurements appropriate to the waveforms, basic statistical techniques will be employed in order to reveal certain aspects of the gray-tone information recorded. These will include measurements of electronic excursions, gray-tone amplitude fluctuation, and other similar parameters. After the complete waveform graphs have been analyzed without regard for electronic factors affecting fidelity of measurement, the data will be corrected to provide a further analytic refinement. Following the data analysis of each image, they will be grouped into sets to determine if additional information can be gained by comparative waveform analysis. These topics are discussed in Chapter IV.

CHAPTER II

THE VISIBLE AND INFRARED IMAGERY

General Characteristics of Visible Panchromatic Imagery

The enormity and complexity of the literature dealing with the characteristics and interpretation of visible panchromatic imagery preclude any extensive historical or integrative treatise dealing with these factors being presented in this report. Instead, the inclusion of a representative bibliography will allow the reader to sample a cross-section of the more significant works pertaining to these topics. Only the factors closely related to the interpretation and analysis of such imagery as is utilized need be presented.

Visible panchromatic imagery, perhaps better known as conventional aerial photography, was the first actual remote sensor which sampled a portion of the electromagnetic spectrum (see Fig. 1). Throughout the span of time that aerial photography has been employed for various reasons, a great number of aerial photographic devices, film emulsions, film-filter combinations, and aerial photographic aircraft

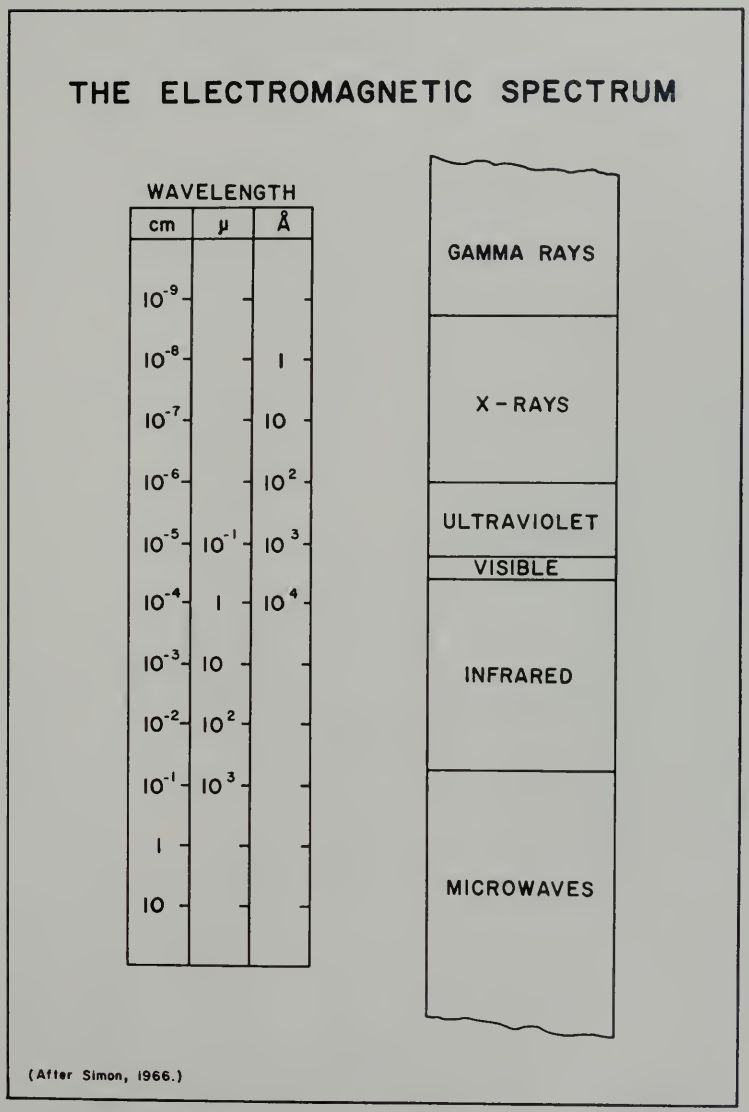

Fig. 1. The electromagnetic spectrum.

platforms have been developed, tested, and used. All of these techniques revolve about several significant characteristics in need of reiteration in this presentation.

The Visible Spectral Region

The first of these significant characteristics is that even though visible light occupies a very small percentage of the electromagnetic spectrum, the wavelength band which comprises visible light (about 0.4-0.7 microns) accounts for a very large percentage of the radiation received at the earth's surface. This is illustrated in Figure 2, which shows that the peak radiation received as visible light corresponds to the radiation wavelengths characteristic of the incandescent temperature of the sun's surface (see peak of 6,000°K curve). Since all natural and cultural earth objects are exposed to light composed of all of the wavelengths which comprise visible light, it is seen that the actual color exhibited by such objects is the result of selective absorption, reflection, and reradiation of light. It is this process which also produces the differences in selectively reflected light so important to the tonal contrasts exhibited on conventional aerial photography. Such photographic sensing would be meaningless and impossible if cultural objects and natural terrain objects did not produce

SPECTRAL RADIANT EMITTANCE CURVES FOR BLACKBODIES AT SEVERAL ABSOLUTE TEMPERATURES

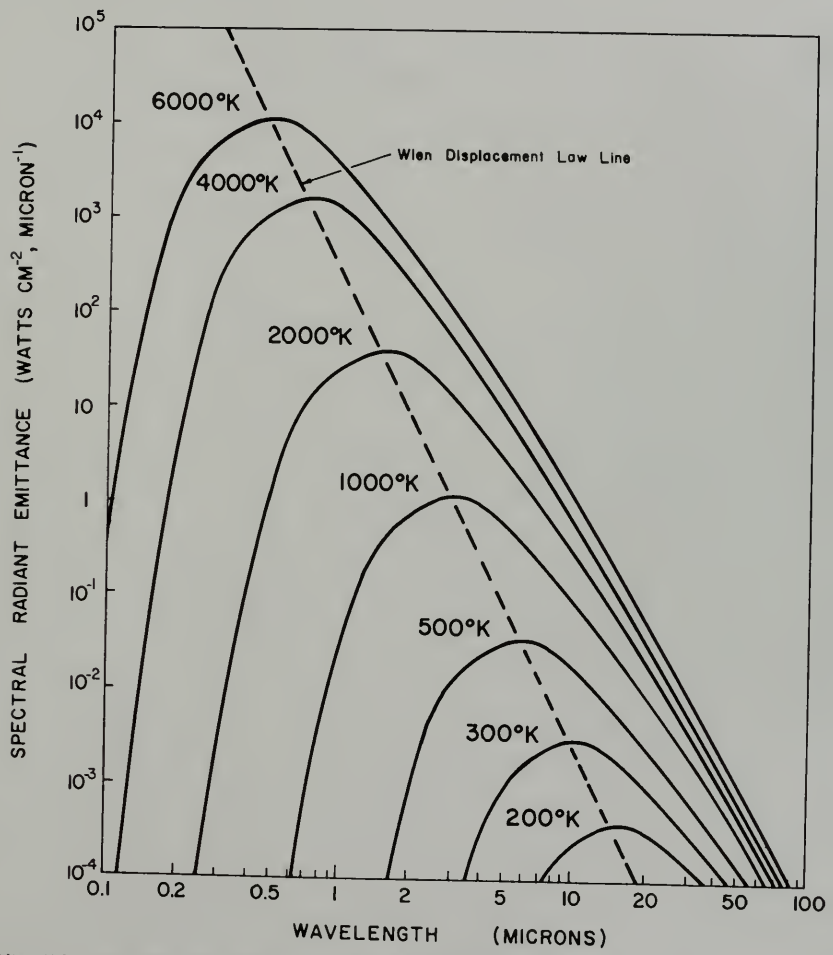

(After U.S. Army, Basic and Advanced Infrared Technology, April 1965.)

Fig. 2. Spectral radiant emittance curves for blackbodies at several absolute temperatures.

differences in gray-tone as recorded on films used in aerial photography.

Spatial Differentiation and Resolution

Another important characteristic of visible panchromatic imagery is its ability to record distributions of geographic phenomena in such a manner that the actual spatial patterns existing among the phenomena are maintained to a predictable degree of accuracy. It is thus possible to use such imagery for the construction of controlled maps or for various spatial measurements of dimensions exhibited by the phenomena. This characteristic has been made possible by the construction of corrected lens systems, gyro-compensated camera mounts, film emulsions and photographic paper whose dimensional stability characteristics are known, and, finally, photogrammetric techniques devised to compensate for errors induced at any stage of the actual photography or its processing.

Continued research into film design and optics has greatly increased the resolution of the aerial photographic camera system. Resolution can be thought of as the smallest linear width that can be recorded on any specific film. The actual resolution of any system, of course, depends not only upon the inherent design characteristics of the camera

and its film system, but also the length of the optical path from target to camera. A standard mapping camera, for example, may be able to discern a certain phenomenon at low altitudes which would be beyond its resolving capability at higher altitudes. The important resolution characteristic of aerial mapping cameras in use at the present is that resolving power can be considered to be constant throughout the angular viewing field of the lens, permitting measurement of similar objects to be made at all locations on a photograph, without resorting to measurements confined to the central area, as is necessary on some other types of remote sensing imagery.

Film-Filter Combinations

Most aerial films used for recording visible light are termed "panchromatic," implying that they are capable of recording all wavelengths comprising the visible part of the spectrum. In normal usage, however, this capability is rarely used. More commonly, an optical filter is placed in front of the camera lens so that a portion of the visible light is filtered out before reaching the film. By using such filters, it is possible to record selectively predetermined parts of the visible spectrum, or to employ such filters in the elimination of atmospheric or gray-tone

contrasts expected to be detrimental to the quality of the desired imagery. Most black-and-white aerial films intended for normal photographic coverage are used with a Wratten 12 (minus-blue) filter to remove any effects of atmospheric haze. When considerable numbers of cultural features are anticipated, a Wratten 25A (red) filter is substituted.[1] Various other film-filter combinations are used in conjunction with other types of aerial photography.

General Characteristics of Infrared Imagery

The Infrared Spectral Region

The infrared spectral region, so named because its included wavelengths extend "beyond the red" wavelengths of the visible portion of the spectrum, extends from 0.7 microns, the upper wavelength limit of visible light, to almost 1,000 microns,[2] the lower wavelength limit of microwave radiation (see Fig. 1).

Of primary interest to geographers are the so-called "near" and "middle" infrared regions. The near-infrared

---

[1]American Society of Photogrammetry, Manual of Photographic Interpretation (Menasha, Wis.: George Banta Co., Inc., 1960), pp. 45-50.

[2]Ivan Simon, Infrared Radiation (Princeton: D. Van Nostrand Co., Inc., 1966), p. 10.

wavelengths extend from 0.7 microns to approximately 2 microns, with the middle-infrared region extending from 2 microns to approximately 20 microns.[3]

All bodies having temperatures above absolute zero ($0^{\circ}K$) emit infrared radiation. The peak wavelength of such radiation is a function of the absolute temperature of the emitting body. As temperature increases, the peak wavelength associated with that temperature decreases, and vice versa. Because of the complexity of all natural bodies, radiation from such bodies is not of one discrete wavelength, but instead includes a spectral distribution of wavelengths. Although Figure 2 deals specifically with blackbodies, those theoretical objects whose radiations are equal to their absorptions, it can still be observed that there is a spectral distribution of wavelengths for an emitter having any specific temperature. The shift in the peak radiant emittance for changing temperature is shown by the Wien Displacement Law line, which connects the peaks of the various blackbody curves.[4]

The near- and middle-infrared spectral regions are

---

[3] Ibid., p. 11.

[4] U.S. Army, Basic and Advanced Infrared Technology (Redstone Arsenal, Ala.: U.S. Army, April, 1965), p. 7.

of special interest to geographers because of the importance of this radiation in the terrestrial and atmospheric heat balance.[5] As with visible light, a considerable part of the sun's radiation reaches the earth as near-infrared radiation.[6] As this radiation is absorbed by natural materials, their temperatures adjust to a state of equilibrium and they reradiate energy. Because the temperatures of the earth objects are considerably lower than the incandescent temperatures which produced the original incoming radiation, the wavelength of the terrestrial reradiation shifts to longer wavelengths. Thus, the temperatures at which most earth objects exist produce radiation whose wavelengths are from about 5 microns to about 15 microns.

Reflection of incoming radiation, however, involves no change of wavelength. Incoming visible light may be reflected as visible light and incoming infrared radiation may be reflected as infrared radiation, both retaining their original respective wavelengths. As with infrared wavelength shifts, however, incoming visible light may also be changed in wavelength, even to the extent of producing

---

[5] Simon, op. cit., p. 23.

[6] A. N. Strahler, The Earth Sciences (New York: Harper and Row, 1963), p. 194.

infrared radiation from the original visible light.

Several different methods have been developed for sensing and recording infrared radiation. These methods may be generalized into those which record reflected and/or reradiated short-wave infrared radiation and those which record reradiated long-wave thermal infrared radiation.[7] Photographic devices are used to record the former types of radiation, and electro-optical devices are used to record the latter. The spectral sensitivities of these two types of recording devices roughly correspond to the near and middle infrared, respectively, and consequently these regions have come to be generally known as the photographic infrared and the thermal infrared.

The Photographic Infrared Spectral Region

Certain photographic emulsions are capable of sensing and recording wavelengths up to about 1.35 microns.[8] In practical use, however, the common films used in infrared photography are sensitive only to about 0.86 microns.[9] The

---

[7] U.S. Army, op. cit., p. 140.

[8] Simon, op. cit., pp. 111-113.

[9] Eastman Kodak Company, Infrared and Ultraviolet Photography, Advanced Data Book M-3 (Rochester, N. Y.: Eastman Kodak Company, 1963), pp. 3-5.

importance of considering such films in a discussion of remote sensing techniques is not merely that an additional spectral region is rendered visible, but more important that all of the advantages of conventional panchromatic aerial photography, namely high contrast ratios, spatial recording fidelity, light resolution, etc., are retained in the additional spectral region being sampled. No other unclassified sensor can hold claim to as many operational attributes.

Since most films capable of infrared sensing also record visible blue light, it is necessary to use optical filters to restrict exposures to the infrared. A number of different filters have been developed for this purpose.[10, 11]

Any camera whose film housing and shutter are opaque to infrared light may be used for infrared photography simply by refocusing the camera for the slightly longer wavelengths. This is accomplished by refocusing approximately one-quarter of one percent of the camera lens focal length forward of the normal "infinity" position, in effect foreshortening the focal plane of the infinity position of the lens.

---

[10] Ibid., p. 5.

[11] Eastman Kodak Company, Kodak Wratten Filters for Scientific and Technical Use, Scientific and Technical Data Book B-3, 22nd edition (Rochester, N. Y.: Eastman Kodak Company, 1965), pp. 27-31, 70-75.

In the United States, infrared aerial photography has been procured for a variety of different reasons. Perhaps the most common utilization has been by the United States Forest Service and private commercial forestry corporations, since infrared photography proves to be very useful in the discrimination of tree types and in the detection of certain diseases. Another common utilization has been its use in the mapping of shoreline features by the United States Coast and Geodetic Survey. Infrared radiation is normally completely absorbed by water, producing a black tone very helpful in distinguishing shoreline features, especially in shallow waters having low bottom-profile gradients.[12]

The Thermal Infrared Spectral Region

As previously mentioned, the thermal infrared spectral region primarily includes radiation whose wavelengths are the result of absorption and reradiation of natural and cultural terrestrial objects. The various potentialities and utilizations of devices capable of recording the thermal patterns resulting from the foregoing process are well

---

[12] L. H. Lattman and R. G. Ray, Aerial Photographs in Field Geology (New York: Holt, Rinehart, and Winston, 1965), p. 21.

documented in the literature (see bibliography). The various types of instruments used, however, deserve brief consideration.

The most common thermal sensing system, and the one whose salient detecting features are employed in most other thermal sensing and mapping systems, is the radiometer.[13] The radiometer employs an infrared detector whose output signal corresponds to the wavelength and intensity of the radiation received and which is portrayed on an oscilloscope or other suitable device. The radiometer normally receives radiation from a point or area source and does not include a scanning function.

The ability to arrange signals analogous to thermal values in a spatial arrangement is produced when a scanning function is added to the radiometer-like detector and a means of recording the voltage outputs of the detector is provided. The scanning function is usually accomplished by placing a rotating 45° mirror in front of the detector, which is placed at right angles to the optical path. As the mirror turns, it receives radiation from a restricted angular

---

[13] John A. Jamieson, Raymond H. McFee, Gilbert N. Plass, Robert H. Grube, and Robert G. Richards, Infrared Physics and Engineering (New York: McGraw-Hill Book Co., Inc., 1963), pp. 612-617.

field of view, which is then focused onto the detector. The voltage-output signal of the detector is used to light a glow tube, providing varying light intensities which can be recorded on a continuously moving strip of normal panchromatic film.

The detector "looks at" a ground strip which lies at right angles to the direction in which the scanner is moving and thus accumulates strip after strip, producing a thermal map on the photographic film. The length of the ground strip being sampled depends on the angular field of view of the scanner, and the length of the entire image is controlled only by the length of the flight path.[14] The resolution of this system is controlled by the instantaneous field of view, which is the smallest ground area whose temperature can be sensed. The width of this area is expressed in milliradians (one milliradian resolution equals a one-foot width discernible at a distance of 1,000 feet). It is thus seen that as the height above terrain over which the sensor is operated increases, the resolution of the resulting imagery decreases. As the slant path to the detector increases, the ground area being sensed in the instantaneous

---

[14] David E. Harris and Caspar L. Woodbridge, "Terrain Mapping by Use of Infrared Radiation," Photogrammetric Engineering, January, 1964, p. 134.

field of view elongates, producing decreasing resolution with greater distance away from the flight path. The central parts of the thermal imagery therefore show greater detail.

Another item of consideration is the geometry peculiar to imagery which has not been range-rate compensated. This scanning geometry is generated by the relative forward motion of the sensor platform with respect to lateral ground areas and produces the effect of having areas on one side of the flight line appear to be ahead of the sensor, while areas on the other appear to be behind it.[15] This effect also increases with greater distance away from the flight path. These two factors, decreasing resolution and increasing spatial distortion on lateral edges of the imagery, inhibit image interpretation and accurate measurement in areas other than the central part of the image.

Another interesting sensor is the Barnes Thermograph Camera. It operates in much the same manner as an aerial infrared scanner but accumulates thermal information over a pre-selected field of view. It is positioned in a certain location and allowed to scan the area of interest. After

---

[15] Eugene E. Derenyi and Gottfried Konecny, "Infrared Scan Geometry," Photogrammetric Engineering, September, 1966, pp. 773-778.

the scanning cycle is completed, a Polaroid camera produces a print of the resulting thermal image.[16] Both types of infrared scanners may be adjusted for the temperature range to be included in the black-to-white ratio of the output signal.

Of primary concern in the design of infrared detectors is the fact that the atmosphere is opaque to certain bandwidths of infrared radiations. Those wavelength regions where infrared radiation may be transmitted are called the atmospheric "windows" (see Fig. 3). The two most prominent of these regions are the 2-5 micron band and the 8-13 micron band. (Also included in Figure 3 are the atmospheric constituents responsible for each of the major absorption bands.)

When interpreting the geographic patterns recorded on photographic infrared imagery, normal photo interpretation and mensuration techniques are applicable. The only additional requirement is that a new set of spectral signatures and their associated phenomena must be added to the interpreter's mental store of information.

When analyzing patterns recorded on thermal infrared

---

[16] William S. Beller, "IR Photos Yield Data on Natural Resources," Technology Week, August 15, 1966, pp. 24-30.

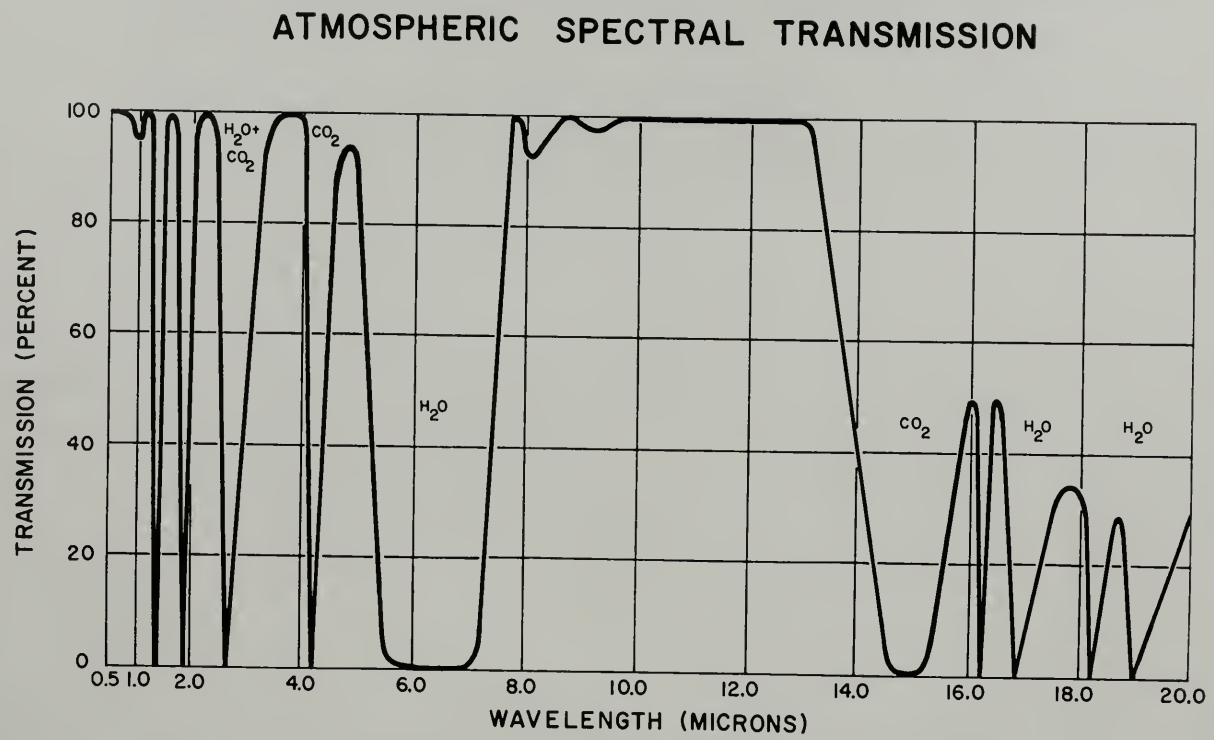

(After SBRC, Infrared Detection, 1965.)

Fig. 3. Atmospheric spectral transmission.

imagery, however, the interpreter must transfer his thinking to distributions of temperatures, rather than distributions of gray-tone resulting from reflected light. He must not only be aware of the atmospheric "window" being utilized but he must also be continuously aware of the resolution changes and scanning geometry distortions found on the thermal image.

Multispectral Remote Sensing Imagery

Several remote sensing systems have been developed which record radiation in several different portions of the electromagnetic spectrum over the same area of the earth's surface at the same time. It has been well established in the literature that this process usually results in more information being derivable than is available merely as the sum of two imagery records (see bibliography). Very often the combination of the interpretations of each set of imagery yields information not at all discernible from one set alone.

These so-called multispectral systems utilize two or more sensors, or similar sensors operating in different spectral regions.

One of the first multispectral systems was the two-camera system employed by the United States Department of

Agriculture. This system used two similar cameras, mounted on a common platform, simultaneously photographing the same terrain area in the panchromatic and photographic infrared.

A different attempt at multispectral sensing was the use of the Sonne Continuous-Strip Camera, using two sets of lenses and filters recording spectrally separate images on each half of the moving film strip.[17]

In a 1964 paper, Molineux[18] presented a report on research in progress at the Air Force Cambridge Research Laboratories dealing with a nine-lens multiband camera manufactured by Itek Corporation, capable of recording nine simultaneous images resulting from photographic sampling of six visible-light bandwidths and three infrared bandwidths.

The important physical characteristics of the nine-lens multiband camera system and the spectral bands covered by each lens are listed in Tables 1 and 2.

Research utilizing combinations of different types

---

[17] John H. Wolvin, "Multi-Channel Photo Spectrum Recording," in Proceedings of the Second Symposium on Remote Sensing of Environment (Ann Arbor: University of Michigan, 1963), pp. 81-88.

[18] Carlton E. Molineux, "Aerial Reconnaissance of Surface Features with the Multiband Spectral System," in Proceedings of the Third Symposium on Remote Sensing of Environment (Ann Arbor: University of Michigan, 1965), pp. 399-421.

TABLE 1

NINE-LENS MULTIBAND CAMERA DATA

Lenses	Nine 6-inch f/2.8 Schneider Xenotar matched lenses.
Film type	Two rolls of 70-mm. Plus-X Aerographic, one roll of 70-mm. Infrared Aerographic.
Frame format	Nine frames, each 2-1/4 inch by 2-1/4 inch.
Exposure technique	Three exposures on each roll of film.
Shutter system	Three parallel focal plane shutters of three slits each, to expose all nine frames simultaneously.
Image motion compensation	Modified A9-B magazine with film drive image motion compensation.

Source: Carlton E. Molineux, "Aerial Reconnaissance of Surface Features with the Multiband Spectral System," in Proceedings of the Third Symposium on Remote Sensing of Environment (Ann Arbor: University of Michigan, 1965), pp. 399-421.

TABLE 2

NINE-LENS MULTIBAND CAMERA SPECTRAL BANDS

Lens No.	Bandwidth (microns)	Filters Used
1	0.40-0.50	Wratten 2B + 35 + 38A
2	0.45-0.51	Wratten 3 + 47
3	0.52-0.55	Wratten 15 + 65
4	0.55-0.60	Wratten 57 + 12 + Balzers 155/116
5	0.59-0.64	Wratten 90 + 24 + Optics Tech. Interference filter
6	0.67-0.72	Wratten 36 + 12
7	0.70-0.81	Wratten 89B + Balzers 455/141
8	0.81-0.90	Wratten 87C
9	Full Sensitivity Range of IR Film	

Source: Carlton E. Molineux, "Aerial Reconnaissance of Surface Features with the Multiband Spectral System," in Proceedings of the Third Symposium on Remote Sensing of Environment (Ann Arbor: University of Michigan, 1965), pp. 399-421.

of sensors has also been reported. Perhaps the most common of these is the aerial mapping camera-thermal infrared mapper combination. This combination, of course, produces imagery which is not photogrammetrically comparable, but is capable of allowing certain types of valid analysis, nevertheless. The panchromatic image developed produces a mapping base on which may be entered thermal information gathered by the infrared scanner, or vice versa. Other combinations of sensors have been proposed and reported at various times.[19, 20] A summary of the various problems, limitations, and a compendium of multispectral potential and present uses have been offered by Colwell.[21]

Selection and Conventional Analysis of the Visible and Infrared Imagery

Imagery Selection

Two types of infrared imagery have been discussed: photographic infrared imagery and thermal infrared imagery.

---

[19] Earl S. Leonardo, "Capabilities and Limitations of Remote Sensors," Photogrammetric Engineering, November, 1964, pp. 1005-1010.

[20] Charles W. Lancaster and Allen M. Feder, "The Multisensor Mission," Photogrammetric Engineering, May, 1966, pp. 484-494.

[21] Robert N. Colwell, "Uses and Limitations of Multispectral Remote Sensing," in Proceedings of the Fourth Symposium on Remote Sensing of Environment (Ann Arbor: University of Michigan, 1966), pp. 71-100.

Both types and their corresponding conventional photographs will be used in the analysis to follow. It will also be informative to use imagery generated by some of the various types of multispectral remote sensors previously mentioned.

The Visible-Photographic Infrared Imagery Set

During the research being reported here, it was possible to acquire various types of multispectral visible and infrared imagery. Among these acquisitions were several rolls of nine-lens multiband camera negative imagery produced for the Air Force Cambridge Research Laboratories. This nine-lens photography was flown in the San Francisco Bay area during January, 1963. After impromptu construction of a viewing stage and light table capable of handling all three rolls of negatives simultaneously, one complete set, Frame 42, of nine negatives was chosen for waveform analysis. This particular frame was chosen because of the variety of natural and cultural features and the variety of geometric shapes and contrast gradients recorded on it. Since some of the spectral bandwidths of the nine-lens system overlap, three of the bands were chosen for use: Lenses 2, 4, and 9 (see Figs. 4, 5, and 6). Lenses 2 and 4 were chosen because of the intermediate bandwidths they recorded,

NINE-LENS MULTIBAND IMAGERY

Frame 42, Lens 2

Fig. 4. Nine-lens multiband imagery, Frame 42, Lens 2.

NINE-LENS MULTIBAND IMAGERY

Frame 42, Lens 4

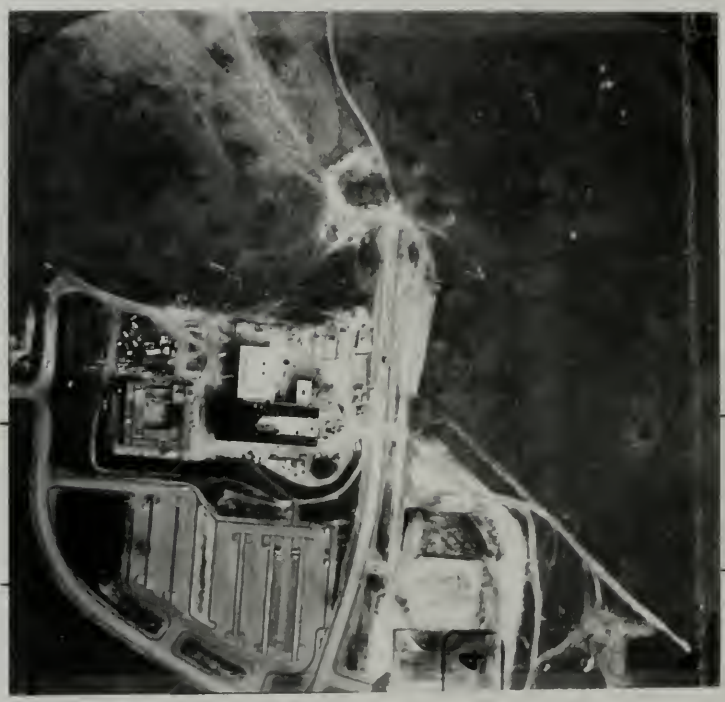

Fig. 5. Nine-lens multiband imagery, Frame 42, Lens 4.

NINE-LENS MULTIBAND IMAGERY

Frame 42, Lens 9

Fig. 6. Nine-lens multiband imagery, Frame 42, Lens 9.

and Lens 9 was chosen because it included the full bandwidth of the photographic infrared (see Table 2).[22] Frame 42 depicts an urban fringe location in Woodside, California, a suburb of Fremont on the southeastern side of the San Francisco-Oakland metropolitan area. The principal features evident in Frame 42 are the construction site in the left center of each image, the road network under construction, the paved parking lot in the lower left, the expanses of open field, with and without grass cover, and the sparse stand of deciduous trees in the upper left (see Fig. 7). The negative scale of Frame 42 is 1:10,000 (six-inch lens and 5,000-foot altitude above terrain).

The Visible-Thermal Infrared Imagery Set

During the summer of 1966, this writer was privileged to attend the first Summer Conference on Remote Sensing of Environment for College Teachers of Natural Sciences, sponsored by the National Science Foundation and conducted by the Institute of Science and Technology at the University of Michigan. Part of the effort of this conference was devoted to field work and multispectral imagery analysis of

---

[22]Molineux, op. cit., p. 410.

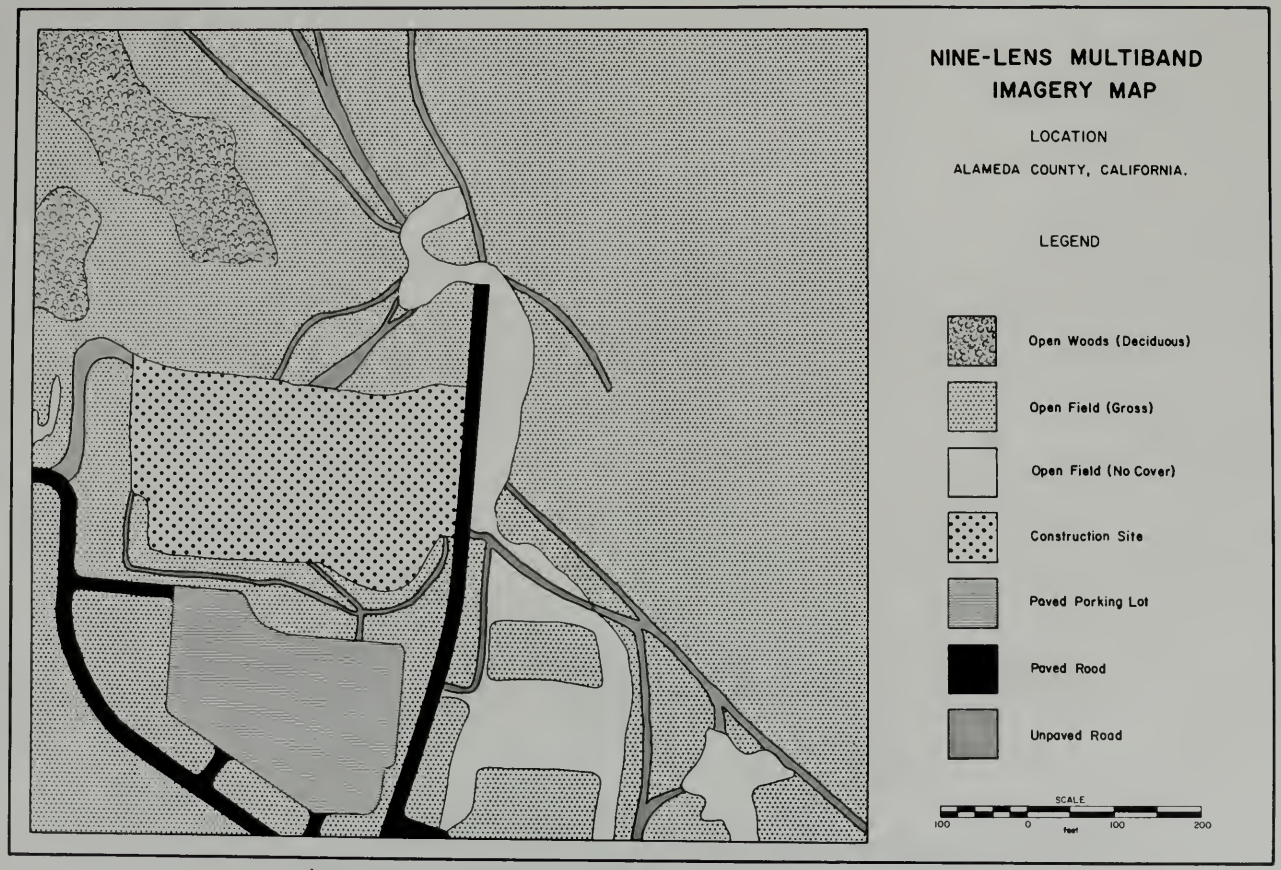

Fig. 7. Nine-lens multiband imagery map.

a specific area northwest of Ann Arbor, Michigan. The imagery available for analysis was: (1) a photomosaic of parts of several 9" x 9" contact prints, and (2) a thermal infrared image. Since considerable field work had been accomplished by this writer in conjunction with this imagery, and the results of the other conference participants were available, this set of multispectral imagery was chosen for comparison of visible and thermal infrared imagery. This imagery set also represents a comparison of two different types of sensors.

The panchromatic photomosaic (see Fig. 8) was produced from parts of several 1:20,000 photographs originally flown for the Soil Conservation Service, United States Department of Agriculture. It is a daylight summertime photograph, with a scale of 1:24,400 as used in the field exercises. The area bounded by this mosaic includes parts of Sections 34, 35, and 36 of Township 1 North, Range 4 East, Livingston County, Michigan, and part of Section 31 of Township 1 North, Range 5 East, Livingston County. Also included are Sections 1, 2, 3, 10, 11, 12, 13, 14, and 15 of Township 1 South, Range 4 East, Washtenaw County, Michigan, and parts of Sections 6, 7, and 18, Township 1 South,

PANCHROMATIC IMAGE

Fig. 8. Panchromatic image, Stinchfield Woods and vicinity.

Range 5 East, also of Washtenaw County, Michigan.[23]

The thermal infrared image was originally produced for the Forest Service, United States Department of Agriculture, and has since been incorporated into the University of Illinois Committee on Aerial Photography series as Image No. 902, entitled "Chain of Lakes." It was used in this form during the field exercises. The image itself results from a night flight during the summer of 1965 and has a scale of 1:46,000, as offered in the University of Illinois series. Since the "Chain of Lakes" image occupies slightly more area than the photomosaic, only that part of the image which is comparable to the mosaic will be used in the waveform analysis (see Fig. 9).

As the University of Illinois Committee title implies, both images are dominated by the series of lakes appearing in the upper portion of each image. The heavily wooded area in the central part of the panchromatic photograph is Stinchfield Woods, an experimental forest operated by the School of Natural Resources of the University of Michigan. Much of the remaining area included is charac-

---

[23] University of Michigan, School of Natural Resources, Stinchfield Woods (Map) (Ann Arbor: University of Michigan, 1961).

THERMAL INFRARED IMAGE

Fig. 9. Thermal infrared image, Stinchfield Woods and vicinity.

terized by open fields, although areas of woodland and swampland are to be found at various locations throughout. The Huron River can be seen on the eastern side of each image, and a well developed road network is also evident.

This particular area is situated in a region characterized by a series of recessional moraines[24] and their associated hydrologic features, and thus exhibits a variety of surface features, vegetation associations, land use differences, and the diverse gray-tones associated with such patterns, both in the panchromatic photograph and the thermal infrared image (see Fig. 10).

The similarities and differences between conventional panchromatic aerial photography and infrared imagery have been presented in this chapter. The imagery sets which have been selected to represent these spectral regions will now be subjected to waveform analysis, with the methodology concerning such analysis being considered in the following chapter.

---

[24] Dieter Brunnschweiler, Physiographic Elements of the Dexter Test Area Relevant to the Interpretation of Remote Sensing Records (unpublished report, NSF Summer Conference on Remote Sensing of Environment, University of Michigan, June, 1966).

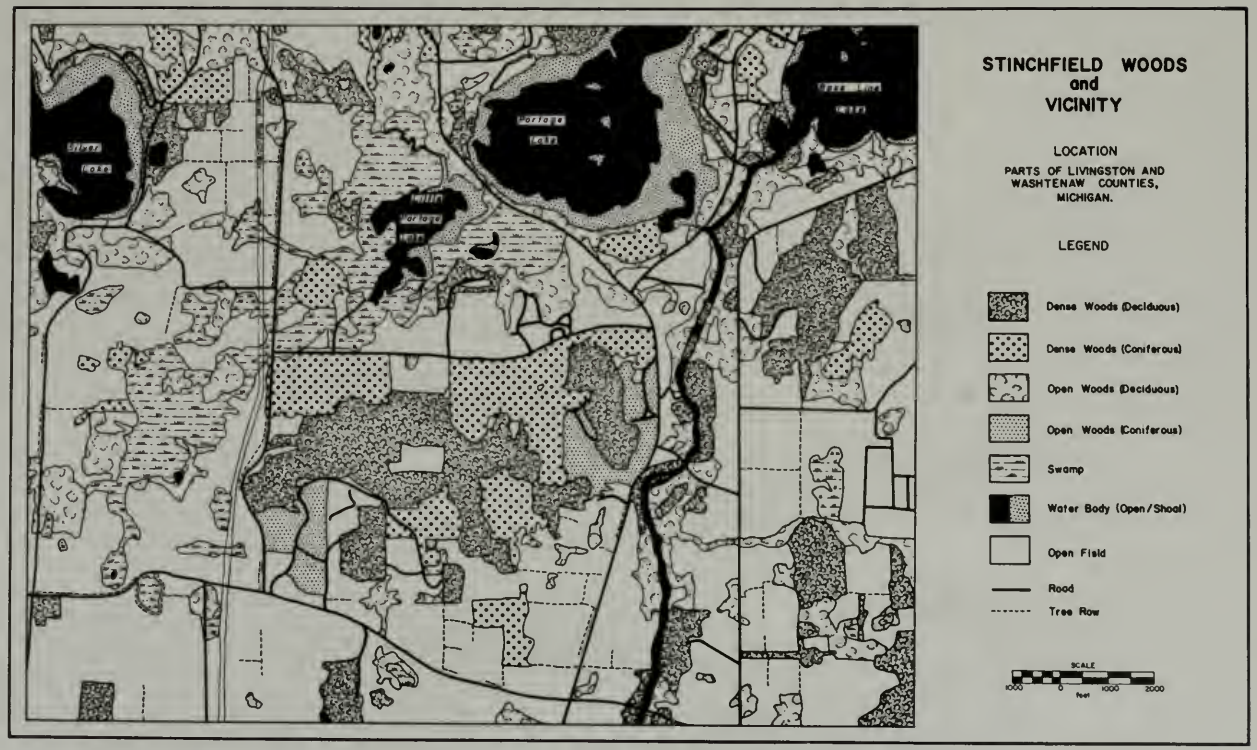

Fig. 10. Map of Stinchfield Woods and vicinity.

CHAPTER III

WAVEFORM ANALYSIS METHODOLOGY

Scan-Line Techniques

For some time electronic engineers have analyzed the character and quality of their signals and tested certain instruments with waveform monitors. These monitors graphically display on a cathode-ray tube the actual cartesian-coordinate waves representing the voltage fluctuations occurring in electronic signals. Among their uses in electronics is the monitoring of signals constituting conventional television transmission. When applied in this manner one of their primary functions is the calibration of gray-tone level and black-to-white contrast ratio of television pictures, using a reference-voltage level. One of the advantages of applying such an instrument to the analysis of television signals is that any scan line contained in the collection of parallel scan lines (termed the TV "raster") may be selected for waveform study.

In order to apply such instrumentation to the problem of quantifying geographic distributions, it is necessary

to review: (1) the instrumentation parameters associated with imagery waveform analysis; (2) the significance of gray-tones recorded in the visible and infrared portions of the electromagnetic spectrum; (3) imagery orientation and display before the television camera; (4) scan-line selection; and (5) consistent sampling of comparable areas on the multispectral imagery sets.

Instrumentation Parameters

When a stationary remote-sensor image is placed before a television camera and the televised image displayed on a conventional monitor, a waveform monitor may be connected to both camera and monitor, allowing any scan line included in the original image to be graphically displayed on the waveform monitor. The waveform derived from any scan line selected reveals certain aspects of the distribution of gray-tone levels occurring along the scan line (see Fig. 11). Any such image being viewed by a conventional television camera is scanned from left to right, but a certain amount of time is required to traverse the image electronically along each scan line. The time required to scan each line is a function of the scanning rate of the system and its resolving capability. As a practical example, the above-stated parameters will be considered for a conventional television system.

Fig. 11. Monitor presentation of thermal infrared image and waveform monitor display of waveform produced by scan line crossing center of image.

The most common television scanning rate employed in the United States is the sixty-cycle, two-field scan. In effect, this means that any image being viewed by a television camera is scanned thirty times each second by each of two scanning systems operating approximately 180 degrees out of phase. The scan rate of each of the scanning systems, in this case thirty scans per second, is commonly called "field rate" and sometimes called the "frame rate."

The other parameter in question, the resolving capability of the television system, is controlled by the number of scan lines being generated during one complete viewing of an image by the television camera, in this case every sixtieth of a second. The most common scan-line generation capability of the television cameras in use in the United States is 525 lines. This is commonly called the "line rate."

From these two parameters, the scan rate and the number of scan lines or line rate, the time required for traversing one single scan line can be computed. (In this case, it is approximately 63 microseconds, or 6.3×10^{-5} seconds.) To realize its import, what can be accomplished by the waveform monitor during this time period must be thoroughly analyzed.

In the interval required for the scanning of each television line, voltage fluctuations representing gray-tone level changes perceived by the camera are presented on the cathode-ray tube of the waveform monitor with some fixed degree of accuracy. The degree of accuracy of this representation is a function of two independent variables and one dependent variable. The two independent variables are inherent characteristics of the waveform monitor and are constants for any particular instrument.

The first independent variable involved is the frequency response characteristic of the monitor itself. This involves the ability of the instrument to discern small voltage fluctuations throughout the range of frequencies contained in the input signal. The second independent variable is the ability of the instrument to record or "write" these small voltage fluctuations as they actually occur. This latter ability is usually expressed in terms of the brevity of "rise time" or, in its opposite sense, "fall time." By definition and convention,[1] rise time is the finite length of time required for the "writing" or recording of 80 percent of the instantaneous maximum amplitude of

---

[1]U.S. Army, Transients and Waveforms, Department of the Army Technical Manual 11-669 (Washington: U.S. Army, November, 1951), p. 5.

the waveform,[2] representing the voltage fluctuations produced by a 100 percent gray-tone level difference, i.e., from black to white. In common parlance, the term "rise time" is not restricted to 100 percent fluctuations, but is used in conjunction with any gray-tone amplitude change. High-frequence response characteristics result in very short rise times, producing more accurate representations of gray-tone level and gray-tone level changes. During this small amount of time required for a signal to change from one amplitude to another, however, certain inaccuracies are produced in the resultant waveform. These inaccuracies are predictable, even though they do obscure the interpretation of a waveform to some degree.

The dependent variable in this analysis of the accuracy of waveform representation is the amount of voltage fluctuation, which may also be stated as the waveform amplitude change, commonly called an "excursion," or fundamentally as the gray-tone level difference itself. Even though the electronic necessity of a certain length of rise time constitutes a misrepresentation of a theoretical waveform, minor excursions are more accurately represented than major

---

[2]John C. Hubbs, "The New Pulse," Journal of the Precision Measurements Association (Instruments and Control Systems), November, 1966, p. 114.

excursions, since the actual length of rise time is directly proportional to the percentage voltage difference. In practice, then, the actual waveform appearing on the monitor is a function not only of the character of the subject matter being televised, but is also influenced to some extent by the frequency response and rise-time characteristics of the waveform monitor.

Gray-Tone Significance

When multispectral systems are employed for imagery production, and this imagery subjected to any sort of interpretive analysis, the gray-tones and their spatial distribution patterns produced on the imagery depend not only on the particular phenomena being sensed, but also on the sensing systems being employed.

Most geographers are familiar to some degree with the patterns and meaning of gray-tones seen on conventional panchromatic aerial photography. Some others are familiar with these items as seen on photographic infrared imagery. Still fewer are the numbers of investigators familiar with the basic significance of gray-tones recorded on other types of remote-sensor imagery.

Because none of the nine-lens multiband-camera lenses records all the visible wavelengths, each of the

lenses produces different spectral signatures for the objects being photographed. On the Lens 2 image, for example (see Fig. 4), light tones are characteristic of cultural features such as buildings, roads, parking lots, cleared fields, etc. Middle-density gray-tones indicate deciduous vegetation, and the darkest tones are produced by the expanses of open field. On the Lens 4 image (see Fig. 5), on the other hand, the lightest tones result from the unpaved roads and roads and buildings under construction, while the intermediate gray-tones are indicative of paved roads. Of special interest on this image are the similar gray-tones produced by open fields and deciduous vegetation, rendering the isolation and identification of the vegetation nearly impossible. The Lens 9 image exhibits the lightest tone for open field (see Fig. 6), with the darker tones representing the cultural features. The road and buildings under construction (center of image) show a slightly lighter tone, however, and also discernible are the two small drainage ditches on the right. Of additional interest is that there is no differentiation of open field and cleared field on this image.

The gray-tones rendered on the thermal infrared image (see Fig. 9) represent reradiation from the earth's

surface. The accumulation of these gray-tones in an orderly manner permits identification of geographic patterns associated with thermal differences, with the warmer areas being recorded as lighter gray-tones. This image is dominated by the warmer lakes in the upper part and the Huron River extending through the right center. The linear road patterns are also prominent, and paved major roads are distinguishable from unpaved secondary roads. Forested areas are characterized by intermediate gray-tones, with coniferous vegetation being slightly warmer in the example than deciduous vegetation. Open fields are slightly cooler than forested areas, and swamplands exhibit the coolest temperatures recorded on this image.

Imagery Orientation and Display

In order to eliminate lighting glare and provide consistent orientation of imagery displayed before the television camera, each image was placed on an easel having a tiltable head. This allowed each image to be oriented perpendicular to the camera on all axes. After the camera was focused, the background lighting was positioned so that no glare was observed on the camera or the monitor. When the camera, easel, and lighting positions were found to be suitable, they were left constant during the video-tape-recording

and/or analysis of each individual multispectral set.

Scan-Line Selection

Two scan lines from each of the nine-lens multiband camera images were selected for waveform recording and analysis (see Figs. 4, 5, and 6). The first scan line recorded traverses of each image through the construction site in the central section. The second scan line crosses the parking lot, several roads, and open fields, both grass-covered and cleared. It was felt that these selections would provide a maximum sampling of different terrain types and different boundary contrasts.

Three scan lines were chosen from each of the panchromatic and thermal infrared images (see Figs. 8 and 9). Line 1 represents a traverse across the lake and swamp region in the upper portion of each image. Line 2 traverses the northern part of the Stinchfield Woods Experimental Forest. This northern traverse of Stinchfield Woods was chosen because of the various types of coniferous vegetation included.[3] Line 3 extends through the southern section of Stinchfield Woods, which differs in that both deciduous and

---

[3]University of Michigan, School of Natural Resources, Stinchfield Woods (Map) (Ann Arbor: University of Michigan, 1961).

coniferous vegetation is present, and in varying ages and densities.

Scan-Line Sampling of Comparable Areas

The nine-lens multiband camera images used in this analysis were originally recorded at the same scale. The negatives were enlarged and printed to the same scale, permitting the sampling of the same scan line on each image merely by substituting images on the easel placed before the television camera. This substitution was accomplished by constructing a slotted template capable of holding each of the images in the same relative position.

Such a procedure was not possible in the panchromatic-thermal infrared multispectral set because of the scanning geometry distortions on the thermal infrared image. In addition, the two images were originally at different scales. After they had been scaled comparably, only the central section of the infrared image was thought to be sufficiently distortion-free for scan-line selection. Two frames were constructed to present the central parts of each image to the same scan line. It must be noted, however, that because of the distortion present, only approximately comparable areas are traversed by subsequent scan lines. This has accounted for some of the differences in spatial

patterns noted on the waveform sets, but these differences are considered to be minor.

The most careful attention was given to the construction of the previously mentioned templates and mounting of the images so that the most comparable results might be obtained.

Gray-Tone Level Recording

Evolution of Recording Instrumentation

The first experimental arrangement of electronic components used in waveform monitoring was in the videotape-recording of test pieces of multispectral imagery (see Fig. 12). In this arrangement, the television camera scanned the image and recorded it on video tape. It was found that recording time in excess of 20 minutes could not be used because the viewing of a stationary image for a longer time "burned" the image into the phosphor coating of the camera's principal cathode-ray tube, and many hours of subsequent viewing of a perfectly white surface were then necessary to erase the image. This effect also eliminated the possibility of recording additional imagery soon afterwards.

After suitable test items had been recorded on video tape, a Tektronix Model 529 Waveform Monitor and a standard

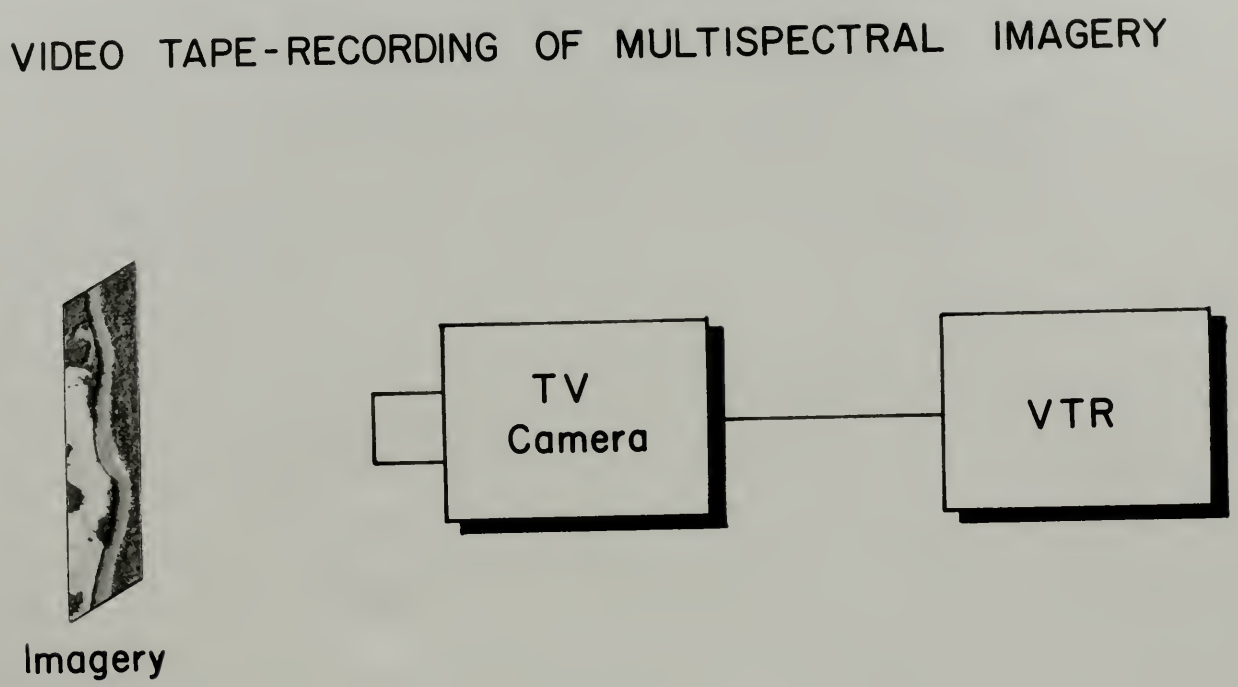

Fig. 12. Schematic illustration of video-tape-recording of multispectral imagery.

Conrac monitor were connected to the video tape-recorder as the imagery tape was replayed (see Fig. 13). The waveform monitor was adjusted appropriately and a Textronix Oscilloscope was attached to its display tube (see Fig. 14). This oscilloscope camera is equipped with a Polaroid film back capable of handling the roll film used to record electronic traces such as waveforms.

Polaroid Type 3000 film (rated 3000 ASA) was used in this introductory experiment, but proved to be unsatisfactory because the time required for the exposure was greater than one complete cycle of the field rate (30 scans per second), producing a blurred trace.

An additional problem was the length of time required for the recording of one waveform. This arose when the waveform magnification feature of the waveform monitor was tested. In the 1X waveform magnification position, the entire waveform is compressed in horizontal-axis length to fit the five-inch display tube (see Fig. 14). In that position, the entire waveform could be seen at one time, but it was sufficiently compressed to render it uninterpretable. The instrument also includes capability for 5X and 25X magnifications of waveforms. The 25X increase in size proved to be too large, but the 5X magnification allowed recording

RECORDING WAVEFORMS WITH OSCILLOSCOPE CAMERA

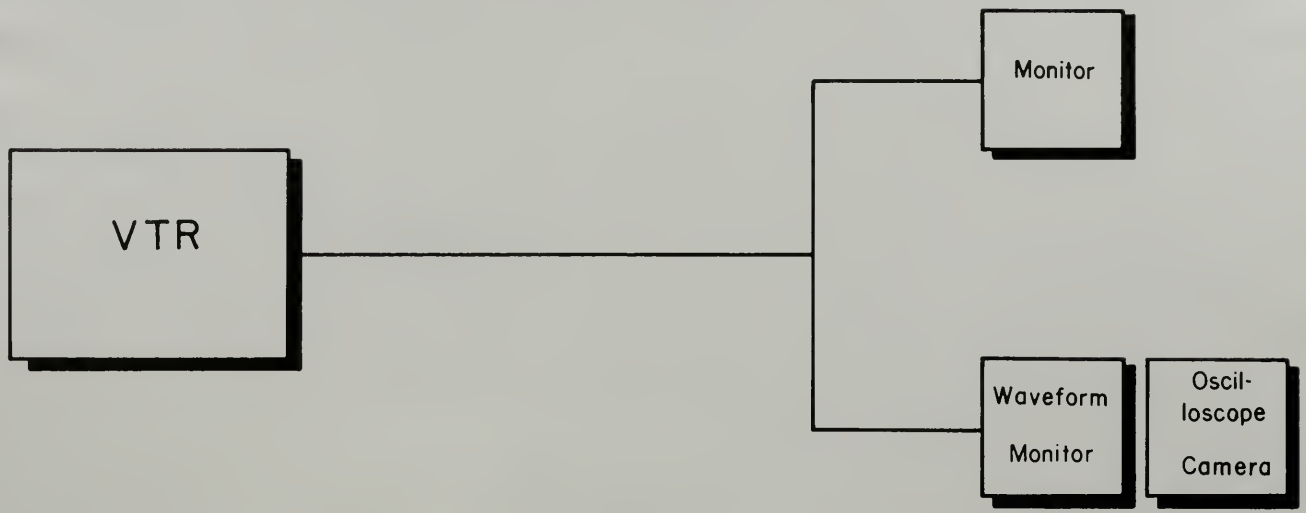

Fig. 13. Schematic illustration of recording waveforms with oscilloscope camera.

Fig. 14. Arrangement of components used in oscilloscope recording of waveforms displayed on Tektronix Model 529 Waveform Monitor. Camera is mounted on hinges and is swung out for inspection of waveform monitor display tube. Waveform can be viewed through upper part of camera while film is being exposed.

of one entire expanded waveform on four or five photographs. Unfortunately, this requires a considerable period of time, at least 20 minutes, for the recording of one single waveform.

Because of the film speed and recording cycle time problems, it was decided to test the capability of another type of waveform monitor, called the Colorado Video Model 302 Video Analyzer (see Fig. 15). This was a new product capable of simultaneously displaying on a conventional monitor the image, the scan line selected, and the resultant waveform superimposed on a changeable and positionable grid (see Fig. 16). In short, this Video Analyzer promised to be the answer to equipment selection problems, since the brightness of the waveform trace and its sampling grid made it possible to record the waveform with conventional films (see Figs. 17 and 18). Various films were tested to determine the best alternative for recording waveforms produced on the Model 302 (see Figs. 19 and 20). All of these films proved to have sufficient resolution to record the image, scan line, grid, and waveform. In fact, their resolution was so great that it was discerned that the waveform produced by the Model 302 was not really a line but a series of dots simulating a line. It was also discovered that the

Fig. 15. Various components used to present and record waveforms produced by the Colorado Video Model 302 Video Analyzer. Note the arrangement of image, waveform, and grid on the Conrac Monitor.

Fig. 16. A 35-millimeter photograph of monitor face. Note scan line vertically presented on left side of image, and waveform indicating gray-tone levels intersected by scan line. Horizontal line at top of image is electronic "straight edge" used for correlating specific locations on scan line and waveform. These elements have been generated by the Model 302 Video Analyzer.

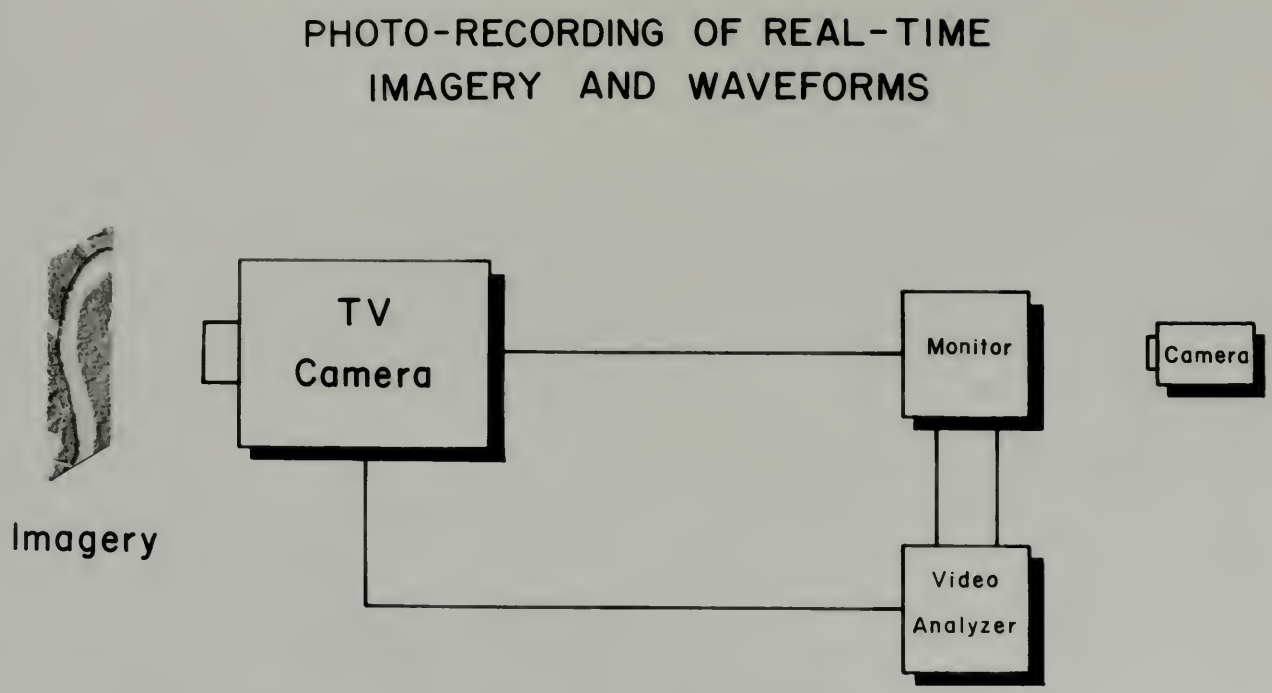

Fig. 17. Schematic illustration of photo-recording of real-time imagery and waveforms.

PHOTO-RECORDING VIDEO-TAPED IMAGERY AND WAVEFORMS

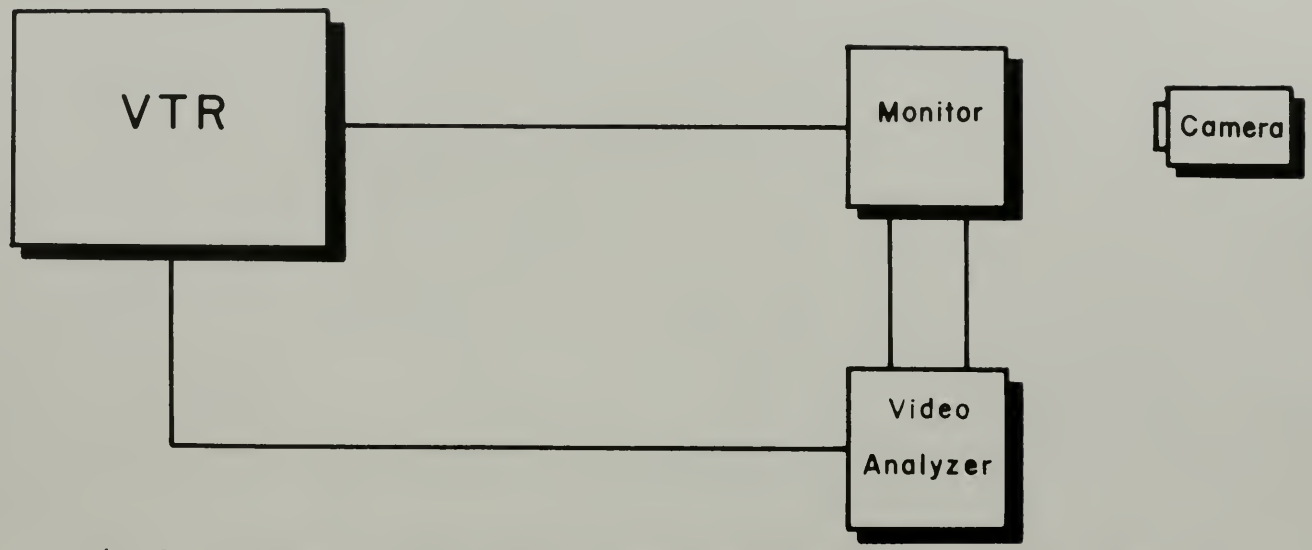

Fig. 18. Schematic illustration of photo-recording of video-taped imagery and waveforms.

Fig. 19. A 35-millimeter camera being used to photograph simultaneously presented waveform, image, and sampling scan line on monitor, while sampling location and other pertinent data are noted. Instrument in right lower foreground is Colorado Video Model 302 Video Analyzer. Controls on front of Model 302 are for choosing location and width of scan line.

Fig. 20. A 4" x 5" Speed Graphic with Polaroid Sheet Film Pack being used in exposure test of Polaroid 55 P/N film. Note grid superimposed on monitor test pattern by Colorado Video Model 302 Video Analyzer.

instrument was very hard to adjust, especially in the calibration of a 100 percent black-to-white ratio. These factors together would not have negated the use of the Model 302, since it was very convenient to have the image, scan line, and waveform simultaneously presented and easily photographable. The one factor which finally made this instrument unusable was the very excessive rise time needed to record gray-tone fluctuations. The time required was so great that only the peaks of excursions were considered valid samples of gray-tone level.

During the period in which the Model 302 Video Analyzer was being evaluated, attention was drawn to a new faster speed oscilloscope-trace recording film, called Polaroid Polascope Type 410 (see Fig. 21). This film has a 10,000 ASA speed and has proven capable of recording waveforms at faster exposure times than the normal television field rate. Because of this film's capability and the much shorter rise times characteristic of the Tektronix Model 529 Waveform Monitor, it was decided to return to the use of that instrument for the monitoring and recording of the waveforms produced by the scan lines previously selected. At the same time, a 35-millimeter camera was used to photograph the position of the scan lines as they actually tra-

Fig. 21. Oscilloscope camera being used to record section of waveform using Polaroid Type 410 film. Photograph has just been removed from camera back.

versed the images, providing a permanent record of their location (see Fig. 22).

Gray-Tone Level Control

Since the gray-tone level finally displayed in a waveform can be altered at many different previous points in the instrumentation, it was necessary to evolve a procedure for maintaining consistent gray-tone levels through the electronic system.

In any rescaling and/or reproduction of the imagery prior to waveform monitoring, an automatic exposure timer was used in conjunction with the photographic enlarger, and a film chip densitometer provided the final control on gray-tone. This alleviated any problem that might arise from inconsistent gray-tones appearing on the imagery.

Before each real-time or video-tape-recording session began, the television camera and/or video-tape-recorder was calibrated for normal contrast brightness and focus using a commercial broadcast test pattern. The camera and recorder controls were then left constant during the session. Each complete set of imagery was scanned and its waveforms recorded during one session, eliminating any inconsistencies engendered by having to recalibrate the camera or tape-recorder.

Fig. 22. A 35-millimeter photograph used for locating traverse of scan line. Image is nine-lens multiband photograph, Frame 42, Lens 2, Line 2.

Gray-tones presented to the conventional monitor are not altered by any adjustment of that monitor. Consequently, it is possible to adjust the brightness and contrast of the monitor to provide the best picture for selecting and recording the location of the scan line (see Fig. 22).

Because of its primary testing function, the Tektronix Model 529 has several controls capable of changing the character and gray-tone level of a waveform. Primary of these is the calibrator switch, which provides a one-volt peak-to-peak reference voltage for calibrating a 100 percent black-to-white contrast signal generated by a ten-division black-to-white "stair-step" test pattern. This signal is then positionable on the 100 percent grid scale illuminated graticule placed in front of the display cathode-ray tube.

A frequency-response switch allows the selection of several conventional response characteristics. In the "flat" response position, considerable signal noise is included in the waveform. Ninety percent of this noise, however, is removed in the "IEEE" (Institute of Electrical and Electronic Engineers) response position, producing a waveform which includes a maximum amount of gray-tone information

and a minimum amount of signal noise. Other controls of the waveform monitor include the magnification feature mentioned previously, a trace-illumination control, and a control for changing the lateral position of the waveform in order to view successive portions of it when either of the magnification positions is used.

Variations in exposure timing of the oscilloscope camera do not influence the gray-tone levels presented on the waveform monitor. Once a usable exposure time and lens setting are found, they are maintained throughout the recording.

Future Instrumentation Additions

Since one of the major drawbacks in the waveform analysis procedure is the recording of the actual waveforms using an oscilloscope camera, it is planned to include an X-Y axis strip-chart recorder (see Figs. 23 and 24) among the experimental components. This will permit direct graphical recording of the traces displayed on the waveform monitor cathode-ray tube, without having to resort to the laborious process of putting the waveform recorded on Polaroid film into analyzable graphical form.

Additional instrumentation plans also include the use of television cameras, monitors, and waveform monitors

STRIP-CHART RECORDING OF REAL-TIME IMAGERY AND WAVEFORMS

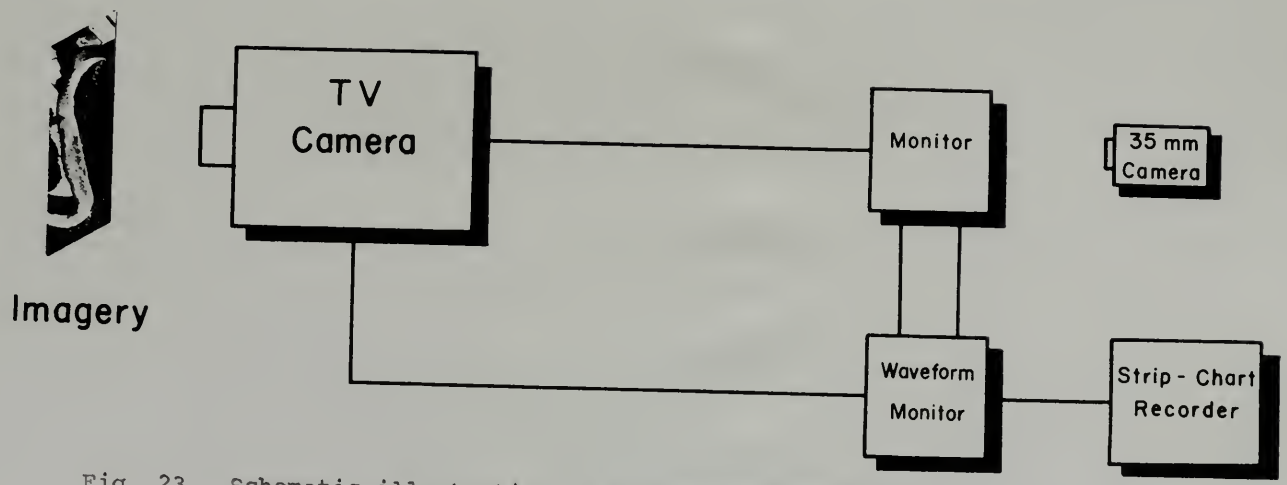

Fig. 23. Schematic illustration of strip-chart recording of real-time imagery and waveforms.

STRIP-CHART RECORDING OF VIDEO-TAPED IMAGERY AND WAVEFORMS

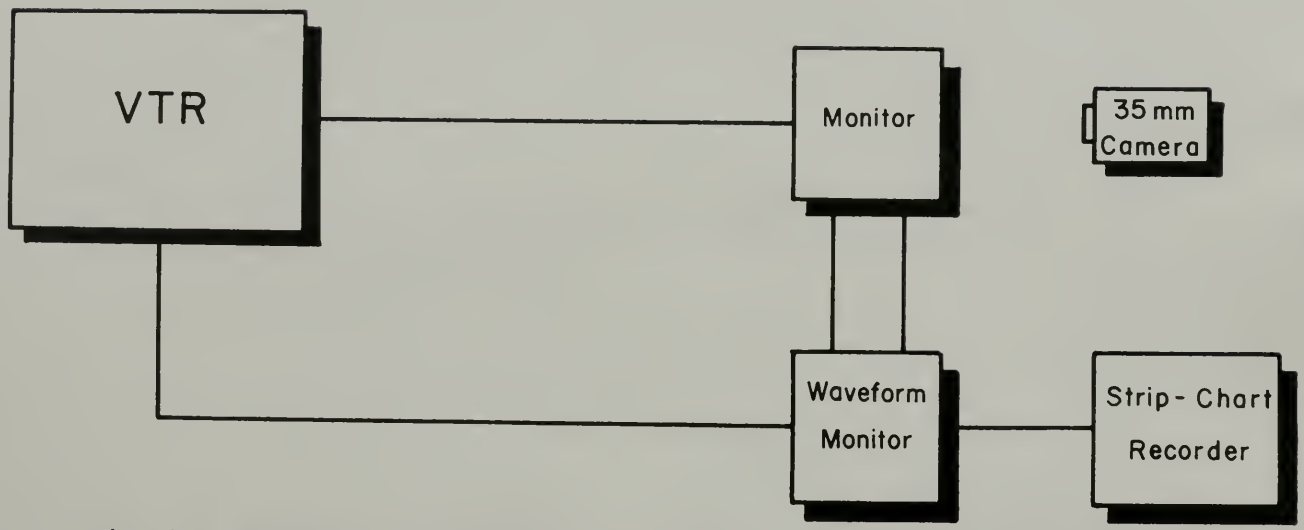

Fig. 24. Schematic illustration of strip-chart recording of video-taped imagery and waveforms.

having several different scan-line rates, such as 729, 875, and 945 lines, and higher frequency response. Such instrumentation sets will permit the comparison of images using systems having increasingly higher resolution capability.

Graphical Presentation of Waveforms

Since each of the original polaroid photographs (Fig. 21) included only part of the waveform magnified to 5X, it was necessary to mosaic these photographs in order to have a composite record of each waveform. This problem had been anticipated before the photography was begun, and hence sufficient overlay between successive Polaroid photographs was retained so that accurate linear mosaicing might be accomplished. After each mosaic was completed, it was projected onto a sampling grid using a Saltzman Auto-Focus Projector. During this process, the waveform was enlarged approximately 3X so that a 100 percent gray-tone fluctuation occupied a five-inch vertical interval on the sampling grid (see Fig. 25). After each waveform had been enlarged, the scan lines traversing each image were segmented according to the specific terrain types crossed. The distances representing these individual terrain-type occurrences were then scaled to the enlarged waveform size, and the specific parts of the wave-

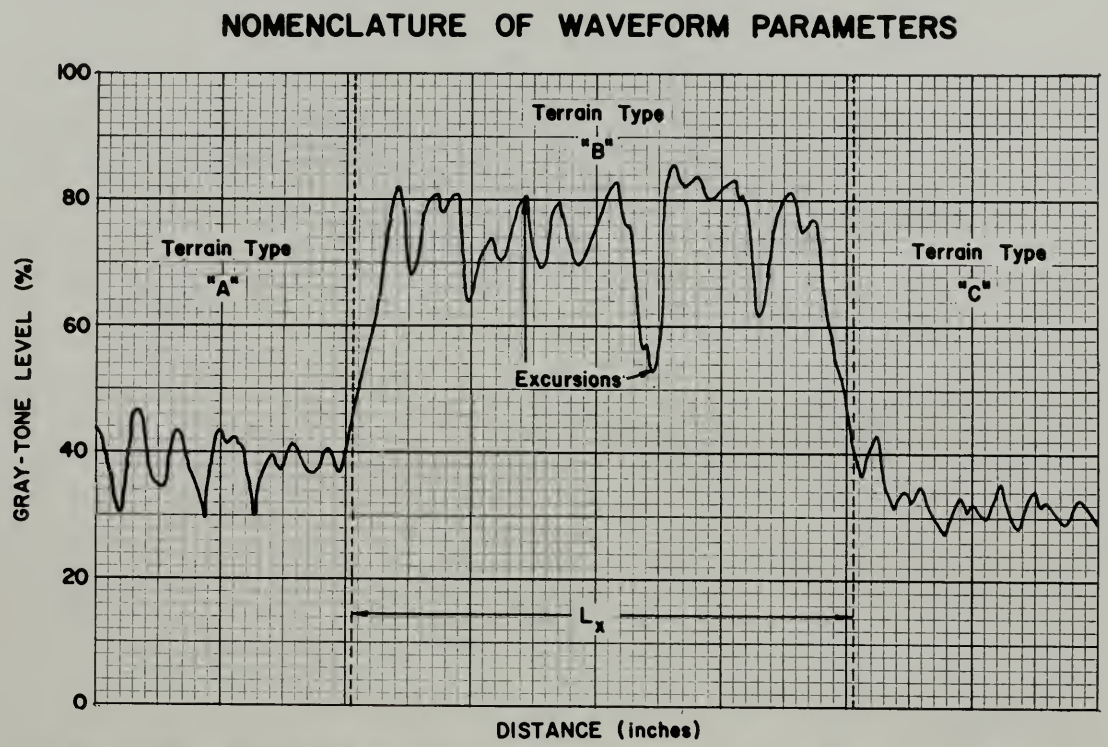

Fig. 25. Graphical example of nomenclature of waveform parameters.

form corresponding to the terrain-type occurrences were identified and isolated by vertical lines (see Figs. 26 through 37).

The sampling grid used for the enlarged waveforms is standard graph paper, with ten divisions per inch along both X and Y axes. This type of graph paper permits the accurate sampling of 1 percent gray-tone level changes along the Y-axis and 0.05-inch distance along the X-axis.

Statistical Presentation of Gray-Tone Levels

In any analysis of waves which are not regular mathematical functions such as simple periodic sinusoidal waves, the conventional wave equations are not applicable. Even Fourier Analysis has been applied to certain waveforms composed of higher order harmonics. This tool, however, does not appear to be applicable to waveforms representative of remote-sensor imagery, which are apparently too complex to be resolved into harmonic components.[4]

Any number of measurements of waveform parameters and subsequent calculations could be made from waveforms, but all such measurements would depend to some degree on the most

---

[4]Hubbs, op. cit., p. 109.

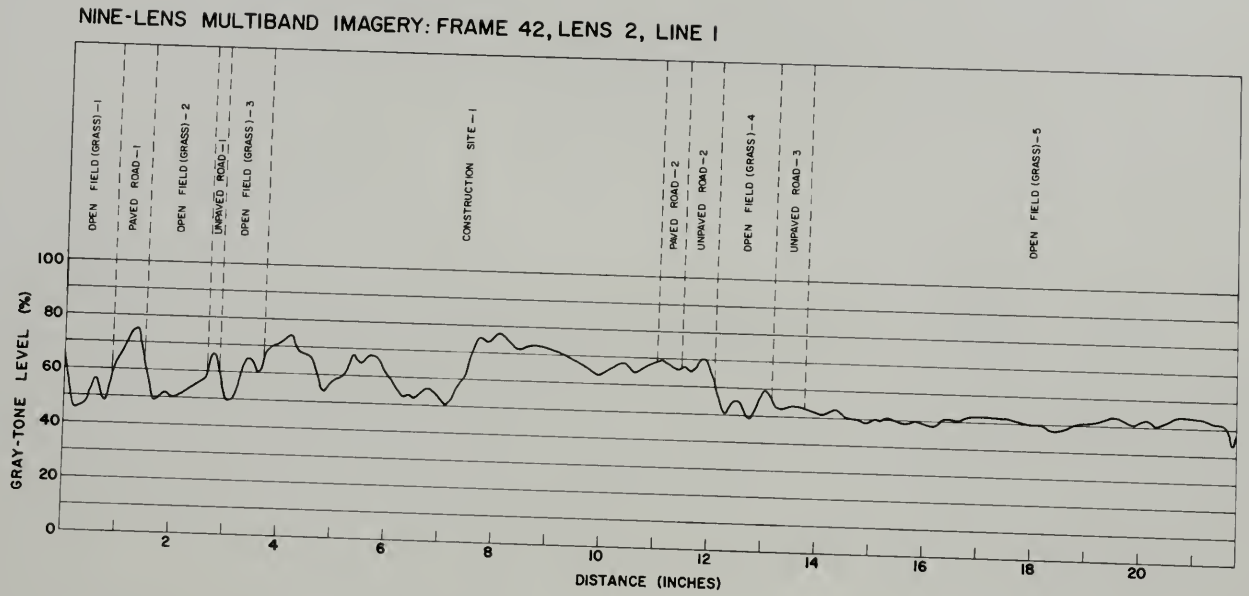

Fig. 26. Graphical presentation of waveform representing nine-lens multiband camera imagery, Frame 42, Lens 2, Line 1.

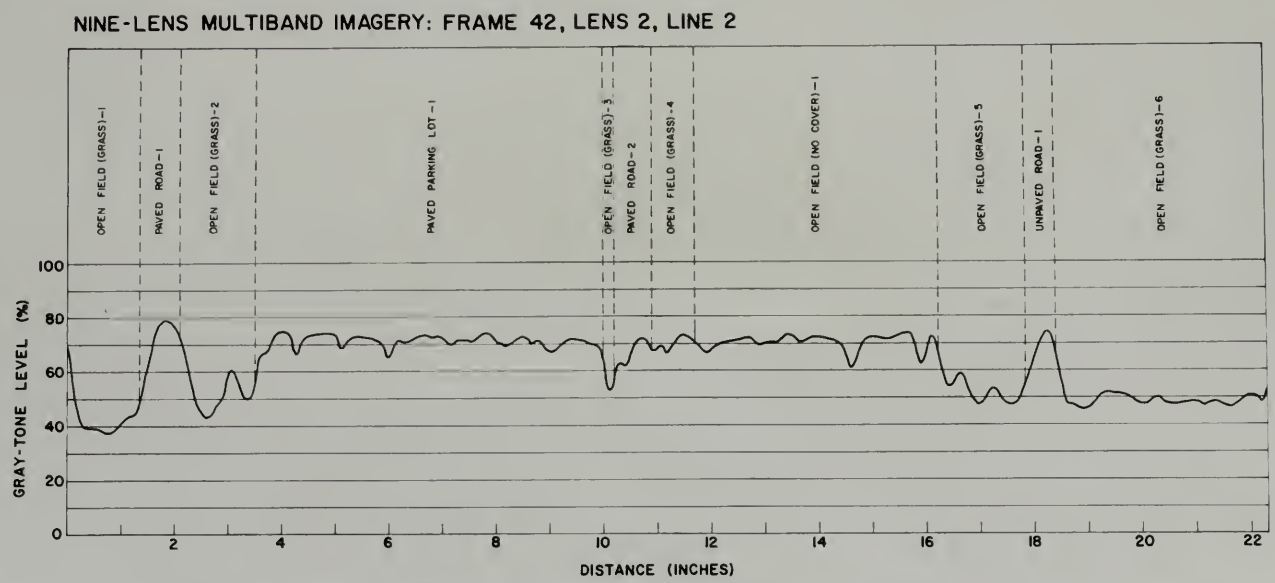

Fig. 27. Graphical presentation of waveform representing nine-lens multiband camera imagery, Frame 42, Lens 2, Line 2.

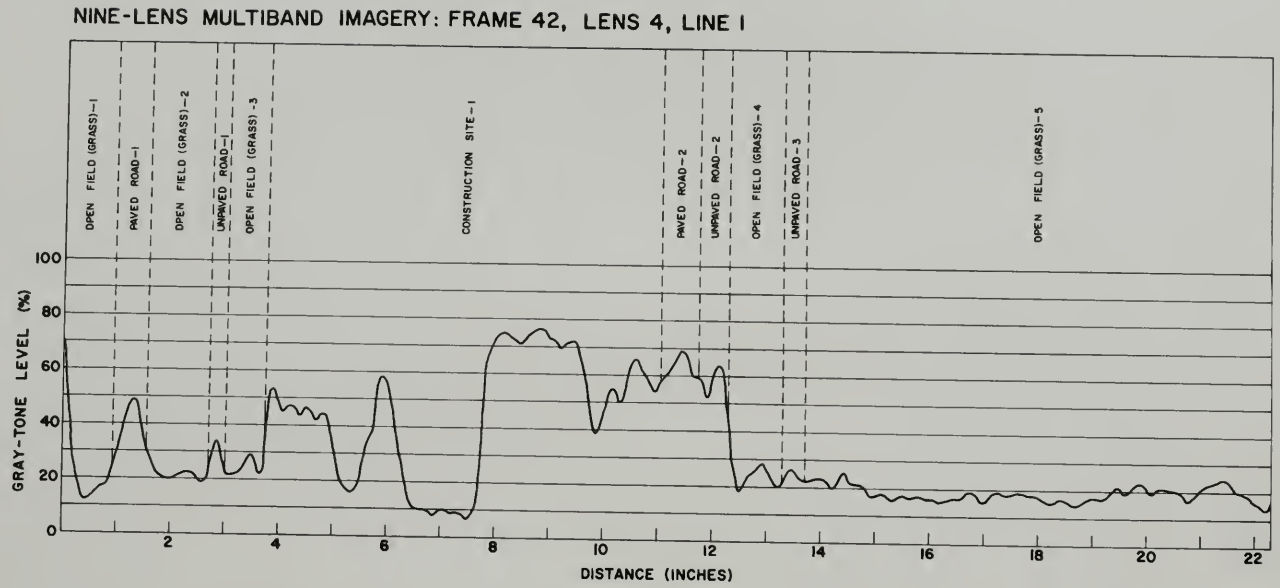

Fig. 28. Graphical presentation of waveform representing nine-lens multiband camera imagery, Frame 42, Lens 4, Line 1.

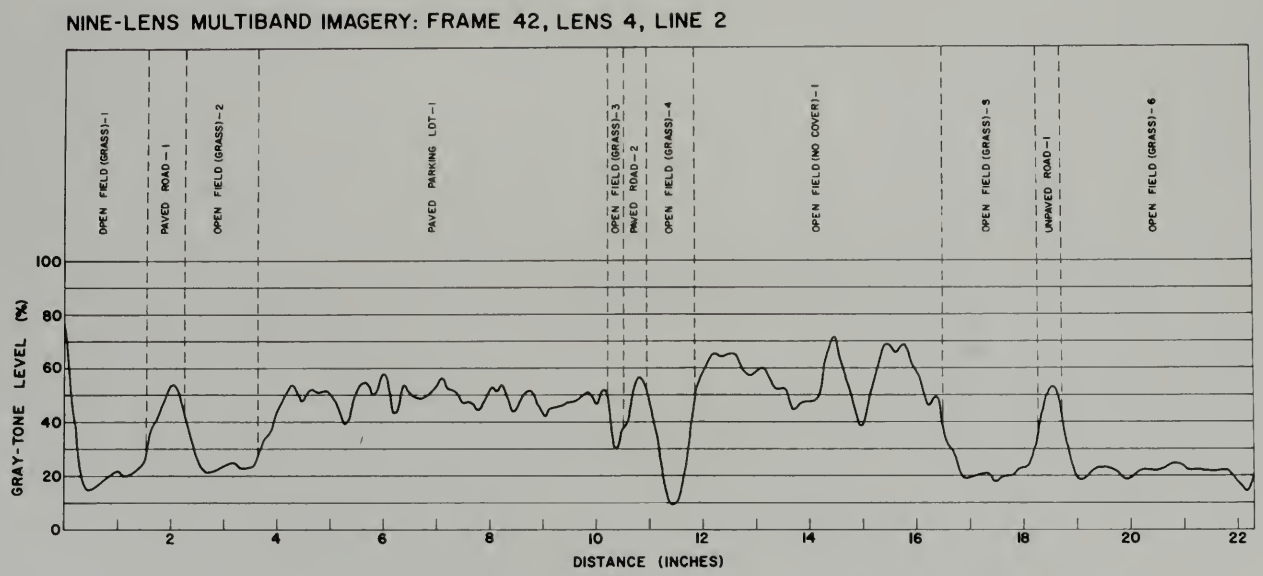

Fig. 29. Graphical presentation of waveform representing nine-lens multiband camera imagery, Frame 42, Lens 4, Line 2.

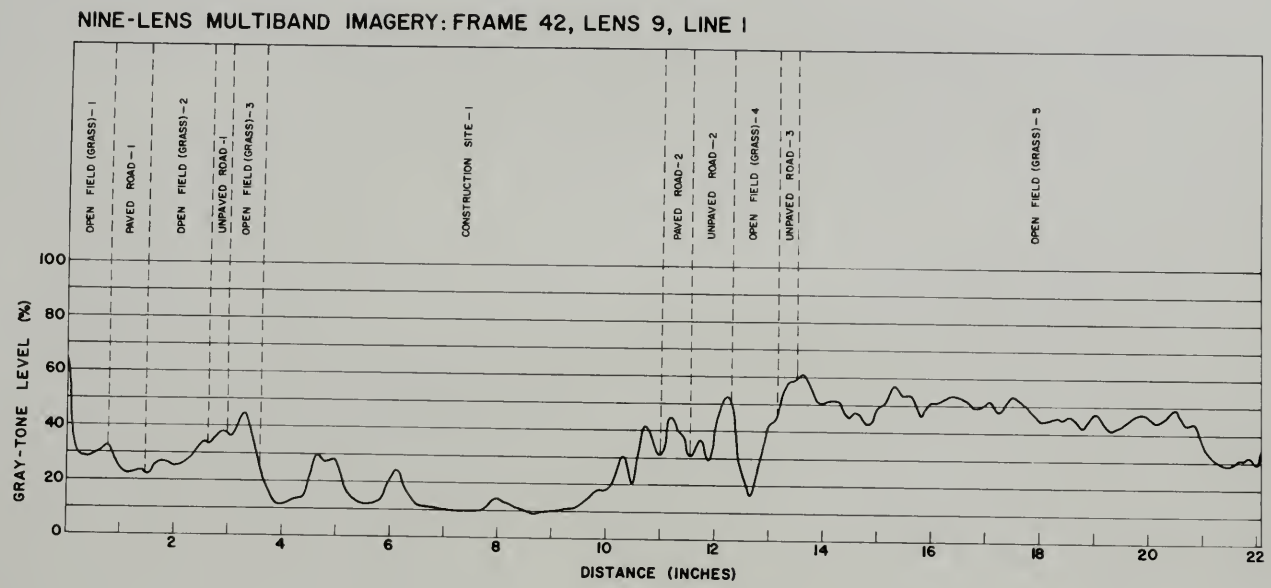

Fig. 30. Graphical presentation of waveform representing nine-lens multiband camera imagery, Frame 42, Lens 9, Line 1.

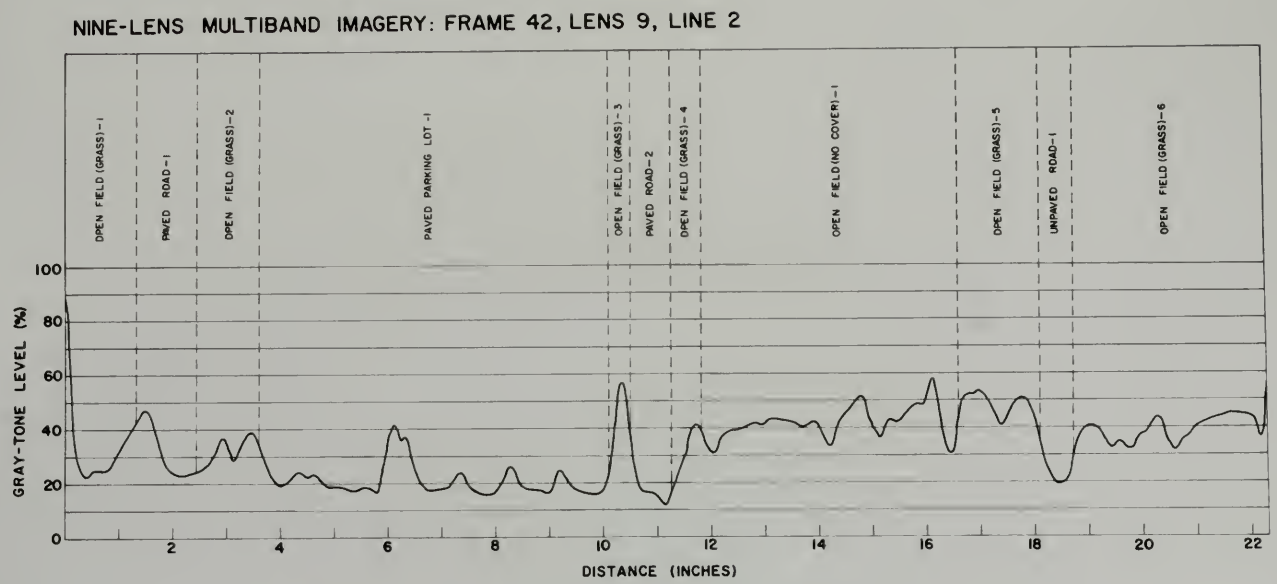

Fig. 31. Graphical presentation of waveform representing nine-lens multiband camera imagery, Frame 42, Lens 9, Line 2.

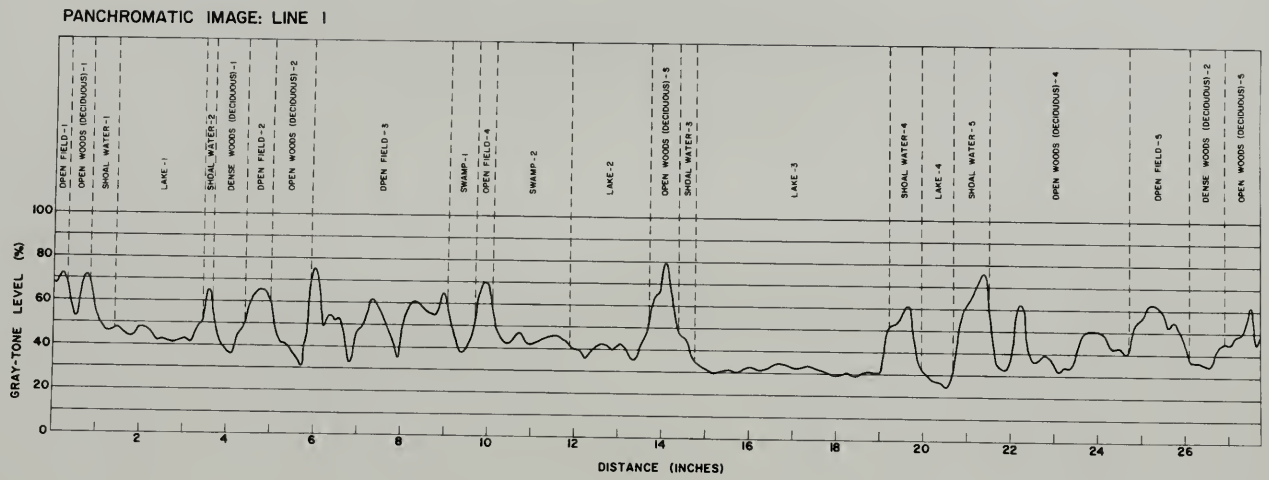

Fig. 32. Graphical presentation of waveform representing panchromatic image, Line 1.

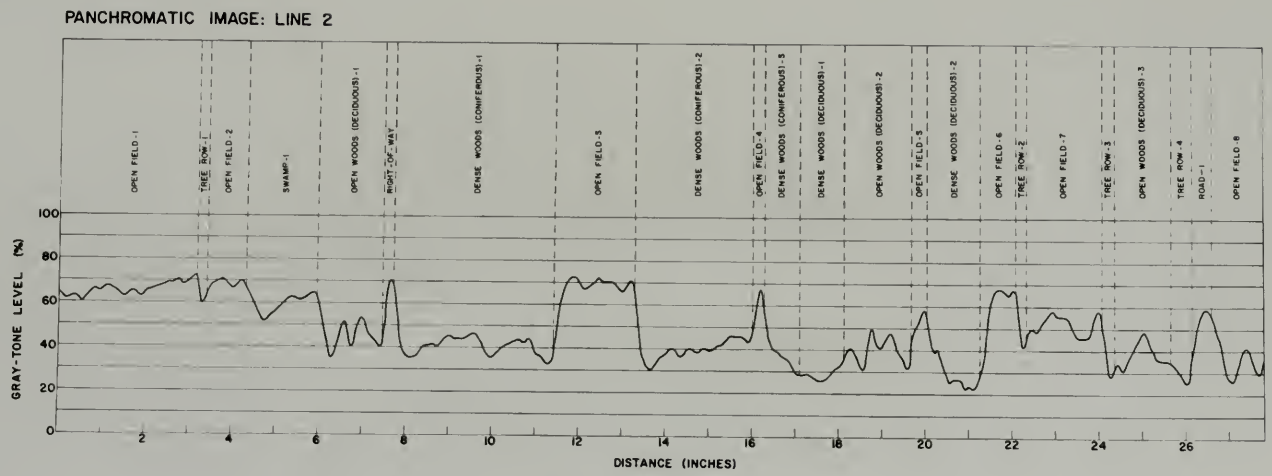

Fig. 33. Graphical presentation of waveform representing panchromatic image, Line 2.

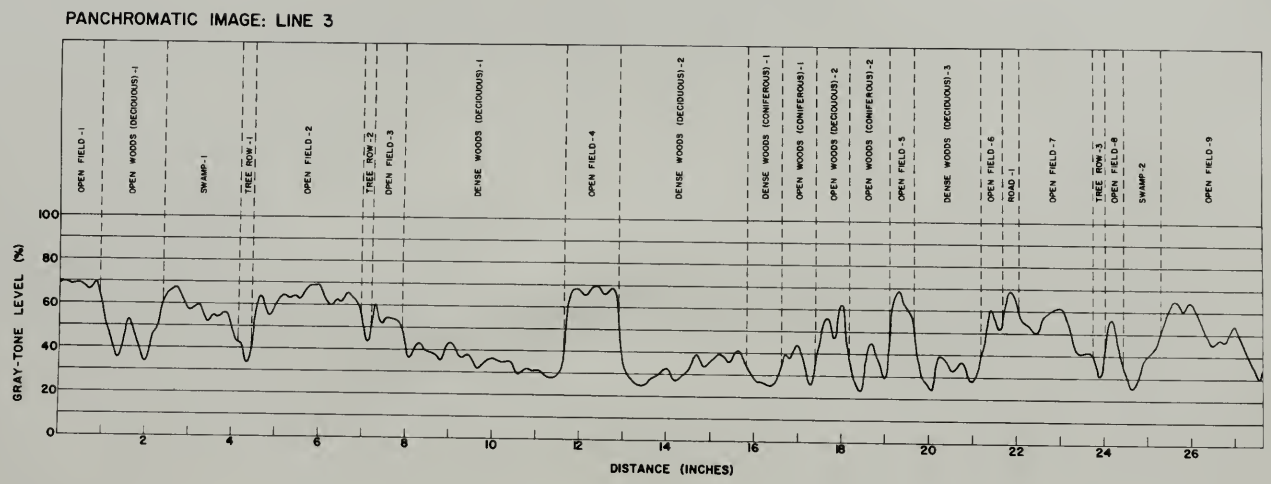

Fig. 34. Graphical presentation of waveform representing panchromatic image, Line 3.

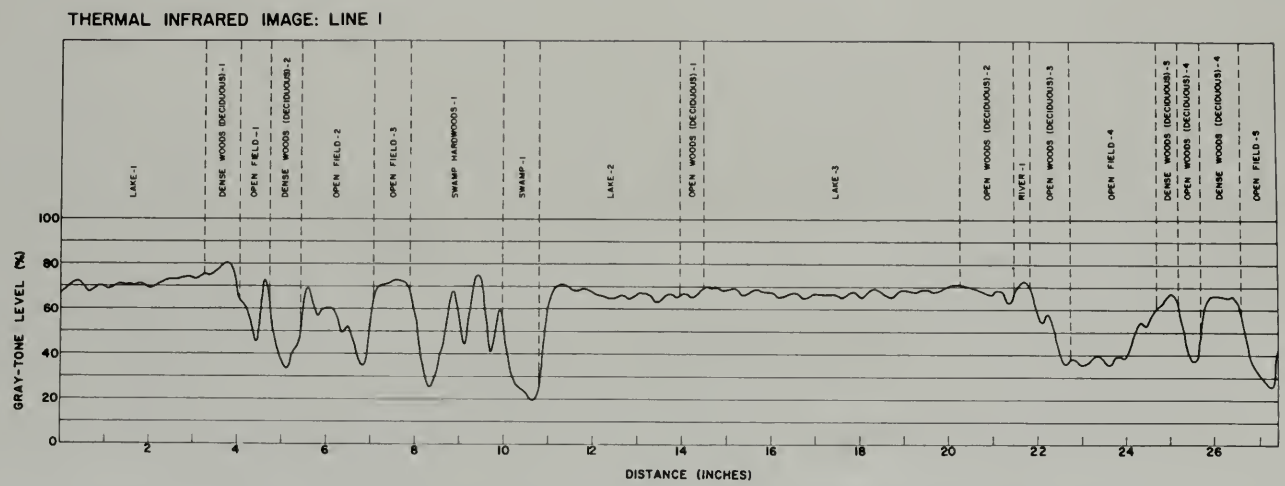

Fig. 35. Graphical presentation of waveform representing thermal infrared image, Line 1.

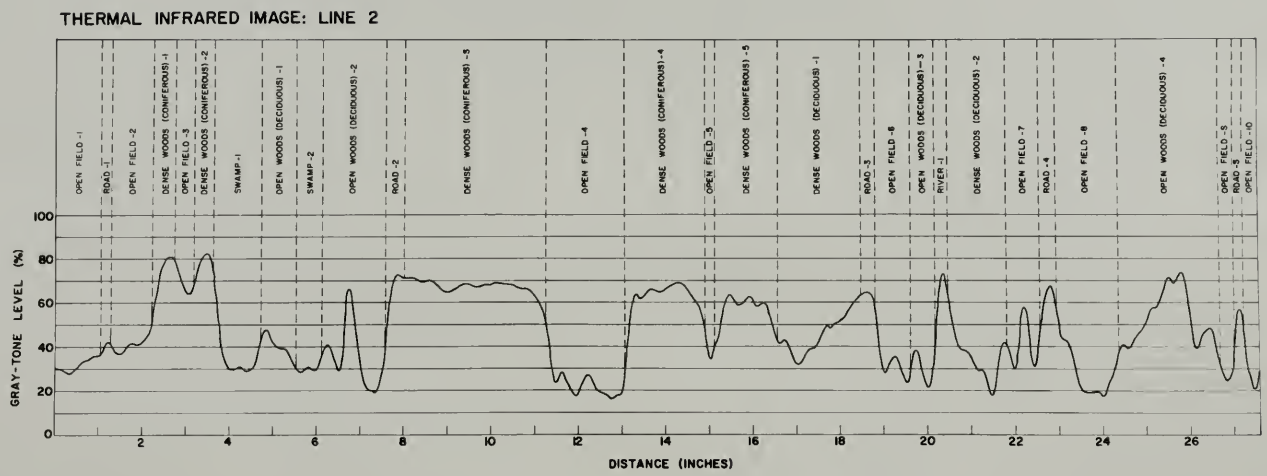

Fig. 36. Graphical presentation of waveform representing thermal infrared image, Line 2.

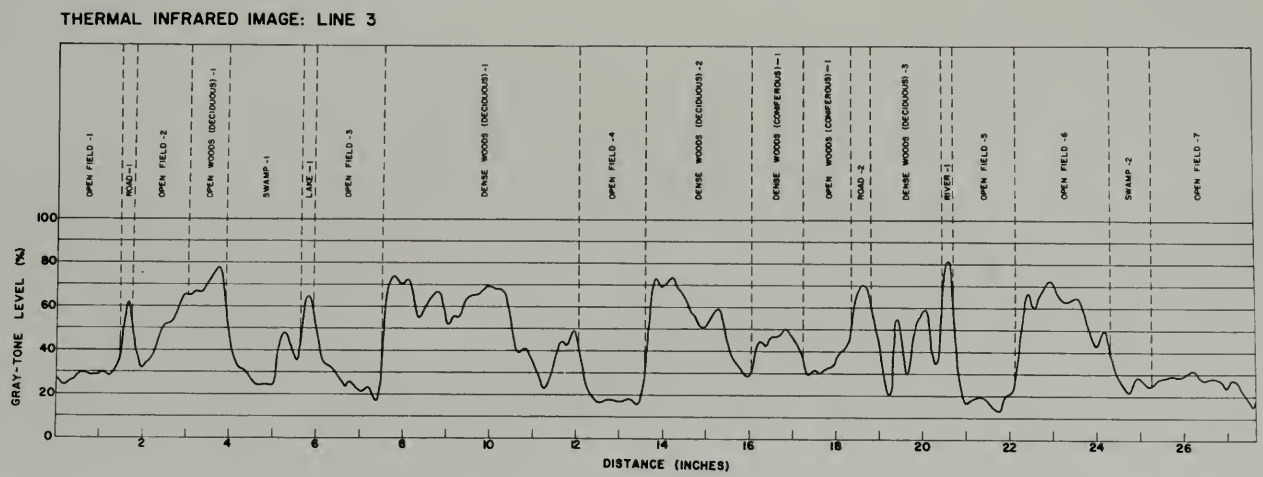

Fig. 37. Graphical presentation of waveform representing thermal infrared image, Line 3.

conventional of all variables dealing with waves. These variables are amplitude and frequency. Amplitude of a wave can be simply stated as the distance away from the base line or reference line of any point on the wave as measured along the Y-axis. In this case, the amplitude of any point on the waveform is in reality the gray-tone level of that point, expressed as a percentage of white (100 percent). On Figure 25, for example, gray-tone level, as sampled every 0.10 inch, would be for Terrain Type "A" (reading left to right): 44 percent, 38 percent, 32 percent, etc.

Frequency, on the other hand, is simply the number of fluctuations occurring per unit length of the curve. A description of the derivation and significance of the statistical parameters pertaining to waveforms which have evolved during this research will occupy several of the following pages.

The Number of Samples (n)

A certain number of gray-tone level samples are taken from each of the terrain-type occurrences. In Figure 25, for example, in Terrain Type "A" n would equal 20 samples. Each 0.1-inch minor grid division is used as a sampling point, and all such divisions crossed or intersected (see left-hand edge of Terrain Type "A") are counted as

sampling points. (N.B. Note that each individual terrain-type occurrence is coded by a number appearing after it, both on the large graphs, i.e., Figures 26 through 37, and on all tables appearing in the Appendices.)

The Summation of Gray-Tone Levels (Σx)

The letter x is used to denote any specific gray-tone level, and the parameter Σx is simply the total of all gray-tone levels in any individual terrain-type occurrence.

The Average Gray-Tone Level ($\bar{x}$)

This parameter is simply the total of the gray-tone levels sampled in any terrain-type occurrence (Σx) divided by the number of samples (n). It denotes the average, or mean, gray-tone level occurring in any particular terrain-type occurrence which has been traversed by a scan line. The unit used with $\bar{x}$ is percent.

The Number of Excursions (E)

As previously noted, a waveform "excursion" is a positive or negative peaking (see Fig. 25) of the curve and represents a local maximum gray-tone level. The symbol E represents the total number of excursions appearing in any waveform segment representing a discrete terrain type. Inflection points, or those positions on the curve where the

rotation of a tangent to the curve changes direction, are counted as one-half of a peaked excursion, since they do represent significant gray-tone fluctuation, although not sufficient to produce a positive or negative peak. In Figure 25, for example, Terrain Type "B" exhibits 27.5 excursions.

The Waveform Segment (L_x)

The symbol L_x represents the length of the waveform segment, in inches, corresponding to an individual terrain-type occurrence, as measured along the X-axis. These X-axis waveform-segment distances can be converted to represent actual ground-scale distances, as determined from the image. When necessary, these segment distances could also be converted to lengths of time, since a constant amount of time is required to traverse the entire length of scan line. This length is measured to the nearest 0.05 inch.

The Scale Waveform Segment (L_s)

In order to reduce L_x to actual imagery scale, it must be multiplied by a constant factor. This constant represents the number of feet of imagery scale corresponding to one inch on the enlarged waveform. For the nine-lens multiband camera imagery, this has been determined to be

94.3 ft./in. For the panchromatic and thermal infrared images used, it is 694 ft./in.

The Excursion Frequency ($\bar{f}$)

The excursion frequency is calculated by dividing the number of excursions (E) occurring in any particular terrain-type occurrence by the length of the corresponding waveform segment. Since there is normally a variation of distance between the individual excursions, this parameter is in reality an average frequency calculation, and thus represents the average X-axis distance occupied by each excursion. The calculation of excursion frequency provides a means for determining the spacing between gray-tone level fluctuations appearing on the imagery. The unit for this measure is reciprocal distance, or inches^{-1}.

The Scale Excursion Frequency ($\bar{f}_s$)

The excursion frequency $\bar{f}$ is converted to scale excursion frequency $\bar{f}_s$ by multiplying $\bar{f}$ by some constant appropriate to the scale of the imagery being analyzed. This scale constant represents the ratio of the number of excursions per mile on the original imagery to the number of excursions per inch on the waveform as it is presented on the sampling grid. For the nine-lens multiband camera imagery,

this constant has been calculated to be 17.95. For the panchromatic and thermal infrared image, it was found to be 3.70. The multiplication of the excursion frequencies by these factors reduces $\bar{f}$ to a scale parameter, $\bar{f}_s$, which can be compared between multispectral sets. The unit of the measure thus becomes excursions per mile.

The Excursion Wavelength ($\bar{\lambda}$)

This parameter is calculated by determining the reciprocal of the excursion frequency ($\bar{f}$). It represents the actual average distance in inches between individual excursions.

The Scale Excursion Wavelength ($\bar{\lambda}_s$)

As was the case with the conversion of L_x to L_s, $\bar{\lambda}$ is converted to $\bar{\lambda}_s$ by using the scale constant of each imagery set, 94.3 ft./in. for the nine-lens imagery and 694 ft./in. for the panchromatic and thermal infrared set. This measure, then, represents the actual average distance in feet between individual excursions.

Mean Deviation of Gray-Tone Level ($\overline{x-\bar{x}}$)

This statistical measure is simply the summation of the absolute (algebraic sign disregarded) departure of each gray-tone level percentage sample from the average gray-tone

level $\bar{x}$, divided by the number of samples n. Fully expressed, it would be $\frac{|x-\bar{x}|}{n}$. This calculation determines the average dispersion of the sampled data about the mean. In this waveform analysis, it provides an estimation of the relative size of the excursions, i.e., the degree of gray-tone fluctuation within any terrain-type occurrence.

Standard Deviation of Gray-Tone Level (s)

This variable, fully denoted by $\left(\frac{(x-\bar{x})^2}{n}\right)^{1/2}$, is a conventional statistical variable which also gives an indication of the dispersion of the data. It expresses, however, percentages of the data which exist within certain ranges from the mean of the data. For example, a standard deviation of 5.00 would indicate, when applied to the gray-tone level data, that, for one standard deviation, approximately 68.3 percent of the data would lie between $\pm$ 5.00 percentage points of the mean; for two standard deviations, 95.4 percent would lie between $\pm$ 10.00 percentage points of the mean; and for three standard deviations, 99.7 percent of the data would be included within $\pm$ 15.00 percentage points of the mean. This provides a more precise measure of the dispersion and relative size of the excursions.

CHAPTER IV

EXPERIMENTAL RESULTS

This chapter presents the results and conclusions derived from the waveform analysis of the nine-lens multiband camera imagery and the panchromatic and thermal infrared images. The calculations for each of the scan lines are reviewed and the significant findings presented. The terrain-type occurrences are then paired, where possible, and waveform-analysis results compared for each individual type of sensor.

Waveform Analysis Results: Nine-Lens Multiband Camera Imagery

Primary Data

The primary sampling data and calculations for the nine-lens multiband camera imagery are summarized in Appendix I. In that section, each specific terrain-type occurrence is listed and denoted by the code number appearing immediately after the occurrence, e.g., open field-1, open field-2, etc. These notations will also be found concurrently on the waveform graphs (Figs. 26 through 37). These

calculations are summarized by individual scan lines so that each data group representing one scan line may be compared directly with its corresponding waveform graph. Also for the sake of clarity, calculations for both scan lines from each of the nine-lens images are included on each data page.

Compiled Data

The primary data has been reorganized in Appendix III by grouping all occurrences from both lines together by terrain type and either totaling or averaging the data where appropriate; e.g., n has been totaled for each terrain type while $\bar{x}$ has been averaged. The mean deviation and standard deviation, because of their mathematical character, must be weighted before being averaged. This is accomplished by multiplying the mean deviation and standard deviation for each occurrence by n, the number of gray-tone level samples, and then calculating the average of the accumulated products.

The light over-all visual impression of the Lens 2 image (see Fig. 4) is manifested in the average gray-tone level calculations. A close grouping of the lightest gray-tones, 68.6 percent for paved road, 70.3 percent for open field (no cover), and 70.6 percent for paved parking lot, substantiates this visual grouping of lighter tones. Inter-

mediate gray-tones are characteristic of unpaved road (62.6 percent) and the construction site (65.4 percent), while the darkest tones on the image are characteristic of open field (grass), which returns 51.6 percent. Excursion frequencies, and similarly excursion wavelengths, show little differentiation between terrain types on the Lens 2 image, providing little opportunity for legitimate discrimination using these two measures related to spacing of textural differences. Even though the two foregoing parameters indicate similar excursion spacing, the standard deviations for each terrain-type group do correspond to texture differences. The most diverse of the gray-tone assemblages are associated with the construction site, whose gray-tone level sampled data shows a standard deviation of 7.03. This is much higher than any other Lens 2 standard deviation, and is demonstrated on Figure 26 by the diverse types of excursion patterns and gradients. Paved road and unpaved road are well separated with standard deviations of 5.07 and 2.58, respectively, but open field (grass), open field (no cover), and the paved parking lot are grouped together with 3.63, 3.06, and 3.08, respectively, again providing little differentiation. Identification of these terrain types would have to be accomplished in conjunction with a graphical inspection of the

waveform gradients which represent the rapidity with which contrasts between terrain types change. Figures 26 and 27 illustrate this well. The construction-site waveform segment is a gradual change from its neighbors, while open field (grass) and paved parking lot are sharp departures from their adjacent terrain types, as is illustrated by the nearly vertical excursions. As was mentioned in Chapter III, the Lens 2 image is excellent for shape measurement and boundary determination, but inferior for general identification purposes. This conclusion has been amplified by the foregoing discussion of calculated gray-tone characteristics.

The Lens 4 calculations exhibit greater diversity among the different terrain types (see Figs. 5, 28, and 29). Again, open field (grass) is the darkest of the terrain types, with an average gray-tone level of 22.0 percent. By contrast, open field (no cover) has the lightest tone (56.3 percent). Paved road and paved parking lot have similar gray-tone levels, 50.3 and 48.3 percent, respectively, indicating the use of similar construction materials, and are well differentiated from unpaved road (39.2 percent).

Excursion frequency is also highest for the construction site (3.42/in.). Unpaved road and paved road are well discriminated by frequencies of 3.24/in. and 1.90/in.,

but again open field (grass) (2.86/in.), open field (no cover) (3.01/in.), and paved parking lot (3.08/in.) are not differentiated.

Standard deviations provide a better measure of gray-tone assemblage. The high score of 22.65 for the construction site illustrates the great diversity of gray-tones associated with such a complex cultural feature. The rough surface of open field (no cover) also produces a standard deviation (8.60) characteristic of a complex cultural feature. The relatively smooth open field (grass), unpaved road, paved road, and paved parking lot can be grouped together with characteristically low scores of 5.35, 3.92, 5.56, and 4.87. The low gray-tone level of the background function performed by open field (grass) in this image plus the relatively higher average gray-tone levels of the other terrain types give Lens 4 the distinction of having the gray-tone diversity necessary for both measurement and identification. This conclusion is also borne out by the calculations.

The Lens 9 image exhibits the light (40.7 percent) open field (grass) gray-tone characteristic of infrared film (see Figs. 6, 30, and 31). With the exception of open field (no cover) (41.6 percent), this large background area

has the lightest return on the image. All other terrain types are darker, with the cultural construction site (16.4 percent), paved parking lot (21.0 percent), and paved road (28.6 percent) being characteristically the darkest features. Unpaved road (37.2 percent) is expectedly similar to open field (no cover)(41.6 percent).

Paved road again exhibits the lowest excursion frequency, 1.88/in., but the construction site does not exhibit the diversity of gray-tone so characteristic of it in Lenses 2 and 4, and thus produces a low $\bar{f}$ also, 2.03/in.

As might have been anticipated, because of the general dark tones and lack of terrain-type contrasts, the standard deviations associated with the Lens 9 image allow little discrimination between terrain types; all values for s lie between 7.73 for the construction site and 5.68 for the open field (no cover), with no significant cultural or natural groupings.

Corrected Data

After all calculations had been made using all sampling points on the grids, an attempt was made to reduce the discrepancies among the data by correcting the calculations for each waveform segment for the inaccuracies produced on the graphs by rise time or fall time. Those

sampling points representing transitional gray-tones produced by rise time were eliminated from the sampling data and the entire range of calculations performed again. This corrected data for the nine-lens multiband camera imagery is compiled in Appendix V.

As can be seen from an inspection of the Lens 2 image corrected data, the elimination of rise-time inaccuracies produces the same basic analytic patterns, but amplifies these patterns by increasing the range of the data for each statistical variable. The difference between highest and lowest, or range of average gray-tone levels has increased from 19.0 to 19.9 percent, excursion frequencies from 0.61/in. to 0.72/in., and standard deviation from 4.45 to 5.02, providing greater differences between calculations for individual terrain types. Substantiating the hypothesis that the elimination of gray-tone samples generated by rise-time discrepancies is the observation that the range of calculations for each waveform segment included with a terrain-type group, such as the eleven waveform segments representing open field (grass), is lower for the corrected data. In effect, this means that the grouping of the data around the various averages is smaller, and is demonstrated by the lower standard deviations in all cases where rise-time corrected waveform segments occur.

The Lens 4 and Lens 9 calculations also exhibit the effects of: (1) separating the data by increasing the range between terrain types, and (2) decreasing the range of data included within each group of terrain-type occurrences. This serves to enhance the use of the Lens 4 image as the most useful for interpretation and measurement, but does not improve the Lens 9 image's position as the least useful in these general matters.

Sensor Comparison Totals: Nine-Lens Multiband Camera Images

In order to compare the statistical trends for each terrain type as exhibited by the various film-filter combinations sampled, the totals and averages for each terrain-type occurrence group have been compiled for all lenses in Tables 3 and 4.

Table 3 includes the data which has not been corrected for rise time. Since no sampling points have been removed, an inspection of the various totals for n, L_x, and L_s will reveal the ability of the waveform monitor to display consistently a waveform which can be dimensionally compared with another waveform from a comparable image. The slight discrepancies existing between these dimension variables for each terrain type are composite errors from several sources.

TABLE 3

SENSOR COMPARISON TOTALS BY TERRAIN TYPE: NINE-LENS MULTIBAND CAMERA IMAGERY

Terrain Type	Lens No.	n	Σx	$\bar{x}$
Construction site	2	74	4,842	65.4
	4	73	3,258	44.6
	9	75	1,234	16.4
Open field (grass)	2	217	11,194	51.6
	4	222	4,873	22.0
	9	212	8,630	40.7
Paved road	2	27	1,852	68.6
	4	24	1,208	50.3
	9	33	944	28.6
Unpaved road	2	22	1,378	62.6
	4	19	745	39.2
	9	23	856	37.2
Open field (no cover)	2	46	3,233	70.3
	4	47	2,646	56.3
	9	47	1,953	41.6
Paved parking lot	2	67	4,733	70.6
	4	66	3,191	48.3
	9	66	1,388	21.0

TABLE 3.--Extension

Statistical Parameters								
E	L_x	L_s	$\bar{f}$	$\bar{f}_s$	$\bar{\lambda}$	$\bar{\lambda}_s$	$\overline{\lvert x-\bar{x}\rvert}$	s
22.0	7.35	693	3.00	53.85	0.33	31	5.71	7.03
25.0	7.30	688	3.42	61.39	0.29	27	18.93	22.65
15.0	7.40	698	2.03	36.44	0.49	46	6.26	7.73
60.5	21.20	1,998	2.85	51.16	0.35	33	2.77	3.63
62.25	21.80	2,056	2.86	51.34	0.35	33	4.01	5.35
57.5	20.60	1,943	2.79	50.08	0.36	34	5.72	7.43
7.0	2.50	236	2.80	50.26	0.36	34	4.28	5.07
4.75	2.50	236	1.90	34.10	0.53	50	4.88	5.56
6.0	3.20	302	1.88	33.75	0.53	50	6.30	7.19
7.0	2.05	194	3.41	61.21	0.29	27	2.13	2.58
5.5	1.70	161	3.24	58.16	0.31	29	3.37	3.92
6.5	2.05	194	3.17	56.90	0.32	30	5.11	5.74
14.0	4.50	424	3.11	55.82	0.32	30	2.16	3.06
14.0	4.65	438	3.01	54.03	0.33	31	7.37	8.60
16.0	4.75	448	3.37	60.49	0.30	28	4.20	5.68
22.0	6.50	613	3.38	60.67	0.30	28	2.03	3.08
26.5	6.60	623	3.08	55.29	0.32	30	3.64	4.87
19.5	6.50	613	3.00	53.85	0.33	31	4.31	5.89

TABLE 4

SENSOR COMPARISON TOTALS BY TERRAIN TYPE: NINE-LENS MULTIBAND CAMERA IMAGERY (CORRECTED FOR RISE TIME)

Terrain Type	Lens No.	n	Σx	$\bar{x}$
Construction site	2	74	4,842	65.4
	4	73	3,258	44.6
	9	75	1,234	16.4
Open field (grass)	2	209	10,666	51.0
	4	209	4,270	20.4
	9	204	8,250	40.4
Paved road	2	26	1,798	69.2
	4	22	1,143	52.0
	9	32	904	28.2
Unpaved road	2	21	1,320	62.9
	4	18	718	39.9
	9	22	820	37.3
Open field (no cover)	2	46	3,233	70.3
	4	47	2,646	56.3
	9	47	1,953	41.6
Paved parking lot	2	66	4,679	70.9
	4	65	3,161	48.6
	9	66	1,388	21.0

TABLE 4.--Extension

Statistical Parameters								
E	L_x	L_s	$\bar{f}$	$\bar{f}_s$	$\bar{\lambda}$	$\bar{\lambda}_s$	$\overline{\lvert x-\bar{x}\rvert}$	s
22.0	7.35	693	3.00	53.85	0.33	31	5.71	7.03
25.0	7.30	688	3.42	61.39	0.29	27	18.93	22.65
15.0	7.40	698	2.03	36.44	0.49	46	6.26	7.73
60.5	20.45	1,926	2.96	53.13	0.34	32	2.27	2.71
62.25	18.55	1,750	3.36	60.31	0.30	28	2.33	2.87
57.5	19.85	1,872	2.90	52.06	0.34	32	4.85	6.09
7.0	2.35	222	2.98	53.49	0.34	32	3.57	4.14
4.5	2.35	222	1.91	34.28	0.52	49	4.16	4.72
6.0	3.10	292	1.94	34.82	0.52	49	5.51	6.13
7.0	1.90	180	3.68	66.06	0.27	25	1.68	2.01
5.5	1.55	148	3.55	63.72	0.28	26	3.02	3.28
6.5	1.95	184	3.33	59.77	0.30	28	4.65	5.15
14.0	4.50	424	3.11	55.82	0.32	30	2.16	3.06
14.0	4.65	438	3.07	54.03	0.33	31	7.37	8.60
16.0	4.75	448	3.37	60.49	0.30	28	4.20	6.13
22.0	6.40	604	3.44	61.75	0.29	27	1.74	2.31
26.5	6.40	604	4.14	74.31	0.24	23	3.37	4.34
19.5	6.50	613	3.00	53.85	0.33	31	4.31	5.89

They are undoubtedly minor dimensional differences between the images displayed before the television camera. There are also minor differences between the waveforms of each image resulting from the determination of the edge of the imagery on the waveform. Minor discrepancies also result from small errors in display placement positions between subsequently scanned images, and, finally, there are small errors engendered in the linear mosaicing of the Polaroid prints to produce the composite waveform. All of these errors totaled average 0.9 of one percent of the total dimensions recorded throughout the imagery-television camera-waveform monitor-oscilloscope camera-mosaic-enlarged waveform progression.

The totals compiled in Table 3 reveal some patterns not previously noticed. There is a general decrease in average gray-tone level from Lens 2 through Lens 9, with the exception of the open field (grass) category. In some cases, this amounts to a complete reversal of gray-tone, as in paved parking lot, and in others it is only a slight shift (unpaved road, for example). Some terrain-type categories exhibit remarkably consistent excursion frequencies between images, such as open field (grass), unpaved road, open field (no cover), and paved parking lot. Others

exhibit widely divergent values for $\bar{f}$, such as the construction site. Categories showing consistent excursion frequencies also show consistent excursion wavelengths, because of the reciprocal mathematical relationship between these two variables. With the exception of the construction site and open field (no cover) categories, there is a general increase in standard deviations from Lens 2 through Lens 9. Most likely this is the result of the wider range of wavelengths sampled by the Lens 9 film-filter combination, which, in effect, produces greater variation within terrain types than between them.

These same trends are exhibited in Table 4, which presents the compiled data after correction for rise-time discrepancies. The significant difference between the two sets of data lies in the standard deviations. The removal of a few sampling points has resulted in a substantial decrease in most average standard deviations, again illustrating the value of this method of data refinement.

Waveform Analysis Results: Panchromatic and Thermal Infrared Images

Primary Data: Panchromatic Image

The primary sampling data and calculations for the panchromatic image are presented in Appendix II. As was the

case with the nine-lens multiband camera imagery presented in Appendix I, the data is listed by specific terrain-type occurrences, and each occurrence is denoted by the code number appearing immediately after the occurrence.

In Appendix II, the data has been grouped for each individual scan line. Where possible, the abbreviations PAN for panchromatic and IR for infrared will be used for the sake of simplicity throughout this discussion.

Compiled Data: Panchromatic Image

The primary sampling data and calculations have been reorganized in Appendix IV by grouping all occurrences of each specific terrain type together from each of the three scan lines across the image. This data has been totaled and/or averaged in the same manner described in the treatment of the nine-lens multiband camera data.

The panchromatic image (see Fig. 8) and its associated waveforms (see Figs. 32, 33, and 34) illustrate the complexity of gray-tone patterns and land uses which influenced the choice of this image as representative of panchromatic aerial photography. Because it is a photographic record of all wavelengths of visible light, it is more difficult to separate out individual terrain types by such stringent gray-tone ranges as was accomplished in the narrow

bandwidth photography generated by the nine-lens multiband camera.

Using all of the grid sampling points, the following ranking of gray-tone levels by terrain type was produced:

Cleared right-of-way	59.0%
Open field	57.9%
Road	57.2%
Shoal water	54.0%
Swamp	50.5%
Open woods (deciduous)	46.0%
Tree row	41.9%
Dense woods (coniferous)	39.3%
Dense woods (deciduous)	37.3%
Lake	36.2%
Open woods (coniferous)	34.8%

As might be expected, the three lightest tones, if grouped together, represent much the same type of terrain as seen by an interpreter. Only the linearity of most roads serves to distinguish them from other similar terrain types. On the PAN image (see Fig. 8) itself, it will be noticed that where roads do cross open fields and/or the cleared right-of-way extending vertically through the left center of the photograph, they occasionally become almost imperceptible except for linearity. It is also interesting to notice the gray-tone similarity between swamp and shoal water (where bottom is visible) in the large lakes. With the exception of gray-tones belonging to the deeper parts of the large lakes, the previous ranking shows all of the lowest gray-tone values to

be associated with forested areas. Of significance here are the similarities between open woods (deciduous) and tree rows, those forested areas generally lining roads or acting as property lines. The slight difference between these two values suggests that they might possibly have been grouped together in the original sampling categorization.

While there appears to be significant differentiation between all terrain types on the basis of gray-tone level, the following ranking of excursion frequencies may add additional information:

Open woods (coniferous)	4.12/in.
Cleared right-of-way	4.00/in.
Tree row	3.66/in.
Open field	3.52/in.
Dense woods (deciduous)	3.45/in.
Open woods (deciduous)	3.25/in.
Lake	3.24/in.
Dense woods (coniferous)	3.23/in.
Swamp	2.61/in.
Road	2.35/in.
Shoal water	1.79/in.

This ranking again points out the similarities between open field, tree row, and cleared right-of-way. While it might appear that open woods (coniferous) should also be included in such a grouping, the recollection of discrete trees with small crowns characteristic of a young pine forest will serve to explain the high excursion frequence noted. The mature deciduous forests exhibit similar frequencies while

the even-crowned nature of the planted coniferous stands produces a slightly lower frequency.

The diverse character of each of the various terrain types is demonstrated even further in the ranking of standard deviations:

Cleared right-of-way	12.18%
Shoal water	8.21%
Open woods (deciduous)	7.13%
Open woods (coniferous)	6.15%
Open field	5.76%
Road	5.70%
Dense woods (coniferous)	5.12%
Dense woods (deciduous)	4.99%
Swamp	4.85%
Lake	3.13%

The extreme range of data included in the calculation for the cleared right-of-way is produced by many different types of terrain which lie adjacent to and which are crossed by the cleared strip. Undoubtedly many of these diverse gray-tone levels will be removed during correction for rise time. The high standard deviation associated with shoal water results from the gray-tone gradient associated with it. As the water deepens and gray-tone decreases, a wide range of values is recorded for each occurrence. Both vegetative types of open woods exhibit similar ranges of gray-tone values, although they are widely separated by average gray-tone. This is indicative of small clearings associated with such forest patterns. Open fields and roads show similar

gray-tone ranges, and both types of dense woods have similar ranges of gray-tone, just as they have nearly identical average gray-tone levels. It is not extraordinary that the gray-tone range of swamp approximates that of dense woods (deciduous), since a considerable portion of the poorly drained lands have just that vegetative cover. The lakes, finally, exhibit their characteristically even-toned return, amplified by the lowest standard-deviation calculation.

Corrected Data: Panchromatic Image

The primary data was corrected for rise time using the same technique as discussed during the correction of the nine-lens multiband camera data.

Approximately the same general ordering of average gray-tone values is exhibited when the corrected data is ranked as follows:

Cleared right-of-way	67.5%
Road	59.6%
Open field	58.0%
Shoal water	54.4%
Swamp	50.5%
Open woods (deciduous)	45.4%
Dense woods (coniferous)	38.5%
Tree row	36.5%
Lake	36.0%
Open woods (coniferous)	34.8%
Dense woods (deciduous)	33.6%

In this ranking, the trio of cleared right-of-way, road, and open field still dominates the lighter gray-tones, although

their relative position is somewhat reversed. The remaining ranking remains generally the same, although relative positions have also changed somewhat among the forest-type occurrences. The general ordering of the terrain types with respect to corrected excursion frequencies also seems to have followed the same pattern as average gray-tone value. The basic ranking remains the same, but relative changes have taken place in conjunction with an increase in the range of values. The ranking of corrected excursion frequencies follows:

Cleared right-of-way	6.67/in.
Tree row	4.41/in.
Open woods (coniferous)	4.12/in.
Open field	3.64/in.
Dense woods (deciduous)	3.61/in.
Open woods (deciduous)	3.38/in.
Dense woods (coniferous)	3.38/in.
Lake	3.33/in.
Road	2.86/in.
Swamp	2.80/in.
Shoal water	1.96/in.

Even though several different terrain types now are listed as having the highest frequencies, it must be pointed out that these types have very few samples included in their calculations. This is especially critical in calculation of excursion frequencies, since one or two additional samples could produce much lower or higher frequencies. It is seen, nevertheless, that the basic ordering observed in the rank-

ing of uncorrected data is basically the same, although minor relative changes have occurred.

In the general ordering of the standard deviations of the corrected data, there has been an extreme contraction of the range of this variable, and a considerable reorganization. The ranking of the corrected standard deviations is as follows:

Open woods (deciduous)	6.47%
Shoal water	6.24%
Open woods (coniferous)	6.15%
Open field	5.34%
Dense woods (deciduous)	4.36%
Swamp	4.33%
Dense woods (coniferous)	4.11%
Road	3.95%
Tree row	2.81%
Cleared right-of-way	2.51%
Lake	2.26%

The most significant change in this ordering is, of course, the relative movement of the cleared right-of-way calculation from highest in uncorrected data to next to lowest in the corrected data. This again illustrates the mathematical instability of a calculation comprising only several samples. This ranking, as does the ranking of the corrected data, illustrates the wide range of gray-tone values contained in waveform segments of <u>both</u> vegetative types of open woods, the intermediate ranges of both types of dense woods, and the very low range of gray-tone values associated with segments of lake traverses.

Primary Data: Thermal Infrared Image

The primary sampling data and calculations for the thermal infrared image are also included in Appendix II. The same listing method and coding of waveform segments applies to this image as applied to the nine-lens multiband camera imagery and the panchromatic image.

Compiled Data: Thermal Infrared Image

As with the previous imagery, the data and calculations reorganized by terrain type are included in Appendix IV. The same totaling and averaging methods have been used in the analysis of this image.

The infrared image (see Fig. 9) and its waveforms (see Figs. 35, 36, and 37) exhibit the great diversity of gray-tone patterns illustrated by the comparable PAN image. Those gray-tones presented here, however, do not imply differences in reflected light as do the PAN gray-tones, but instead represent relative heat differences, with white and black representing relatively warmer and colder areas, respectively. It is interesting to note that three patterns discernible on the PAN image, shoal water, tree row, and cleared right-of-way, are not discernible on the IR image. The shoal water is not seen on the IR image because of the more complete mixing of warm waters within the lakes set up

during summer convectional movements. The tree rows are not seen because they are undoubtedly smaller than the instantaneous field-of-view (resolution) of this unclassified sensor, and the cleared right-of-way, while vaguely visible on the image itself, was not noticeable on any of the waveforms because of the boundary positions and contrasts in those areas where scan lines traversed it.

By contrast, however, the river is one of the prominent features of the infrared image, while it goes unnoticed on the PAN waveforms because of its similar gray-tone level and position within forested areas in the vicinity of its scan-line traverses. Another terrain-type category is also recognized on the IR image. On Line 1, a small stand of deciduous vegetation is found just to the left of Little Portage Lake. Since it lies on poorly drained soils, and is therefore different from the other deciduous occurrences, it has been called "swamp hardwoods," and its totals separated from both deciduous and swamp occurrences in the Appendices. Consequently, after omitting three terrain types and adding another, ten types are recognized on the IR image.

Re-emphasizing the nighttime origin of this infrared image, and keeping in mind the thermal significance of

the gray-tone level, the following ranking of average gray-tone levels as calculated from the primary sampling data provides a significant distribution:

River	68.7%
Lake	67.4%
Dense woods (coniferous)	61.6%
Road	57.8%
Dense woods (deciduous)	52.1%
Swamp hardwood	51.7%
Open woods (deciduous)	51.5%
Open field	37.5%
Open woods (coniferous)	35.2%
Swamp	31.8%

This distribution illustrates emphatically the meteorological phenomenon usually referred to as the "differential heating and cooling of land and water." It is seen that the water surfaces returned much higher temperatures at this late evening time than did the land surfaces. Interesting to note are the slightly higher temperatures in the Huron River. This is to be expected because of the lack of convectional circulation common to the lakes, allowing the river water to heat to a higher temperature during the long summer days.

One terrain type, dense woods (coniferous), appears to retain its higher temperature even though surrounding terrain types have cooled off considerably. A good example of this is seen on Line 2 of the IR image, occurrence-3. The high temperatures at this and similar locations occur

because the air space beneath the dense crowns of such vegetation acts as a heat sink during the day and as an insulator at night, creating the very even distribution of high temperatures recorded by the infrared scanner.

The closely grouped average gray-tone levels of dense woods (deciduous), swamp hardwoods, and open woods (deciduous) illustrate the similar physical character of each of these subtypes. They act as heat sinks also, but to a lesser degree because of the vertical stratification common to such stands, which permits faster loss of heat at night.

Also physically grouped together are the coolest terrain types, open field, open woods (coniferous), and swamp. The similar heating and cooling characteristics of these types result from their lack of insulating vertical stratification, plus easy access by advection currents, which import regional temperatures.

Excursion frequency, when calculated for a thermal infrared image, represents the local distribution of temperature fluctuations within a specific waveform segment. By this means, it gives an indication of the homogeneity of temperatures within a specific terrain type. It does not, however, indicate the magnitude of the fluctuation. The

following array of ranked excursion frequencies illustrates this significance:

Lake	3.76/in.
Open woods (coniferous)	3.64/in.
Dense woods (deciduous)	3.45/in.
Road	3.27/in.
Open field	3.20/in.
River	3.16/in.
Open woods (deciduous)	3.03/in.
Dense woods (coniferous)	2.86/in.
Swamp hardwoods	2.83/in.
Swamp	2.69/in.

This close grouping of excursion frequencies points out the frequent convectional temperature differences in the lakes, open woods (coniferous), and dense woods (deciduous) terrain types. It also illustrates the homogeneous temperatures characteristic of dense woods (coniferous), swamp hardwoods, and swamp, the latter two low frequencies being produced by the ameliorating effects of considerable soil moisture.

The magnitude of these temperature fluctuations is illustrated by the following order of standard deviations of gray-tone level fluctuations:

Swamp hardwoods	14.60%
Dense woods (deciduous)	10.98%
Open woods (deciduous)	8.54%
Swamp	7.57%
Open field	7.24%
Road	6.63%
Dense woods (coniferous)	5.99%
Open woods (coniferous)	5.92%
River	5.78%
Lake	3.50%

This ranking illustrates the larger temperature fluctuations associated with the three deciduous subtypes. In the case of swamp hardwoods, it becomes apparent that while a low excursion frequency exists, when fluctuations do occur they are very significant, pointing out the wet or dry characteristic expected of such a forest stand. Both coniferous terrain types show low magnitude of temperature fluctuation, emphasizing the even crown and homogeneous heights of planted coniferous forest plots. As would be theorized, both water types have the least range of temperature.

Corrected Data: Thermal Infrared Image

The compiled data was corrected for rise time using the same techniques concerning such corrections as previously discussed. An inspection of the following ranking of corrected average gray-tone levels illustrates characteristics of such corrected data as were previously noted:

River	68.7%
Lake	68.1%
Dense woods (coniferous)	63.0%
Road	60.3%
Dense woods (deciduous)	52.1%
Swamp hardwoods	51.7%
Open woods (deciduous)	51.5%
Open field	37.2%
Open woods (coniferous)	33.9%
Swamp	30.2%

A slight decrease in the range of the average gray-tone values is noted, but the order remains the same. This

latter characteristic indicates the stability of the relative thermal levels associated with each individual terrain type.

The ranking of excursion frequencies, as follows, however, shows minor changes:

Open woods (coniferous)	4.00/in.
Road	3.90/in.
Lake	3.85/in.
Dense woods (deciduous)	3.53/in.
Open field	3.30/in.
River	3.16/in.
Dense woods (coniferous)	3.12/in.
Open woods (deciduous).	3.03/in.
Swamp	3.01/in.
Swamp hardwoods	2.83/in.

The minor changes here involve a slight increase in the range of the data and a reordering of open woods (coniferous) and road terrain types. As was mentioned with reference to the PAN image, however, these two types involve few sampling points, and thus significant frequency changes are expected in conjunction with the elimination of only one or two samples. The remaining part of the array, however, is constant.

The elimination of a few sampling points from those terrain types having few primary samples also produces a reorganization of the array of standard deviations of gray-tone levels:

Swamp hardwoods	14.60%
Dense woods (deciduous)	10.73%

Open woods (deciduous)	8.54%
Open field	6.03%
River	5.78%
Swamp	5.40%
Open woods (coniferous)	4.08%
Dense woods (coniferous)	3.38%
Road	3.21%
Lake	1.81%

The road and river terrain types have exchanged approximate locations, as have open and dense woods (coniferous). The most notable change in the standard deviations, however, is the near-nullifying effect of lake-temperature fluctuation with the removal of several boundary rise-time-induced values.

Sensor Comparison Totals: Panchromatic and Thermal Infrared Images

In order to compare the utility of each image in discerning certain gray-tone patterns, the compiled data and corrected data have been grouped together for each type of sensor. Only the terrain types which appear simultaneously on both images are presented.

Table 5 presents the compiled data which has not been corrected for rise-time inaccuracies. The comparative interpretation of the average gray-tone levels depends on an overwhelming number of factors, such as time of day, season, climatological factors, etc. A large backlog of data would be needed to isolate any particular combination of variables

TABLE 5

SENSOR COMPARISON TOTALS BY TERRAIN TYPE: PANCHROMATIC AND THERMAL INFRARED IMAGES (PAIRED OCCURRENCES)

Terrain Type	Sensor	n	Σx	$\bar{x}$
Dense woods (deciduous)	PAN	111	4,137	37.3
	IR	152	7,922	52.1
Open woods (deciduous)	PAN	126	5,793	46.0
	IR	95	4,888	51.5
Swamp	PAN	66	3,330	50.5
	IR	53	1,686	31.8
Open field	PAN	278	16,090	57.9
	IR	265	9,940	37.5
Lake	PAN	93	3,369	36.2
	IR	123	8,291	67.4
Dense woods (coniferous)	PAN	83	3,266	39.3
	IR	87	5,357	61.6
Open woods (coniferous)	PAN	17	591	34.8
	IR	12	423	35.2
Road	PAN	8	458	57.2
	IR	26	1,504	57.8

TABLE 5.--Extension

Statistical Parameters								
E	L_x	L_s	$\bar{f}$	$\bar{f}_s$	$\bar{\lambda}$	$\bar{\lambda}_s$	$\overline{\lvert x-\bar{x}\rvert}$	s
43.0	12.45	8,634	3.45	12.76	0.29	201	4.21	4.99
51.0	14.80	10,272	3.45	12.76	0.29	201	9.19	10.98
40.0	12.30	8,536	3.25	12.02	0.31	215	5.85	7.13
28.0	9.25	6,420	3.03	11.21	0.33	229	7.15	8.54
17.5	6.70	4,649	2.61	9.66	0.38	264	4.01	4.85
14.0	5.20	3,608	2.69	9.95	0.37	257	5.55	7.57
96.0	27.25	18,914	3.52	13.02	0.28	194	4.61	5.76
83.0	25.95	17,974	3.20	11.84	0.31	215	5.81	7.24
29.5	9.10	6,315	3.24	11.99	0.31	215	2.10	3.13
47.0	12.50	8,675	3.76	13.91	0.27	187	2.26	3.50
26.0	8.05	5,586	3.23	11.95	0.31	215	4.10	5.66
25.0	8.75	6,073	2.86	10.58	0.35	243	4.26	5.99
7.0	1.70	1,180	4.12	15.24	0.24	167	5.12	6.15
4.0	1.10	763	3.64	13.47	0.27	187	4.83	5.92
2.0	0.85	590	2.35	8.70	0.43	298	4.85	5.70
8.0	2.45	1,701	3.27	12.10	0.31	215	5.52	6.63

dealing with gray-tones. As an example, while there is a complete gray-tone reversal for the lakes between the PAN and IR images, their gray-tones would be approximately similar if the infrared scanner had been used during the daytime. For this reason, it appears that the usefulness of gray-tone level comparisons is more restricted to simultaneously procured imagery.

Of great importance, however, are the similarities noted between the scale excursion frequencies. In all cases except for roads, the only cultural terrain-type category in this multispectral set, there appears to be some suggestion of natural terrain frequencies being demonstrated by the similar excursion frequencies.

With respect to the standard deviation of gray-tone levels, however, there is a general increase in the range of the gray-tone samples from PAN to IR. This suggests an increase in the amount of information available from the uncorrected gray-tone data on the infrared image.

Table 6 presents the corrected comparisons of the PAN and IR images. The gray-tone data still illustrates its dependence on a variety of factors, but the differences between the scale excursion frequencies have decreased with the elimination of rise-time inaccuracies, increasing their

TABLE 6

SENSOR COMPARISON TOTALS BY TERRAIN TYPE: PANCHROMATIC AND THERMAL INFRARED IMAGES (PAIRED OCCURRENCES; CORRECTED FOR RISE TIME)

Terrain Type	Sensor	n	Σx	$\bar{x}$
Dense woods (deciduous)	PAN	116	3,892	33.6
	IR	149	7,763	52.1
Open woods (deciduous)	PAN	122	5,544	45.4
	IR	95	4,888	51.5
Swamp	PAN	63	3,180	50.5
	IR	49	1,482	30.2
Open field	PAN	271	15,729	58.0
	IR	257	9,569	37.2
Lake	PAN	91	3,279	36.0
	IR	120	8,174	68.1
Dense woods (coniferous)	PAN	80	3,082	38.5
	IR	80	5,037	63.0
Open woods (coniferous)	PAN	17	591	34.8
	IR	11	373	33.9
Road	PAN	7	417	59.6
	IR	22	1,327	60.3

TABLE 6.--Extension

Statistical Parameters								
E	L_x	L_s	$\bar{f}$	$\bar{f}_s$	$\bar{\lambda}$	$\bar{\lambda}_s$	$\overline{\lvert x-\bar{x}\rvert}$	s
43.0	11.90	8,259	3.61	13.36	0.28	194	3.69	4.36
51.0	14.45	10,099	3.53	13.06	0.28	194	8.94	10.73
40.0	11.85	8,225	3.38	12.51	0.30	208	5.36	6.47
28.0	9.25	6,420	3.03	11.21	0.33	229	7.15	8.54
17.5	6.25	4,337	2.80	10.36	0.36	250	3.72	4.33
14.0	4.65	3,226	3.01	11.14	0.33	229	4.41	5.40
96.0	26.40	18,324	3.64	13.47	0.27	187	4.21	5.34
83.0	24.95	17,281	3.30	12.21	0.30	208	5.03	6.03
29.5	8.85	6,142	3.33	12.32	0.30	208	1.82	2.26
47.0	12.20	8,467	3.85	14.24	0.26	180	1.48	1.81
26.0	7.70	5,344	3.38	12.51	0.30	208	3.39	4.11
25.0	8.00	5,552	3.12	11.54	0.32	222	2.54	3.38
7.0	1.70	1,180	4.12	15.24	0.24	167	5.12	6.15
4.0	1.00	694	4.00	14.80	0.25	174	3.52	4.08
2.0	0.70	486	2.86	10.58	0.35	243	2.94	3.95
8.0	2.05	1,423	3.90	14.43	0.26	180	2.74	3.21

usefulness. A reduction in the ranges of data as presented by the standard deviations of the IR gray-tone samples, with the exception of dense woods (deciduous), has produced similar values for that variable for both sensors.

Analysis of Scale and Resolution Differences

The nine-lens multiband camera image was originally recorded at a scale of 1:10,000. An inspection of one of these images reveals that resolutions on the order of one foot are recorded. For example, notice that single tire tracks are reproduced on the Lens 4 image (see Fig. 5). This appears to be quite smaller than the resolving power of the television camera-waveform monitor system. The smallest measurement made was nine feet. Of course, as the size of the pattern being traversed increased, the percentage of error introduced through waveform measurement became smaller. As an example, measurement of the width of various roads crossed varied widely up to 100 percent, but the measurement of the paved parking lot varied only between 613 and 623 feet. It must be pointed out, however, that roads were traversed at all angles, and not always at right angles across minimum widths.

Originally photographed at contact scale of 1:20,000,

the photomosaic scaled to 1:24,400 reveals resolutions on the order of five or six feet. This can be verified by the identification of single isolated crowns of young conifers on the photograph (see Fig. 8). This resolution could not be matched by the video system, however, with approximately 20 feet being the minimum distance recorded. Because of rise-time inaccuracies and the IEEE frequency response selected, however, approximately 100 feet is the minimum distance reproducible on the waveform graph.

Although rescaled to the same size as the PAN image, the original IR image had a scale of 1:46,000. Because of security restrictions on the resolving capability of this instrument, only ground-scale resolutions on the order of 40 feet were possible.

This dimension is approximately the width of a paved road, and, as can be seen from the IR image (see Fig. 9), these roads can be identified only when they are oriented to the general direction of the scanning function, i.e., from top to bottom. In other cases, roads are distinguished by their function of field separations, etc. In no case did the minimum distance reproducible on the waveform monitor decrease to the resolution capability of the imagery. This may eventually necessitate the use of the "flat" frequency response previously described.

CHAPTER V

CONCLUSION

Summary

This study is the most recent in a series of continuing investigations into the feasibility and methodology associated with the objective measurement of geographic patterns and distributions using electronic instrumentation. The research objectives described at the onset of this report included: (1) the application and refinement of an electronic scanning technique; (2) the development of a waveform discrimination methodology; (3) the evaluation of this methodology; (4) an investigation of the utility of such techniques; and (5) the continuation of a long-range research program. A summary of the results of each of these investigations is included in the following pages.

The Scan-Line Technique

After the imagery to be included in the study was chosen, which included multispectral sets of nine-lens multiband camera imagery and panchromatic and thermal infrared

images, the problems of display, orientation, and consistent scan-line sampling were defined and solved. A consistent display methodology was developed by constructing templates capable of positioning the image at the same location and with the same orientation before the television camera. A variety of different electronic components were tested, with the advantages and disadvantages of each being presented. The best method of recording the scan-line waveform was also investigated, with various cameras, films, and exposures being tested. An experimental arrangement utilizing a conventional oscilloscope-type waveform monitor and compatible oscilloscope camera was finally chosen as the best combination. The particular waveform monitor was chosen because of its high-frequency response and brief rise-time characteristics, and the camera chosen because of its use of extremely fast film, permitting the recording of the smallest trace fluctuation.

Waveform Discrimination Methodology

A technique for identifying the particular waveform segments associated with specific occurrences of various types of geographic phenomena was developed. The results of this technique were transferred to a sampling framework and the average gray-tone level associated with each terrain-type

occurrence was calculated. Other calculations included the frequencies of waveform excursions and the mean and standard deviations of the sampled gray-tone data. These calculations were reviewed for each individual scan-line recorded, and the significant results presented.

It was pointed out that, with respect to the three nine-lens images sampled, the Lens 4 image provided the best results for identification and measurement of patterns recorded. Average gray-tone levels were indicative of different terrain types on each of the images, with excursion frequencies and gray-tone standard deviations providing back-up information for terrain-type discrimination purposes. The advantages of correcting the primary and compiled data for discrepancies introduced by rise-time differences were also reviewed and a comparison of the results and trends between different film-filter combinations was discussed.

Pattern discrimination on each of the separate panchromatic and thermal infrared images was also accomplished by calculating average gray-tone level. The advantages of combining this data with the results of excursion-frequency and standard-deviation calculations was also discussed. The problems concerning comparative waveform analysis of multi-sensor imagery procured at different times and under different conditions were also presented.

Methodology Evaluation

The accuracy of each individual technique and measurement was discussed in the respective section in which it was described and presented. In all techniques, however, an effort was made to retain dimensional and gray-tone stability and record these characteristics in an unbiased manner so that the most objective results could be achieved. This author feels that these characteristics were maintained to the degree possible with the instrumentation and techniques which were used. The basic agreement of the gray-tone calculations with visual inspection and the comparable excursion frequencies encountered between sensors indicate that this objectivity has been achieved.

The significant gap between methodology and usable analytic tool became apparent, however, when it was mentioned that a large mass of data must be accumulated before non-simultaneous multispectral sensor imagery can be validly compared. The following paragraph contains some of the ideas relevant to this problem.

Continuation of the Research

The analysis of the data and calculations presented in the various chapters of this report indicate the need for continuing research along several significant lines. First,

an effort must be made to procure significant amounts of representative simultaneous multispectral imagery which can be subjected to the same sort of waveform analysis. Second, different instruments capable of higher resolving and recording of phenomena displayed on such imagery must be tested and utilized. Third, additional techniques must be developed for recording spatial characteristics of distributions. These might include development of different sampling patterns, rotation of the imagery, or utilization of mathematical techniques such as line integrals. Additional research must also include the use of strip-chart recorders to alleviate the degradation of the waveforms by enlargement and recopying.

Potential Utilization of Waveform Analysis in Geographic Research

The most significant and immediate utilization of the techniques and methodology presented above might possibly be in the identification and inventory of outstanding geographic distributions such as forested areas, water bodies, urban areas, etc. After sufficient data has been accumulated, seasonal changes and annual trends of such distributions and their physical characteristics will be available for analysis.

Such techniques as have been developed will be used in the near future in an analysis of the instrumentation to be used in the resource-observing and measuring satellites. This analysis will include an examination of the resolution characteristics and gray-tone assemblages produced by the sensors to be used. This analysis will aid in the evolution of resolution and gray-tone pattern keys which can be used in conjunction with the video-type information which will be returned from these satellites.

Any number of potential utilizations of geographic pattern analysis can be imagined using such multispectral imagery interpretation techniques. This author hopes that such techniques as have been discussed and evaluated will prove helpful in extensive sampling and comparison of different earth environments.

APPENDICES

APPENDIX I

PRIMARY DATA: NINE-LENS MULTIBAND CAMERA IMAGERY

TABLE 7

PRIMARY DATA: FRAME 42, LENS 2, LINES 1 AND 2

Terrain Type	Waveform Segment	n	Σx	$\bar{x}$
Line 1				
Construction site	-1	74	4,842	65.4
Open field (grass)	-1	9	466	51.8
	-2	12	639	53.4
	-3	9	526	58.4
	-4	10	540	54.0
	-5	80	4,072	50.9
Paved road	-1	7	475	67.9
	-2	5	337	67.4
Unpaved road	-1	2	130	65.0
	-2	7	467	66.7
	-3	7	375	53.6
Line 2				
Open field (no cover)	-1	46	3,233	70.3
Paved parking lot	-1	67	4,733	70.6
Open field (grass)	-1	14	616	44.0
	-2	15	806	53.7
	-3	3	175	58.3
	-4	9	538	59.8
	-5	16	839	52.4
	-6	40	1,977	49.4
Unpaved road	-1	6	406	67.7
Paved road	-1	8	572	71.5
	-2	7	468	66.8

TABLE 7.--Extension

Statistical Parameters								
E	L_x	L_s	$\bar{f}$	$\bar{f}_s$	$\bar{\lambda}$	$\bar{\lambda}_s$	$\overline{\lvert x-\bar{x}\rvert}$	s
22.0	7.35	693	3.00	53.85	0.33	31	5.71	7.03
3.0	0.90	85	3.33	59.77	0.30	28	4.20	5.41
3.0	1.15	108	2.61	46.85	0.38	36	2.83	3.52
3.0	0.80	75	3.75	67.31	0.27	25	5.06	5.68
4.0	1.10	104	3.64	65.34	0.28	26	2.20	2.93
21.0	8.00	754	2.62	47.03	0.38	36	1.36	1.67
1.0	0.60	57	1.67	29.98	0.60	57	5.02	5.67
2.0	0.45	42	4.44	79.70	0.23	22	0.88	1.02
1.0	0.25	24	4.00	71.80	0.25	24	1.00	1.00
3.0	0.65	61	4.62	82.93	0.22	21	1.76	2.37
2.0	0.60	57	3.33	59.77	0.30	28	0.65	0.73
14.0	4.50	424	3.11	55.82	0.32	30	2.16	3.06
22.0	6.50	613	3.38	60.67	0.30	28	2.03	3.08
2.0	1.35	127	1.48	26.57	0.68	64	5.71	8.64
3.0	1.40	132	2.14	38.41	0.47	44	6.65	8.23
1.0	0.20	19	5.00	89.75	0.20	19	4.44	4.78
4.0	0.80	75	5.00	89.75	0.20	19	1.80	2.10
5.0	1.60	151	3.12	56.00	0.32	30	3.31	4.03
11.5	3.90	368	2.95	52.95	0.34	32	2.25	3.51
1.0	0.55	52	1.82	32.67	0.55	52	4.67	5.50
1.0	0.75	71	1.33	23.87	0.75	71	6.62	8.22
3.0	0.70	66	4.28	76.83	0.23	22	3.31	3.76

TABLE 8

PRIMARY DATA: FRAME 42, LENS 4, LINES 1 AND 2

Terrain Type	Waveform Segment	n	Σx	$\bar{x}$
Line 1				
Construction site	-1	73	3,258	44.6
Open field (grass)	-1	10	262	26.2
	-2	12	261	21.8
	-3	7	171	24.4
	-4	10	259	25.9
	-5	87	1,614	18.6
Unpaved road	-1	4	110	27.5
	-2	5	293	58.6
	-3	5	119	23.8
Paved road	-1	6	243	40.5
	-2	7	442	63.1
Line 2				
Open field (no cover)	-1	47	2,646	56.3
Paved parking lot	-1	66	3,191	48.3
Unpaved road	-1	5	233	46.6
Paved road	-1	7	323	46.1
	-2	4	200	50.0
Open field	-1	16	425	26.6
	-2	14	352	25.1
	-3	3	103	34.3
	-4	9	229	25.4
	-5	18	417	23.2
	-6	36	780	21.7

TABLE 8.--Extension

Statistical Parameters								
E	L_x	L_s	$\bar{f}$	$\bar{f}_s$	$\bar{\lambda}$	$\bar{\lambda}_s$	$\overline{\lvert x-\bar{x}\rvert}$	s
25.0	7.30	688	3.42	61.39	0.29	27	18.93	22.65
1.5	0.90	85	1.66	29.80	0.60	57	13.88	18.25
3.0	1.15	108	2.61	46.85	0.38	36	1.58	2.28
3.0	0.75	71	4.00	71.80	0.25	24	2.03	2.70
3.0	1.00	94	3.00	53.85	0.33	31	4.90	7.20
31.5	8.60	811	3.66	65.70	0.27	25	2.24	2.66
1.0	0.30	29	3.33	59.77	0.30	28	4.50	4.50
2.25	0.55	52	4.09	73.42	0.24	23	3.12	3.98
1.25	0.40	38	3.12	56.00	0.32	30	1.76	1.83
1.0	0.65	61	1.53	27.46	0.65	61	6.17	6.65
1.25	0.70	66	1.74	31.23	0.56	53	3.02	3.40
14.0	4.65	438	3.01	54.03	0.33	31	7.37	8.60
26.5	6.60	623	3.08	55.29	0.32	30	3.64	4.87
1.0	0.45	42	2.22	39.85	0.45	42	4.32	5.50
1.25	0.70	66	1.78	31.95	0.56	53	5.55	6.45
1.25	0.45	42	2.77	49.72	0.36	34	5.00	6.16
3.0	1.55	146	1.94	34.82	0.52	49	11.16	15.94
3.0	1.40	132	2.14	38.41	0.47	44	3.22	4.87
1.25	0.30	29	4.17	74.85	0.24	23	2.89	3.09
1.0	0.90	85	1.11	19.92	0.90	85	11.60	13.20
6.0	1.65	156	3.64	65.34	0.27	25	4.04	5.41
6.0	3.60	339	1.67	29.98	0.60	57	1.83	2.95

TABLE 9

PRIMARY DATA: FRAME 42, LENS 9, LINES 1 AND 2

Terrain Type	Waveform Segment	n	Σx	$\bar{x}$
Line 1				
Construction site	-1	75	1,234	16.4
Open field (grass)	-1	8	286	35.8
	-2	12	330	27.5
	-3	7	255	36.4
	-4	9	295	32.8
	-5	86	3,983	46.3
Unpaved road	-1	4	142	35.5
	-2	8	319	39.8
	-3	4	222	55.5
Paved road	-1	7	174	24.8
	-2	6	222	37.0
Line 2				
Open field (no cover)	-1	47	1,953	41.6
Paved parking lot	-1	66	1,388	21.0
Unpaved road	-1	7	173	24.7
Paved road	-1	12	392	32.7
	-2	8	156	19.5
Open field (grass)	-1	14	498	35.6
	-2	12	381	31.8
	-3	5	212	42.4
	-4	6	187	31.2
	-5	16	756	47.2
	-6	37	1,447	39.1

TABLE 9.--Extension

Statistical Parameters								
E	L_x	L_s	$\bar{f}$	$\bar{f}_s$	$\bar{\lambda}$	$\bar{\lambda}_s$	$\overline{\lvert x-\bar{x}\rvert}$	s
15.0	7.40	698	2.03	36.44	0.49	46	6.26	7.73
1.0	0.75	71	1.33	28.87	0.75	71	8.88	11.81
4.0	1.15	108	3.48	62.47	0.29	27	2.67	3.38
2.0	0.65	61	3.08	55.29	0.32	30	4.82	6.16
1.5	0.85	80	1.77	31.77	0.57	54	9.80	11.10
30.0	8.60	811	3.48	62.47	0.29	27	5.23	7.14
2.0	0.35	33	5.71	102.49	0.18	17	2.00	2.06
3.0	0.75	71	4.00	71.80	0.25	24	7.84	8.61
0.5	0.35	33	1.43	25.67	0.70	66	3.25	3.90
1.0	0.75	71	1.33	23.87	0.75	71	2.94	3.48
1.5	0.55	52	2.73	49.00	0.37	35	4.33	4.73
16.0	4.75	448	3.37	60.49	0.30	28	4.20	5.68
19.5	6.50	613	3.00	53.85	0.33	31	4.31	5.89
1.0	0.60	57	1.67	29.98	0.60	57	4.82	5.60
2.0	1.15	108	1.74	31.23	0.57	54	9.11	9.64
1.5	0.75	71	2.00	35.90	0.50	47	6.50	8.59
1.5	1.30	123	1.15	20.64	0.87	82	12.24	17.30
3.0	1.15	108	2.61	46.85	0.38	36	4.25	4.97
1.0	0.40	38	2.50	44.88	0.40	38	10.08	11.67
1.5	0.60	57	2.50	44.88	0.40	38	8.17	8.69
3.5	1.55	146	2.26	40.57	0.44	41	3.97	4.67
8.5	3.60	339	2.36	42.36	0.42	40	5.32	4.14

APPENDIX II

PRIMARY DATA: PANCHROMATIC AND THERMAL INFRARED IMAGES

TABLE 10

PRIMARY DATA: PANCHROMATIC IMAGE, LINE 1

Terrain Type	Waveform Segment	n	Σx	$\bar{x}$
Dense woods (deciduous)	-1	8	344	43.0
	-2	9	342	38.0
Open woods (deciduous)	-1	5	323	64.6
	-2	10	445	44.5
	-3	8	505	63.1
	-4	32	1,341	41.9
	-5	9	442	49.1
Open field	-1	4	277	69.2
	-2	6	376	62.7
	-3	31	1,642	53.0
	-4	5	316	63.2
	-5	15	799	53.3
Swamp	-1	7	318	45.4
	-2	16	711	44.4
Shoal water	-1	6	305	50.8
	-2	2	125	62.5
	-3	4	175	43.7
	-4	7	364	52.0
	-5	9	542	60.2
Lake	-1	21	936	44.6
	-2	19	772	40.6
	-3	45	1,436	31.9
	-4	8	225	28.1

TABLE 10.--Extension

Statistical Parameters								
E	L_x	L_s	$\bar{f}$	$\bar{f}_s$	$\bar{\lambda}$	$\bar{\lambda}_s$	$\overline{\lvert x-\bar{x}\rvert}$	s
1.5	0.75	520	2.00	7.40	0.50	347	4.75	5.36
1.5	0.80	555	1.88	6.96	0.53	368	2.33	2.92
2.0	0.55	382	3.64	13.45	0.27	187	4.32	4.54
3.0	0.90	624	3.33	12.30	0.30	208	8.50	10.74
1.5	0.70	486	2.14	7.92	0.47	326	8.38	9.78
11.0	3.20	2,221	3.44	12.72	0.29	201	6.34	7.72
3.5	0.85	590	4.12	15.25	0.24	167	3.93	5.04
2.0	0.30	208	6.67	24.70	0.15	104	1.38	1.64
1.0	0.60	416	1.67	6.18	0.60	416	2.78	3.20
11.5	3.15	2,186	3.65	13.50	0.27	187	7.13	9.17
1.0	0.40	278	2.50	9.25	0.40	278	5.76	6.76
3.5	1.40	972	2.50	9.25	0.40	278	5.68	7.08
1.0	0.65	451	1.30	4.81	0.77	534	5.63	6.39
4.0	1.80	1,249	2.22	8.21	0.45	312	1.81	2.18
1.0	0.55	382	1.82	6.74	0.55	382	5.11	6.09
1.0	0.35	243	2.86	12.95	0.35	243	2.50	2.50
0.5	0.35	243	1.43	5.29	0.70	486	3.38	4.15
1.5	0.75	520	2.00	7.40	0.50	347	6.00	7.80
1.0	0.80	555	1.25	4.63	0.80	555	10.15	13.03
8.5	2.05	1,423	4.15	15.35	0.24	167	2.46	2.74
6.0	1.80	1,249	3.33	12.30	0.30	208	2.24	3.23
13.5	4.50	3,123	3.00	11.10	0.33	229	1.82	3.33
1.5	0.75	520	2.00	7.40	0.50	347	2.41	2.76

TABLE 11

PRIMARY DATA: PANCHROMATIC IMAGE, LINE 2

Terrain Type	Waveform Segment	n	Σx	$\bar{x}$
Dense woods (deciduous)	-1	10	286	28.6
	-2	12	362	30.2
Dense woods (coniferous)	-1	37	1,517	41.0
	-2	28	1,144	40.9
	-3	9	348	38.7
Open woods (deciduous)	-1	15	694	46.3
	-2	11	462	42.0
	-3	13	495	38.1
Swamp	-1	16	952	59.5
Tree row	-1	3	192	64.0
	-2	3	155	51.2
	-3	3	113	37.7
	-4	5	148	29.6
Open field	-1	33	2,172	65.8
	-2	9	619	68.8
	-3	19	1,285	67.6
	-4	2	123	61.5
	-5	4	206	51.5
	-6	9	525	58.3
	-7	17	874	51.4
	-8	13	484	37.2
Road	-1	5	266	53.2
Cleared right-of-way	-1	3	177	59.0

TABLE 11.--Extension

Statistical Parameters								
E	L_x	L_s	$\bar{f}$	$\bar{f}_s$	$\bar{\lambda}$	$\bar{\lambda}_s$	$\overline{\lvert x-\bar{x}\rvert}$	s
2.5	1.55	1,076	1.61	5.96	0.62	430	2.12	2.58
7.0	1.20	833	5.83	21.60	0.17	118	7.06	8.15
12.0	3.70	2,568	3.24	11.96	0.31	215	3.57	4.86
11.5	2.75	1,908	4.18	15.45	0.24	167	4.47	6.54
1.0	0.80	555	1.25	4.63	0.80	555	6.30	8.50
5.0	1.50	1,041	3.33	12.30	0.30	208	5.25	6.39
4.0	1.05	729	3.81	14.10	0.26	180	3.64	4.82
3.5	1.30	902	2.69	9.95	0.37	257	4.40	5.25
4.0	1.65	1,145	2.42	8.95	0.41	285	3.62	4.21
1.0	0.20	139	5.00	18.50	0.20	139	4.00	4.32
1.0	0.25	174	4.00	14.80	0.25	174	9.56	10.34
1.0	0.30	208	3.33	12.30	0.30	208	8.22	9.18
1.0	0.45	312	2.22	8.21	0.45	312	2.88	3.20
14.0	3.20	2,221	4.38	16.20	0.23	160	2.43	2.92
3.0	0.90	625	3.33	12.30	0.30	208	1.14	1.32
5.5	1.85	1,284	2.97	11.00	0.34	236	3.24	5.29
1.0	0.25	174	4.00	14.80	0.25	174	5.50	5.50
1.0	0.35	243	2.86	10.58	0.35	243	4.50	5.17
3.0	0.85	590	3.53	13.07	0.28	194	10.67	13.28
5.5	1.75	1,214	3.14	11.60	0.32	222	3.80	4.23
3.0	1.25	868	2.40	8.85	0.42	291	7.05	8.62
1.0	0.45	312	2.22	8.21	0.45	312	5.76	6.72
1.0	0.25	174	4.00	14.80	0.25	174	11.33	12.18

TABLE 12

PRIMARY DATA: PANCHROMATIC IMAGE, LINE 3

Terrain Type	Waveform Segment	n	Σx	$\bar{x}$
Dense woods (deciduous)	-1	37	1,322	35.7
	-2	30	987	32.9
	-3	15	494	32.9
Dense woods (coniferous)	-1	9	257	28.6
Open woods (deciduous)	-1	15	677	45.1
	-2	8	409	51.1
Open woods (coniferous)	-1	8	287	35.9
	-2	9	304	33.8
Swamp	-1	18	1,031	57.3
	-2	9	318	35.3
Tree row	-1	3	112	37.3
	-2	2	94	47.0
	-3	2	66	33.0
Open field	-1	10	681	68.1
	-2	25	1,577	63.1
	-3	7	374	53.4
	-4	12	800	66.7
	-5	6	363	60.5
	-6	5	263	52.6
	-7	17	876	51.5
	-8	5	235	47.0
	-9	24	1,223	51.0
Road	-1	3	192	64.0

TABLE 12.--Extension

Statistical Parameters								
E	L_x	L_s	$\bar{f}$	$\bar{f}_s$	$\bar{\lambda}$	$\bar{\lambda}_s$	$\overline{\lvert x-\bar{x}\rvert}$	s
15.5	3.70	2,568	4.19	15.50	0.24	167	3.81	4.96
10.0	2.95	2,047	3.39	12.35	0.30	208	4.63	5.41
5.0	1.50	1,041	3.33	12.30	0.30	208	3.81	4.49
1.5	0.80	555	1.88	6.96	0.53	368	2.96	3.37
3.5	1.45	1,006	2.41	8.91	0.42	291	6.66	8.17
3.0	0.80	555	3.75	13.85	0.27	187	6.12	7.18
4.0	0.80	555	5.00	18.50	0.20	139	4.66	5.46
3.0	0.90	625	3.33	12.30	0.30	208	5.53	6.76
7.0	1.75	1,214	4.00	14.80	0.25	174	4.98	6.32
1.5	0.85	590	1.76	6.51	0.57	396	5.93	6.63
1.5	0.30	208	5.00	18.50	0.20	139	2.89	3.30
1.0	0.25	174	4.00	14.80	0.25	174	3.00	3.00
1.0	0.30	208	3.33	12.30	0.30	208	2.00	2.00
5.0	0.95	659	5.26	19.45	0.19	132	1.48	1.81
11.0	2.55	1,770	4.31	15.95	0.23	160	2.56	3.43
3.0	0.75	520	4.00	14.80	0.25	174	1.92	2.77
5.0	1.25	868	4.00	14.80	0.25	174	1.44	2.06
1.5	0.55	382	2.73	10.10	0.37	257	5.17	6.13
2.0	0.50	347	4.00	14.80	0.25	174	4.48	5.99
4.5	1.70	1,180	2.65	9.81	0.38	264	6.32	7.46
1.0	0.40	278	2.50	9.25	0.40	278	6.00	7.13
8.0	2.35	1,631	3.40	12.58	0.29	201	7.96	9.62
1.0	0.40	278	2.50	9.25	0.40	278	3.33	4.00

TABLE 13

PRIMARY DATA: THERMAL INFRARED IMAGE, LINE 1

Terrain Type	Waveform Segment	n	$\sum x$	$\bar{x}$
Lake	-1	33	2,341	70.9
	-2	31	1,998	64.5
	-3	56	3,777	67.4
River	-1	4	281	70.2
Open woods (deciduous)	-1	6	400	66.7
	-2	12	813	67.8
	-3	9	459	51.0
	-4	6	277	46.2
Swamp	-1	9	259	28.8
Swamp hardwoods	-1	21	1,086	51.7
Open field	-1	7	418	59.7
	-2	16	860	53.8
	-3	9	635	70.6
	-4	20	858	42.9
	-5	9	335	37.2
Dense woods (deciduous)	-1	8	609	76.1
	-2	7	288	41.1
	-3	6	381	63.5
	-4	10	625	62.5

TABLE 13.--Extension

Statistical Parameters								
E	L_x	L_s	$\bar{f}$	$\bar{f}_s$	$\bar{\lambda}$	$\bar{\lambda}_s$	$\overline{\lvert x-\bar{x}\rvert}$	s
12.5	3.25	2,256	3.85	14.25	0.26	180	1.64	2.01
10.0	3.15	2,186	3.17	11.74	0.32	222	4,28	8.40
23.5	5.80	4,025	4.05	15.00	0.25	174	1.25	1.47
1.0	0.40	278	2.50	9.25	0.40	278	1.62	1.92
2.0	0.55	382	3.64	13.45	0.27	187	1.22	1.37
3.0	1.20	833	2.50	9.25	0.40	278	1.62	2.13
3.0	0.90	625	3.33	12.30	0.30	208	8.89	10.04
1.0	0.50	347	2.00	7.40	0.50	347	7.22	8.61
1.5	0.85	590	1.76	6.51	0.57	396	7.26	9.44
6.0	2.10	1,457	2.83	10.54	0.35	243	12.33	14.60
2.5	0.70	486	3.57	13.20	0.28	194	7.47	8.68
6.0	1.65	1,145	3.64	13.45	0.27	187	7.78	9.38
1.5	0.85	590	1.76	6.51	0.57	396	1.70	2.11
8.0	1.95	1,353	4.10	15.15	0.24	167	7.07	8.07
1.5	0.80	555	1.88	6.95	0.53	368	8.69	10.39
3.0	0.80	555	3.75	13.88	0.27	187	2.62	3.59
1.5	0.70	486	2.14	7.92	0.47	326	4.45	5.46
1.0	0.50	347	2.00	7.40	0.50	347	2.17	2.36
3.0	0.90	625	3.33	12.30	0.30	208	4.30	5.97

TABLE 14

PRIMARY DATA: THERMAL INFRARED IMAGE, LINE 2

Terrain Type	Waveform Segment	n	$\sum x$	$\bar{x}$
River	-1	4	244	61.0
Dense woods (deciduous)	-1	20	914	45.7
	-2	14	510	36.4
Open woods (deciduous)	-1	15	545	36.3
	-2	8	321	40.1
	-3	6	188	31.3
	-4	24	1,254	52.2
Swamp	-1	11	396	36.0
	-2	6	178	29.7
Dense woods (coniferous)	-1	5	368	73.6
	-2	4	320	80.0
	-3	32	2,137	66.8
	-4	19	1,157	60.9
	-5	15	846	56.4
Road	-1	3	121	40.3
	-2	5	315	63.0
	-3	4	251	62.8
	-4	4	241	60.2
	-5	2	107	53.5
Open field	-1	10	316	31.6
	-2	10	409	40.9
	-3	5	347	69.4
	-4	19	450	23.7
	-5	2	74	37.0
	-6	8	259	32.4
	-7	8	334	41.8
	-8	15	439	28.6
	-9	3	80	26.7
	-10	4	118	29.5

TABLE 14.--Extension

Statistical Parameters								
E	L_x	L_s	$\bar{f}$	$\bar{f}_s$	$\bar{\lambda}$	$\bar{\lambda}_s$	$\overline{\lvert x-\bar{x}\rvert}$	s
1.0	0.30	208	3.33	12.30	0.30	208	9.50	11.51
5.5	1.90	1,319	2.90	10.70	0.34	236	7.67	8.99
4.5	1.35	937	3.33	12.30	0.30	208	8.86	11.65
4.0	1.45	1,006	2.76	10.20	0.36	250	11.02	13.93
1.5	0.80	555	1.88	6.94	0.53	368	3.66	4.62
2.0	0.65	451	3.08	11.38	0.32	222	6.33	6.97
7.5	2.35	1,631	3.19	11.75	0.31	215	10.96	12.27
3.0	1.05	729	2.86	10.57	0.35	243	7.82	10.57
3.0	0.60	416	5.00	18.50	0.20	139	1.22	1.60
1.0	0.55	382	1.82	6.73	0.55	382	6.88	7.81
1.0	0.45	312	2.22	8.22	0.45	312	2.00	2.45
9.5	3.25	2,256	2.92	10.80	0.34	236	2.70	4.11
5.0	1.85	1,284	2.70	10.00	0.37	257	6.38	9.79
5.0	1.45	1,006	3.45	12.73	0.29	201	5.33	6.55
1.0	0.25	174	4.00	14.70	0.25	174	1.56	1.70
2.0	0.45	312	4.44	16.42	0.22	153	9.60	11.68
1.0	0.35	243	2.86	10.58	0.35	243	1.38	1.64
1.0	0.40	278	2.50	9.25	0.40	278	5.75	6.94
1.0	0.25	174	4.00	14.70	0.25	174	3.50	3.50
3.5	1.00	694	3.50	12.95	0.28	194	2.60	2.90
3.0	0.95	625	3.15	11.65	0.32	222	1.94	2.62
1.0	0.45	312	2.22	8.22	0.45	312	4.48	5.04
6.0	1.80	1,249	3.33	12.30	0.30	208	5.21	7.62
1.0	0.20	139	5.00	18.50	0.20	139	2.00	2.00
3.0	0.80	555	3.75	13.87	0.27	187	4.97	6.87
3.0	0.80	555	3.75	13.87	0.27	187	8.69	9.43
3.5	1.45	1,006	2.41	8.93	0.41	285	9.74	11.45
1.0	0.35	243	2.86	10.58	0.35	243	1.11	1.25
1.0	0.35	243	2.86	10.58	0.35	243	6.75	8.20

TABLE 15

PRIMARY DATA: THERMAL INFRARED IMAGE, LINE 3

Terrain Type	Waveform Segment	n	Σx	$\bar{x}$
Dense woods (deciduous)	-1	46	2,516	54.7
	-2	24	1,325	55.2
	-3	17	754	44.0
Dense woods (coniferous)	-1	12	529	44.1
Open woods (coniferous)	-1	12	423	35.2
River	-1	3	231	77.0
Open field	-1	15	428	28.5
	-2	13	611	47.0
	-3	15	424	28.3
	-4	16	328	20.5
	-5	14	283	20.2
	-6	22	1,274	57.9
	-7	25	660	26.4
Open woods (deciduous)	-1	9	631	70.1
Lake	-1	3	175	58.3
Road	-1	3	150	50.0
	-2	5	319	63.8
Swamp	-1	17	577	33.9
	-2	10	276	26.7

TABLE 15.--Extension

Statistical Parameters								
E	L_x	L_s	$\bar{f}$	$\bar{f}_s$	$\bar{\lambda}$	$\bar{\lambda}_s$	$\overline{\lvert x-\bar{x}\rvert}$	s
21.0	4.55	3,158	4.62	17.10	0.22	153	12.11	14.09
6.5	2.45	1,700	2.65	9.80	0.38	264	11.42	13.77
5.0	1.65	1,145	3.03	11.20	0.33	229	10.59	12.20
3.5	1.20	833	2.92	10.80	0.34	236	3.40	4.75
4.0	1.10	763	3.64	13.47	0.27	187	4.83	5.92
1.0	0.25	174	4.00	14.80	0.25	174	2.67	3.27
5.5	1.45	1,006	3.79	13.65	0.26	181	1.89	2.73
2.5	1.30	902	1.92	7.11	0.52	361	8.77	10.09
5.5	1.55	1,076	3.55	13.15	0.28	194	7.56	9.84
5.0	1.55	1,076	3.23	11.92	0.31	215	5.00	7.00
3.5	1.40	971	2.50	9.25	0.40	278	4.76	7.78
7.0	2.20	1,527	3.18	11.77	0.31	215	9.12	10.65
8.5	2.40	1,666	3.54	13.10	0.28	194	2.74	3.69
4.0	0.85	590	4.71	17.40	0.21	146	3.68	5.91
1.0	0.30	208	3.33	12.30	0.30	208	6.89	7.32
1.0	0.30	208	3.33	12.30	0.30	208	8.67	10.23
1.0	0.45	312	2.22	8.22	0.45	312	5.84	7.35
3.5	1.75	1,214	2.00	7.40	0.50	347	7.70	8.95
3.0	0.95	659	3.16	11.67	0.32	222	3.14	3.82

APPENDIX III

TERRAIN-TYPE COMPILATIONS: NINE-LENS MULTIBAND CAMERA IMAGERY

TABLE 16

TERRAIN-TYPE COMPILATIONS: FRAME 42, LENS 2, LINES 1 AND 2

Terrain Type	Waveform Segment	n	Σx	$\bar{x}$
Construction site	L1-1	74	4,842	65.4
Open field (grass)	L1-1	9	466	51.8
	-2	12	639	53.4
	-3	9	526	58.4
	-4	10	540	54.0
	-5	80	4,072	50.9
	L2-1	14	616	44.0
	-2	15	806	53.7
	-3	3	175	58.3
	-4	9	538	59.8
	-5	16	839	52.4
	-6	40	1,977	49.4
Totals		217	11,194	51.6
Paved road	L1-1	7	475	67.9
	-2	5	337	67.4
	L2-1	8	572	71.5
	-2	7	468	66.8
Totals		27	1,852	68.6
Unpaved road	L1-1	2	130	65.0
	-2	7	467	66.7
	-3	7	375	53.6
	L2-1	6	406	67.7
Totals		22	1,378	62.6
Open field (no cover)	L2-1	46	3,233	70.3
Paved parking lot	L2-1	67	4,733	70.6

TABLE 16.--Extension

Statistical Parameters								
E	L_x	L_s	$\bar{f}$	$\bar{f}_s$	$\bar{\lambda}$	$\bar{\lambda}_s$	$\overline{\lvert x-\bar{x}\rvert}$	s
22.0	7.35	693	3.00	53.85	0.33	31	5.71	7.03
3.0	0.90	85	3.33	59.77	0.30	28	4.20	5.41
3.0	1.15	108	2.61	46.85	0.38	36	2.83	3.52
3.0	0.80	75	3.75	67.31	0.27	25	5.06	5.70
4.0	1.10	104	3.64	65.34	0.28	26	2.20	2.93
21.0	8.00	754	2.62	47.03	0.38	36	1.36	1.67
2.0	1.35	127	1.48	26.57	0.68	64	5.71	8.64
3.0	1.40	132	2.14	38.41	0.47	44	6.65	8.23
1.0	0.20	19	5.00	89.75	0.20	19	4.44	4.78
4.0	0.80	75	5.00	89.75	0.20	19	1.80	2.10
5.0	1.60	151	3.12	56.00	0.32	30	3.31	4.03
11.5	3.90	368	2.95	52.95	0.34	32	2.25	3.51
60.5	21.20	1,998	2.85	51.16	0.35	33	2.77	3.63
1.0	0.60	57	1.67	29.98	0.60	57	5.02	5.67
2.0	0.45	42	4.44	79.70	0.23	22	0.88	1.02
1.0	0.75	71	1.33	23.87	0.75	71	6.62	8.22
3.0	0.70	66	4.28	76.83	0.23	22	3.31	3.76
7.0	2.50	236	2.80	50.26	0.36	34	4.28	5.07
1.0	0.25	24	4.00	71.80	0.25	24	1.00	1.00
3.0	0.65	61	4.62	82.93	0.22	21	1.76	2.37
2.0	0.60	57	3.33	59.77	0.30	28	0.65	0.73
1.0	0.55	52	1.82	32.67	0.55	52	4.67	5.50
7.0	2.05	194	3.41	61.21	0.29	27	2.13	2.58
14.0	4.50	424	3.11	55.82	0.32	30	2.16	3.06
22.0	6.50	613	3.38	60.67	0.30	28	2.03	3.08

TABLE 17

TERRAIN-TYPE COMPILATIONS: FRAME 42, LENS 4, LINES 1 AND 2

Terrain Type	Waveform Segment	n	Σx	$\bar{x}$
Construction site	L1-1	73	3,258	44.6
Open field (grass)	L1-1	10	262	26.2
	-2	12	261	21.8
	-3	7	171	24.4
	-4	10	259	25.9
	-5	87	1,614	18.6
	L2-1	16	425	26.6
	-2	14	352	25.1
	-3	3	103	34.3
	-4	9	229	25.4
	-5	18	417	23.2
	-6	36	780	21.7
Totals		222	4,873	22.0
Unpaved road	L1-1	4	110	27.5
	-2	5	293	58.6
	-3	5	119	23.8
	L2-1	5	223	46.6
Totals		19	745	39.2
Paved road	L1-1	6	243	40.5
	-2	7	442	63.1
	L2-1	7	323	46.1
	-2	4	200	50.0
Totals		24	1,208	50.3
Open field (no cover)	L2-1	47	2,646	56.3
Paved parking lot	L2-1	66	3,191	48.3

TABLE 17.--Extension

Statistical Parameters								
E	L_x	L_s	$\bar{f}$	$\bar{f}_s$	$\bar{\lambda}$	$\bar{\lambda}_s$	$\overline{\lvert x-\bar{x}\rvert}$	s
25.0	7.30	688	3.42	61.39	0.29	27	18.93	22.65
1.5	0.90	85	1.66	29.80	0.60	57	13.88	18.25
3.0	1.15	108	2.61	46.85	0.38	36	1.58	2.28
3.0	0.75	71	4.00	71.80	0.25	24	2.03	2.70
3.0	1.00	94	3.00	53.85	0.33	31	4.90	7.20
31.5	8.60	811	3.66	65.70	0.27	25	2.24	2.66
3.0	1.55	146	1.94	34.82	0.52	49	11.16	15.94
3.0	1.40	132	2.14	38.41	0.47	44	3.22	4.87
1.25	0.30	29	4.17	74.85	0.24	23	2.89	3.09
1.0	0.90	85	1.11	19.92	0.90	85	11.60	13.20
6.0	1.65	156	3.64	65.34	0.27	25	4.04	5.41
6.0	3.60	339	1.67	29.98	0.60	57	1.83	2.95
62.25	21.80	2,056	2.86	51.34	0.35	33	4.01	5.35
1.0	0.30	29	3.33	59.77	0.30	28	4.50	4.50
2.25	0.55	52	4.09	73.42	0.34	23	3.12	3.98
1.25	0.40	38	3.12	56.00	0.32	30	1.76	1.83
1.0	0.45	42	2.22	39.85	0.45	42	4.32	5.50
5.5	1.70	161	3.24	58.16	0.31	29	3.37	3.92
1.0	0.65	61	1.53	27.46	0.65	61	6.17	6.65
1.25	0.70	66	1.74	31.23	0.56	53	3.02	3.40
1.25	0.70	66	1.78	31.95	0.56	53	5.55	6.45
1.25	0.45	42	2.77	49.72	0.36	34	5.00	6.16
4.75	2.50	235	1.90	34.10	0.53	50	4.88	5.56
14.0	4.65	438	3.01	54.03	0.33	31	7.37	8.60
26.5	6.60	623	3.08	55.29	0.32	30	3.64	4.87

TABLE 18

TERRAIN-TYPE COMPILATIONS: FRAME 42, LENS 9, LINES 1 AND 2

Terrain Type	Waveform Segment	n	$\sum x$	$\bar{x}$
Construction site	L1-1	75	1,234	16.4
Open field (grass)	L1-1	8	286	35.8
	-2	12	330	27.5
	-3	7	255	36.4
	-4	9	295	32.8
	-5	86	3,983	46.3
	L2-1	14	498	35.6
	-2	12	381	31.8
	-3	5	212	42.4
	-4	6	187	31.2
	-5	16	756	47.2
	-6	37	1,447	39.1
Totals		212	8,630	40.7
Unpaved road	L1-1	4	142	35.5
	-2	8	319	39.8
	-3	4	222	55.5
	L2-1	7	173	24.7
Totals		23	856	37.2
Paved road	L1-1	7	174	24.8
	-2	6	222	37.0
	L2-1	12	392	32.7
	-2	8	156	19.5
Totals		33	944	28.6
Open field (no cover)	L2-1	47	1,953	41.6
Paved parking lot	L2-1	66	1,388	21.0

TABLE 18.--Extension

Statistical Parameters								
E	L_x	L_s	$\bar{f}$	$\bar{f}_s$	$\bar{\lambda}$	$\bar{\lambda}_s$	$\overline{\lvert x-\bar{x}\rvert}$	s
15.0	7.40	698	2.03	36.44	0.49	46	6.26	7.73
1.0	0.75	71	1.33	28.87	0.75	71	8.88	11.81
4.0	1.15	108	3.48	62.47	0.29	27	2.67	3.38
2.0	0.65	61	3.08	55.29	0.32	30	4.82	6.16
1.5	0.85	80	1.77	31.77	0.57	54	9.80	11.10
30.0	8.60	811	3.48	62.47	0.29	27	5.23	7.14
1.5	1.30	123	1.15	20.64	0.87	82	12.24	17.30
3.0	1.15	108	2.61	46.85	0.38	36	4.25	4.97
1.0	0.40	38	2.50	44.88	0.40	38	10.08	11.67
1.5	0.60	57	2.50	44.88	0.40	38	8.17	8.69
3.5	1.55	147	2.26	40.57	0.44	41	3.97	4.67
8.5	3.60	339	2.36	42.36	0.42	40	4.14	5.32
57.5	20.60	1,943	2.79	50.08	0.36	34	5.72	7.43
2.0	0.35	33	5.71	102.49	0.18	17	2.00	2.06
3.0	0.75	71	4.00	71.80	0.25	24	7.84	8.61
0.5	0.35	33	1.43	25.67	0.70	66	3.25	3.90
1.0	0.60	57	1.67	29.98	0.60	57	4.82	5.60
6.5	2.05	194	3.17	56.90	0.32	30	5.11	5.74
1.0	0.75	71	1.33	23.87	0.75	71	2.94	3.48
1.5	0.55	52	2.73	49.00	0.37	35	4.33	4.73
2.0	1.15	108	1.74	31.23	0.57	54	9.11	9.64
1.5	0.75	71	2.00	35.90	0.50	47	6.50	8.59
6.0	3.20	302	1.88	33.75	0.53	50	6.30	7.19
16.0	4.75	448	3.37	60.49	0.30	28	4.20	5.68
19.5	6.50	613	3.00	53.85	0.33	31	4.31	5.89

APPENDIX IV

TERRAIN-TYPE COMPILATIONS: PANCHROMATIC AND THERMAL INFRARED IMAGES

TABLE 19

TERRAIN-TYPE COMPILATIONS: PANCHROMATIC IMAGE, ALL LINES

Terrain Type	Waveform Segment	n	Σx	$\bar{x}$
Open field	PAN 1-1	4	277	69.2
	-2	6	376	62.7
	-3	31	1,642	53.0
	-4	5	316	63.2
	-5	15	799	53.2
	PAN 2-1	33	2,172	65.8
	-2	9	619	68.8
	-3	19	1,285	67.6
	-4	2	123	61.5
	-5	4	206	51.5
	-6	9	525	58.3
	-7	17	874	51.4
	-8	13	484	37.2
	PAN 3-1	10	681	68.1
	-2	25	1,577	63.1
	-3	7	374	53.4
	-4	12	800	66.7
	-5	6	363	60.5
	-6	5	263	52.6
	-7	17	876	51.5
	-8	5	235	47.0
	-9	24	1,223	51.0
Totals		278	16,090	57.9
Shoal water	PAN 1-1	6	305	50.8
	-2	2	125	62.5
	-3	4	175	43.7
	-4	7	364	52.0
	-5	9	542	60.2
Totals		28	1,511	54.0
Lake	PAN 1-1	21	936	44.6
	-2	19	772	40.6
	-3	45	1,436	31.9
	-4	8	225	28.1
Totals		93	3,369	36.2

TABLE 19.--Extension

Statistical Parameters								
E	L_x	L_s	$\bar{f}$	$\bar{f}_s$	$\bar{\lambda}$	$\bar{\lambda}_s$	$\overline{\lvert x-\bar{x}\rvert}$	s
2.0	0.30	208	6.67	24.70	0.15	104	1.38	1.64
1.0	0.60	416	1.67	6.18	0.60	416	2.78	3.20
11.5	3.15	2,186	3.65	13.50	0.27	187	7.13	9.17
1.0	0.40	278	2.50	9.25	0.40	278	5.76	6.76
3.5	1.40	972	2.50	9.25	0.40	278	5.68	7.08
14.0	3.20	2,221	4.38	16.20	0.23	160	2.43	2.92
3.0	0.90	625	3.33	12.30	0.30	208	1.14	1.32
5.5	1.85	1,284	2.97	11.00	0.34	236	3.24	5.29
1.0	0.25	174	4.00	14.80	0.25	174	5.50	5.50
1.0	0.35	243	2.86	10.58	0.35	243	4.50	5.17
3.0	0.85	590	3.53	13.07	0.28	194	10.67	13.28
5.5	1.75	1,214	3.14	11.60	0.32	222	3.80	4.23
3.0	1.25	868	2.40	8.88	0.42	291	7.05	8.62
5.0	0.95	659	5.26	19.45	0.19	132	1.48	1.81
11.0	2.55	1,770	4.31	15.95	0.23	160	2.56	3.43
3.0	0.75	520	4.00	14.80	0.25	174	1.92	2.77
5.0	1.25	868	4.00	14.80	0.25	174	1.44	2.06
1.5	0.55	382	2.73	10.10	0.37	257	5.17	6.13
2.0	0.50	347	4.00	14.80	0.25	174	4.48	5.99
4.5	1.70	1,180	2.65	9.81	0.38	264	6.32	7.46
1.0	0.40	278	2.50	9.25	0.40	278	6.00	7.13
8.0	2.35	1,631	3.40	12.58	0.29	201	7.96	9.62
96.0	27.25	18,914	3.52	13.02	0.28	194	4.61	5.76
1.0	0.55	382	1.82	6.74	0.55	382	5.11	6.09
1.0	0.35	243	2.86	12.95	0.35	243	2.50	2.50
0.5	0.35	243	1.43	5.29	0.70	486	3.38	4.15
1.5	0.75	520	2.00	7.40	0.50	347	6.00	7.80
1.0	0.80	555	1.25	4.63	0.80	555	10.15	13.03
5.0	2.80	1,943	1.79	6.62	0.56	389	6.52	8.21
8.5	2.05	1,423	4.15	15.35	0.24	167	2.46	2.74
6.0	1.80	1,249	3.33	12.30	0.30	208	2.24	3.23
13.5	4.50	3,123	3.00	11.10	0.33	229	1.82	3.33
1.5	0.75	520	2.00	7.40	0.50	347	2.41	2.76
29.5	9.10	6,315	3.24	11.99	0.31	215	2.10	3.13

TABLE 19.--Continued

Terrain Type	Waveform Segment	n	Σx	$\bar{x}$
Dense woods (coniferous)	PAN 2-1	37	1,517	41.0
	-2	28	1,144	40.9
	-3	9	348	38.7
	PAN 3-1	9	257	28.6
Totals		83	3,266	39.3
Open woods (coniferous)	PAN 3-1	8	287	35.9
	-2	9	304	33.8
Totals		17	591	34.8
Tree row	PAN 2-1	3	192	64.0
	-2	3	155	51.2
	-3	3	113	37.7
	-4	5	148	29.6
	PAN 3-1	3	112	37.3
	-2	2	94	47.0
	-3	2	66	33.0
Totals		21	880	41.9
Road	PAN 2-1	5	266	53.2
	PAN 3-1	3	192	64.0
Totals		8	458	57.2
Cleared right-of-way	PAN 2-1	3	177	59.0
Dense woods (deciduous)	PAN 1-1	8	344	43.0
	-2	9	342	38.0
	PAN 2-1	10	286	28.6
	-2	12	362	30.2
	PAN 3-1	27	1,322	35.7
	-2	30	987	32.9
	-3	15	494	32.9
Totals		111	4,137	37.3

TABLE 19.--Extension (Continued)

Statistical Parameters								
E	L_x	L_s	$\bar{f}$	$\bar{f}_s$	$\bar{\lambda}$	$\bar{\lambda}_s$	$\overline{\lvert x-\bar{x}\rvert}$	s
12.0	3.70	2,568	3.24	11.96	0.31	215	3.57	4.86
11.5	2.75	1,908	4.18	15.45	0.24	167	4.47	6.54
1.0	0.80	555	1.25	4.63	0.80	555	6.30	8.50
1.5	0.80	555	1.88	6.96	0.53	368	2.96	3.37
26.0	8.05	5,586	3.23	11.95	0.31	215	4.10	5.66
4.0	0.80	555	5.00	18.50	0.20	139	4.66	5.46
3.0	0.90	625	3.33	12.30	0.30	208	5.53	6.76
7.0	1.70	1,180	4.12	15.24	0.24	167	5.12	6.15
1.0	0.20	139	5.00	18.50	0.20	139	4.00	4.32
1.0	0.25	174	4.00	14.80	0.25	174	9.56	10.34
1.0	0.30	208	3.33	12.30	0.30	208	8.22	9.18
1.0	0.45	312	2.22	8.21	0.45	312	2.88	3.20
1.5	0.30	208	5.00	18.50	0.20	139	2.89	3.30
1.0	0.25	174	4.00	14.80	0.25	174	3.00	3.00
1.0	0.30	208	3.33	12.30	0.30	208	2.00	2.00
7.5	2.05	1,423	3.66	13.54	0.27	187	4.69	5.12
1.0	0.45	312	2.22	8.21	0.45	312	5.76	6.72
1.0	0.40	278	2.50	9.25	0.40	278	3.33	4.00
2.0	0.95	590	2.35	8.70	0.43	298	4.85	5.70
1.0	0.25	174	4.00	14.80	0.25	174	11.33	12.18
1.5	0.75	520	2.00	7.40	0.50	347	4.75	5.36
1.5	0.80	555	1.88	6.96	0.53	368	2.67	3.20
2.5	1.55	1,070	1.61	5.96	0.62	430	2.12	2.58
7.0	1.20	833	5.83	21.60	0.17	118	7.06	8.15
15.5	3.70	2,568	4.19	15.50	0.24	167	3.81	4.76
10.0	2.95	2,047	3.39	12.35	0.30	208	4.63	5.41
5.0	1.50	1,041	3.33	12.30	0.30	208	3.81	4.49
43.0	12.45	8,634	3.45	12.76	0.29	201	4.21	4.99

TABLE 19.--Continued

Terrain Type	Waveform Segment	n	Σx	$\bar{x}$
Open woods (deciduous)	PAN 1-1	5	323	64.6
	-2	10	445	44.5
	-3	8	505	63.1
	-4	32	1,341	41.9
	-5	9	442	49.1
	PAN 2-1	15	694	46.3
	-2	11	462	42.0
	-3	13	495	38.1
	PAN 3-1	15	677	45.1
	-2	8	409	51.1
Totals		126	5,793	46.0
Swamp	PAN 1-1	7	318	45.4
	-2	16	711	44.4
	PAN 2-1	16	952	59.5
	PAN 3-1	18	1,031	57.3
	-2	9	318	35.3
Totals		66	3,330	50.5

TABLE 19.--Extension (Continued)

Statistical Parameters								
E	L_x	L_s	$\bar{f}$	$\bar{f}_s$	$\bar{\lambda}$	$\bar{\lambda}_s$	$\overline{\lvert x-\bar{x}\rvert}$	s
2.0	0.55	382	3.64	13.45	0.27	187	4.32	4.54
3.0	0.90	624	3.33	12.30	0.30	208	8.50	10.74
1.5	0.70	486	2.14	7.92	0.47	326	8.38	9.78
11.0	3.20	2,221	3.44	12.72	0.29	201	6.34	7.72
3.5	0.85	590	4.12	15.25	0.24	167	3.93	5.04
5.0	1.50	1,041	3.33	12.30	0.30	208	5.25	6.39
4.0	1.05	729	3.81	14.10	0.26	180	3.64	4.82
3.5	1.30	902	2.69	9.95	0.37	257	4.40	5.25
3.5	1.45	1,006	2.41	8.91	0.42	291	6.66	8.17
3.0	0.80	555	3.75	13.85	0.27	187	6.12	7.18
40.0	12.30	8,536	3.25	12.02	0.31	215	5.85	7.13
1.0	0.65	451	1.30	4.81	0.77	534	5.63	6.39
4.0	1.80	1,249	2.22	8.21	0.45	312	1.81	2.18
4.0	1.65	1,145	2.42	8.95	0.41	285	3.62	4.21
7.0	1.75	1,214	4.00	14.80	0.25	174	4.98	6.32
1.5	0.85	590	1.76	6.51	0.57	396	5.93	6.63
17.5	6.70	4,649	2.61	9.66	0.38	264	4.01	4.85

TABLE 20

TERRAIN-TYPE COMPILATIONS: THERMAL INFRARED IMAGE, ALL LINES

Terrain Type	Waveform Segment	n	Σx	$\bar{x}$
Lake	IR 1-1	33	2,341	70.9
	-2	31	1,998	64.5
	-3	56	3,777	67.4
	IR 3-1	3	175	58.3
Totals		123	8,291	67.4
River	IR 1-1	4	281	70.2
	IR 2-1	4	244	61.0
	IR 3-1	3	231	77.0
Totals		11	756	68.7
Open woods (deciduous)	IR 1-1	6	400	66.7
	-2	12	813	67.8
	-3	9	459	51.0
	-4	6	277	46.2
	IR 2-1	15	545	36.3
	-2	8	321	40.1
	-3	6	188	31.3
	-4	24	1,254	52.2
	IR 3-1	9	631	70.1
Totals		95	4,888	51.5
Swamp	IR 1-1	9	259	28.8
	IR 2-1	11	396	36.0
	-2	6	178	29.7
	IR 3-1	17	577	33.9
	-2	10	276	26.7
Totals		53	1,686	31.8
Swamp hardwoods	IR 1-1	21	1,086	51.7

TABLE 20.--Extension

Statistical Parameters								
E	L_x	L_s	$\bar{f}$	$\bar{f}_s$	$\bar{\lambda}$	$\bar{\lambda}_s$	$\overline{\lvert x-\bar{x}\rvert}$	s
12.5	3.25	2,256	3.85	14.25	0.26	180	1.64	2.01
10.0	3.15	2,186	3.17	11.74	0.32	222	4.28	8.40
23.5	5.80	4,025	4.05	15.00	0.25	174	1.25	1.47
1.0	0.30	208	3.33	12.30	0.30	208	6.89	7.32
47.0	12.50	8,675	3.76	13.91	0.27	187	2.26	3.50
1.0	0.40	278	2.50	9.25	0.40	278	1.62	1.92
1.0	0.30	208	3.33	12.30	0.30	208	9.50	11.51
1.0	0.25	174	4.00	14.80	0.25	174	2.67	3.27
3.0	0.95	660	3.16	11.69	0.32	222	4.77	5.78
2.0	0.55	382	3.64	13.45	0.27	187	1.22	1.37
3.0	1.20	833	2.50	9.25	0.40	278	1.62	2.13
3.0	0.90	625	3.33	12.30	0.30	208	8.89	10.04
1.0	0.50	347	2.00	7.40	0.50	347	7.22	8.61
4.0	1.45	1,006	2.76	10.20	0.36	250	11.02	13.93
1.5	0.80	555	1.88	6.94	0.53	368	3.66	4.62
2.0	0.65	451	3.08	11.38	0.32	222	6.33	6.97
7.5	2.35	1,631	3.19	11.75	0.31	215	10.96	12.27
4.0	0.85	590	4.71	17.40	0.21	146	3.68	5.91
28.0	9.25	6,420	3.03	11.21	0.33	229	7.15	8.54
1.5	0.85	590	1.76	6.51	0.57	396	4.25	9.44
3.0	1.05	729	2.86	10.57	0.35	243	7.82	10.56
3.0	0.60	416	5.00	18.50	0.20	139	1.22	1.60
3.5	1.75	1,214	2.00	7.40	0.50	347	7.70	8.95
3.0	0.95	659	3.16	11.67	0.32	222	3.14	3.82
14.0	5.20	3,608	2.69	99.53	0.37	257	5.55	7.57
6.0	2.10	1,457	2.83	10.54	0.35	243	12.33	14.60

TABLE 20.--Continued

Terrain Type	Waveform Segment	n	Σx	$\bar{x}$
Open field	IR 1-1	7	418	59.7
	-2	16	860	53.8
	-3	9	635	70.6
	-4	20	858	42.9
	-5	9	335	37.2
	IR 2-1	10	316	31.6
	-2	10	409	40.9
	-3	5	347	69.4
	-4	19	450	23.7
	-5	2	74	37.0
	-6	8	259	32.4
	-7	8	334	41.8
	-8	15	439	28.6
	-9	3	80	26.7
	-10	4	118	29.5
	IR 3-1	15	428	28.5
	-2	13	611	47.0
	-3	15	424	28.3
	-4	16	328	20.5
	-5	14	283	20.2
	-6	22	1,274	57.9
	-7	25	660	26.4
Totals		265	9,940	37.5
Dense woods (deciduous)	IR 1-1	8	609	76.1
	-2	7	288	41.1
	-3	6	381	63.5
	-4	10	625	62.5
	IR 2-1	20	914	45.7
	-2	14	510	36.4
	IR 3-1	46	2,516	54.7
	-2	24	1,325	55.2
	-3	17	754	44.3
Totals		152	7,922	52.1

TABLE 20.--Extension (Continued)

Statistical Parameters								
E	L_x	L_s	$\bar{f}$	$\bar{f}_s$	$\bar{\lambda}$	$\bar{\lambda}_s$	$\overline{\lvert x-\bar{x}\rvert}$	s
2.5	0.70	486	3.57	13.20	0.28	194	7.47	8.68
6.0	1.65	1,145	3.64	13.45	0.27	187	7.78	9.38
1.5	0.85	590	1.76	6.51	0.57	396	1.70	2.11
8.0	1.95	1,353	4.10	15.15	0.24	167	7.07	8.07
1.5	0.80	555	1.88	6.95	0.53	368	8.69	10.39
3.5	1.00	694	3.50	12.95	0.28	194	2.60	2.90
3.0	0.95	625	3.15	11.65	0.32	222	1.94	2.62
1.0	0.45	312	2.22	8.22	0.45	312	4.48	5.04
6.0	1.80	1,249	3.33	12.30	0.30	208	5.21	7.62
1.0	0.20	139	5.00	18.50	0.20	139	2.00	2.00
3.0	0.80	555	3.75	13.87	0.27	187	4.97	6.87
3.0	0.80	555	3.75	13.87	0.27	187	8.69	9.43
3.5	1.45	1,006	2.41	8.93	0.41	285	9.74	11.45
1.0	0.35	243	2.86	10.58	0.35	243	1.11	1.25
1.0	0.35	243	2.86	10.58	0.35	243	6.75	8.20
5.5	1.45	1,006	3.79	13.65	0.26	181	1.89	2.73
2.5	1.30	902	1.92	7.11	0.52	361	8.77	10.09
5.5	1.55	1,076	3.55	13.15	0.28	194	7.56	9.84
5.0	1.55	1,076	3.23	11.92	0.31	215	5.00	7.00
3.5	1.40	971	2.50	9.25	0.40	278	4.76	7.78
7.0	2.20	1,527	3.18	11.77	0.31	215	9.12	10.65
8.5	2.40	1,666	3.54	13.10	0.28	194	2.74	3.69
83.0	25.95	17,974	3.20	11.84	0.31	215	5.81	7.24
3.0	0.80	555	3.75	13.88	0.27	187	2.62	3.59
1.5	0.70	486	2.14	7.92	0.47	326	4.45	5.46
1.0	0.50	347	2.00	7.40	0.50	347	2.17	2.36
3.0	0.90	625	3.33	12.30	0.30	208	4.30	5.97
5.5	1.90	1,319	2.90	10.70	0.34	236	7.67	8.99
4.5	1.35	937	3.33	12.30	0.30	208	8.86	11.65
21.0	4.55	3,158	4.62	17.10	0.22	153	12.11	14.09
6.5	2.45	1,700	2.65	9.80	0.38	264	11.42	13.77
5.0	1.65	1,145	3.03	11.20	0.33	229	10.57	12.20
51.0	14.80	10,272	3.45	12.76	0.29	201	9.19	10.98

TABLE 20.--Continued

Terrain Type	Waveform Segment	n	Σx	$\bar{x}$
Dense woods (coniferous)	IR 2-1	5	368	73.6
	-2	4	320	80.0
	-3	32	2,137	66.8
	-4	19	1,157	60.9
	-5	15	846	56.4
	IR 3-1	12	529	44.1
Totals		87	5,357	61.6
Open woods (coniferous)	IR 3-1	12	423	35.2
Road	IR 2-1	3	121	40.3
	-2	5	315	63.0
	-3	4	251	62.8
	-4	4	241	60.2
	-5	2	107	53.5
	IR 3-1	3	150	50.0
	-2	5	319	63.8
Totals		26	1,504	57.8

TABLE 20.--Extension (Continued)

Statistical Parameters								
E	L_x	L_s	$\bar{f}$	$\bar{f}_s$	$\bar{\lambda}$	$\bar{\lambda}_s$	$\overline{\lvert x-\bar{x}\rvert}$	s
1.0	0.55	382	1.82	6.73	0.55	382	6.88	7.81
1.0	0.45	312	2.22	8.22	0.45	312	2.00	2.45
9.5	3.25	2,256	2.92	10.80	0.34	236	2.70	4.11
5.0	1.85	1,284	2.70	10.00	0.37	257	6.38	9.79
5.0	1.45	1,006	3.45	12.73	0.29	201	5.33	6.50
3.5	1.20	833	2.92	10.80	0.34	236	3.40	4.75
25.0	8.75	6,073	2.86	10.58	0.35	243	4.26	5.99
4.0	1.10	763	3.64	13.47	0.27	187	4.83	5.92
1.0	0.25	174	4.00	14.70	0.25	174	1.56	1.70
2.0	0.45	312	4.44	16.42	0.22	153	9.60	11.68
1.0	0.35	243	2.86	10.58	0.35	243	1.38	1.64
1.0	0.40	278	2.50	9.25	0.40	278	5.75	6.94
1.0	0.25	174	4.00	14.70	0.25	174	3.50	3.50
1.0	0.30	208	3.33	12.30	0.30	208	8.67	10.23
1.0	0.45	312	2.22	8.22	0.45	312	5.84	7.35
8.0	2.45	1,701	3.27	12.10	0.31	215	5.52	6.63

APPENDIX V

TERRAIN-TYPE COMPILATIONS CORRECTED FOR RISE TIME: NINE-LENS MULTIBAND CAMERA IMAGERY

TABLE 21

TERRAIN-TYPE COMPILATIONS CORRECTED FOR RISE TIME: FRAME 42, LENS 2, LINES 1 AND 2

Terrain Type	Waveform Segment	n	$\sum x$	$\bar{x}$
Construction site	L1-1	74	4,842	65.4
Open field (grass)	L1-1	8	402	50.2
	-2	11	577	52.4
	-3	9	526	58.4
	-4	10	540	54.0
	-5	80	4,072	50.9
	L2-1	13	546	42.0
	-2	13	666	51.2
	-3	2	110	55.0
	-4	9	538	59.8
	-5	15	778	51.9
	-6	39	1,911	49.0
Totals		209	10,666	51.0
Paved road	L1-1	7	475	67.9
	-2	5	337	67.4
	L2-1	7	518	74.0
	-2	7	468	66.8
Totals		26	1,798	69.2
Unpaved road	L1-1	2	130	65.0
	-2	7	467	66.7
	-3	7	375	53.6
	L2-1	5	348	69.6
Totals		21	1,320	62.9
Open field (no cover)	L2-1	46	3,233	70.3
Paved parking lot	L2-1	66	4,679	70.9

TABLE 21.--Extension

Statistical Parameters								
E	L_x	L_s	$\bar{f}$	$\bar{f}_s$	$\bar{\lambda}$	$\bar{\lambda}_s$	$\overline{\lvert x-\bar{x}\rvert}$	s
22.0	7.35	693	3.00	53.85	0.33	31	5.71	7.03
3.0	0.80	75	3.75	67.31	0.27	25	3.00	3.46
3.0	1.05	99	2.86	51.34	0.35	33	2.03	2.43
3.0	0.80	75	3.75	67.31	0.27	25	5.06	5.68
4.0	1.10	104	3.64	65.34	0.28	26	2.20	2.93
21.0	8.00	754	2.62	47.03	0.38	36	1.36	1.67
2.0	1.25	118	1.60	28.72	0.62	58	3.54	4.93
3.0	1.20	113	2.50	44.88	0.40	38	4.59	5.46
1.0	0.10	9	10.00	179.50	0.10	9	1.00	1.00
4.0	0.80	75	5.00	89.75	0.20	19	1.80	2.10
5.0	1.55	146	3.23	57.98	0.31	29	2.94	3.48
11.5	3.80	358	3.03	54.39	0.33	31	2.15	2.32
60.5	20.45	1,926	2.96	53.13	0.34	32	2.27	2.71
1.0	0.60	57	1.67	29.98	0.60	57	5.02	5.67
2.0	0.45	42	4.44	79.70	0.23	22	0.88	1.02
1.0	0.60	57	1.67	29.98	0.60	57	4.29	5.21
3.0	0.70	66	4.28	76.83	0.23	22	3.31	3.76
7.0	2.35	222	2.98	53.49	0.34	32	3.57	4.14
1.0	0.25	24	4.00	71.80	0.25	24	1.00	1.00
3.0	0.65	61	4.62	82.93	0.22	21	1.76	2.37
2.0	0.60	57	3.33	59.77	0.30	28	0.65	0.73
1.0	0.40	38	2.50	44.88	0.40	38	3.28	3.72
7.0	1.90	180	3.68	66.06	0.27	25	1.68	2.01
14.0	4.50	424	3.11	55.82	0.32	30	2.16	3.06
22.0	6.40	604	3.44	61.75	0.29	27	1.74	2.31

TABLE 22

TERRAIN-TYPE COMPILATIONS CORRECTED FOR RISE TIME: FRAME 42, LENS 4, LINES 1 AND 2

Terrain Type	Waveform Segment	n	Σx	$\bar{x}$
Construction site	L1-1	73	3,258	44.6
Open field (grass)	L1-1	8	141	17.6
	-2	11	233	21.2
	-3	7	171	24.4
	-4	9	214	23.8
	-5	87	1,614	18.6
	L2-1	13	256	19.7
	-2	13	312	24.0
	-3	3	103	34.3
	-4	6	103	17.2
	-5	17	378	22.2
	-6	35	745	21.3
Totals		209	4,270	20.4
Unpaved road	L1-1	4	110	27.5
	-2	5	293	58.6
	-3	5	119	23.8
	L2-1	4	196	49.0
Totals		18	718	39.9
Paved road	L1-1	5	213	42.6
	-2	7	442	63.1
	L2-1	6	288	48.0
	-2	4	200	50.0
Totals		22	1,143	52.0
Open field (no cover)	L2-1	47	2,646	56.3
Paved parking lot	L2-1	65	3,161	48.6

TABLE 22.--Extension

Statistical Parameters								
E	L_x	L_s	$\bar{f}$	$\bar{f}_s$	$\bar{\lambda}$	$\bar{\lambda}_s$	$\overline{\lvert x-\bar{x}\rvert}$	s
25.0	7.30	688	3.42	61.39	0.29	27	18.93	22.65
1.5	0.70	66	2.14	38.41	0.47	44	3.53	4.58
3.0	1.00	94	3.00	53.85	0.33	31	1.11	1.34
3.0	0.75	71	4.00	71.80	0.25	24	2.03	2.70
3.0	0.90	85	3.33	59.77	0.30	28	3.14	3.55
31.5	8.60	811	3.66	65.70	0.27	25	2.24	2.66
3.0	1.25	118	2.40	43.08	0.42	40	2.22	2.78
3.0	1.25	118	2.40	43.08	0.42	40	1.85	2.69
1.25	0.30	29	4.17	74.85	0.24	23	2.89	3.09
1.0	0.70	66	1.43	25.67	0.70	66	6.22	6.99
6.0	1.55	146	3.87	69.47	0.26	25	3.01	3.92
6.0	1.55	146	3.87	69.47	0.26	25	1.70	2.22
62.25	18.55	1,750	3.36	60.31	0.30	28	2.33	2.87
1.0	0.30	29	3.33	59.77	0.30	28	4.50	4.50
2.25	0.55	52	4.09	73.42	0.34	23	3.12	3.98
1.25	0.40	38	3.12	56.00	0.32	30	1.76	1.83
1.0	0.30	29	3.33	59.77	0.30	28	3.00	3.00
5.5	1.55	148	3.55	63.72	0.28	26	3.02	3.28
1.0	0.65	61	1.54	27.64	0.65	61	4.88	5.16
1.25	0.70	66	1.74	31.23	0.56	53	3.02	3.40
1.0	0.55	52	1.82	32.67	0.55	52	4.33	4.93
1.25	0.45	42	2.77	49.72	0.36	34	5.00	6.16
4.5	2.35	221	1.91	34.28	0.52	49	4.16	4.72
14.0	4.65	438	3.07	54.03	0.33	31	7.37	8.60
26.5	6.40	604	4.14	74.31	0.24	23	3.37	4.34

TABLE 23

TERRAIN-TYPE COMPILATIONS CORRECTED FOR RISE TIME: FRAME 42, LENS 9, LINES 1 AND 2

Terrain Type	Waveform Segment	n	Σx	$\bar{x}$
Construction site	L1-1	75	1,234	16.4
Open field (grass)	L1-1	6	179	29.8
	-2	12	330	27.5
	-3	7	255	36.4
	-4	8	244	30.5
	-5	86	3,983	46.3
	L2-1	12	351	29.2
	-2	12	381	31.8
	-3	5	212	42.4
	-4	5	169	33.8
	-5	16	756	47.2
	-6	35	1,390	39.7
Totals		204	8,250	40.4
Unpaved road	L1-1	4	142	35.5
	-2	8	319	39.8
	-3	4	222	55.5
	L2-1	6	137	22.8
Totals		22	820	37.3
Paved road	L1-1	7	174	24.8
	-2	6	222	37.0
	L2-1	12	392	32.7
	-2	7	116	16.6
Totals		32	904	28.2
Open field (no cover)	L2-1	47	1,953	41.6
Paved parking lot	L2-1	66	1,388	21.0

TABLE 23.--Extension

Statistical Parameters								
E	L_x	L_s	$\bar{f}$	$\bar{f}_s$	$\bar{\lambda}$	$\bar{\lambda}_s$	$\overline{\lvert x-\bar{x}\rvert}$	s
15.0	7.40	698	2.03	36.44	0.49	46	6.26	7.73
1.0	0.55	52	1.82	32.67	0.55	52	1.16	1.34
4.0	1.15	108	3.48	62.47	0.29	27	2.67	3.38
2.0	0.65	61	3.08	55.29	0.32	30	4.82	6.16
1.5	0.75	71	2.00	35.90	0.50	47	8.75	9.59
30.0	8.60	811	3.48	62.47	0.29	27	5.23	7.14
1.5	1.10	104	1.36	24.41	0.74	70	5.46	6.25
3.0	1.15	108	2.61	46.85	0.38	36	4.25	4.97
1.0	0.40	38	2.50	44.88	0.40	38	10.08	11.67
1.5	0.45	42	3.33	59.77	0.30	28	6.64	7.00
3.5	1.55	147	2.26	40.57	0.44	41	3.96	4.67
8.5	3.50	330	2.43	43.61	0.41	39	3.80	4.48
57.5	19.85	1,872	2.90	52.06	0.34	32	4.85	6.09
2.0	0.35	33	5.71	102.49	0.18	17	2.00	2.06
3.0	0.75	71	4.00	71.80	0.25	24	7.84	8.61
0.5	0.35	33	1.43	25.67	0.70	66	3.25	3.90
1.0	0.50	47	2.00	35.90	0.50	47	3.11	3.44
6.5	1.95	184	3.33	59.77	0.30	28	4.65	5.15
1.0	0.75	71	1.33	23.87	0.75	71	2.94	3.48
1.5	0.55	52	2.73	49.00	0.37	35	4.33	4.73
2.0	1.15	108	1.74	31.23	0.57	54	9.11	9.64
1.5	0.65	61	2.31	41.46	0.43	41	2.94	3.96
6.0	3.10	292	1.94	34.82	0.52	49	5.51	6.13
16.0	4.75	448	3.37	60.49	0.30	28	4.20	5.68
19.5	6.50	613	3.00	53.85	0.33	31	4.31	5.89

APPENDIX VI

TERRAIN-TYPE COMPILATIONS CORRECTED FOR RISE TIME: PANCHROMATIC AND THERMAL INFRARED IMAGES

TABLE 24

TERRAIN-TYPE COMPILATIONS CORRECTED FOR RISE TIME: PANCHROMATIC IMAGE, ALL LINES

Terrain Type	Waveform Segment	n	$\sum x$	$\bar{x}$
Open field	PAN 1-1	4	277	69.2
	-2	6	376	62.7
	-3	29	1,498	49.9
	-4	5	316	63.2
	-5	15	799	53.3
	PAN 2-1	33	2,172	65.8
	-2	9	619	68.8
	-3	18	1,237	68.7
	-4	2	123	61.5
	-5	3	162	54.0
	-6	7	456	65.1
	-7	17	874	51.4
	-8	12	428	35.7
	PAN 3-1	10	681	68.1
	-2	25	1,577	63.1
	-3	7	374	53.4
	-4	12	800	66.7
	-5	6	363	60.5
	-6	5	263	52.6
	-7	17	876	51.5
	-8	5	235	47.0
	-9	24	1,223	51.0
Totals		271	15,729	58.0
Shoal water	PAN 1-1	5	242	48.4
	-2	2	125	62.5
	-3	4	175	43.7
	-4	7	364	52.0
	-5	8	510	63.8
Totals		26	1,416	54.4

TABLE 24.--Extension

Statistical Parameters								
E	L_x	L_s	$\bar{f}$	$\bar{f}_s$	$\bar{\lambda}$	$\bar{\lambda}_s$	$\overline{\lvert x-\bar{x}\rvert}$	s
2.0	0.30	208	6.67	24.70	0.15	104	1.38	1.64
1.0	0.60	416	1.67	6.18	0.60	416	2.78	3.20
11.5	2.90	2,013	3.97	14.69	0.25	174	6.43	7.91
1.0	0.40	278	2.50	9.25	0.40	278	5.76	6.76
3.5	1.40	972	2.50	9.25	0.40	278	5.68	7.08
14.0	3.20	2,221	4.38	16.20	0.23	160	2.43	2.92
3.0	0.90	625	3.33	12.30	0.30	208	1.14	1.32
5.5	1.70	1,180	3.24	11.99	0.31	215	2.09	2.64
1.0	0.25	174	4.00	14.80	0.25	174	5.50	5.50
1.0	0.25	174	4.00	14.80	0.25	174	2.67	3.27
3.0	0.60	416	5.00	18.50	0.20	139	10.67	13.28
5.5	1.75	1,214	3.14	11.60	0.32	222	2.10	3.85
3.0	1.15	798	2.61	9.66	0.38	264	5.78	8.98
5.0	0.95	659	5.26	19.45	0.19	132	1.48	1.81
11.0	2.55	1,770	4.31	15.95	0.23	160	2.56	3.43
3.0	0.75	520	4.00	14.80	0.25	174	1.92	2.77
5.0	1.25	868	4.00	14.80	0.25	174	1.44	2.06
1.5	0.55	382	2.73	10.10	0.37	257	5.17	6.13
2.0	0.50	347	4.00	14.80	0.25	174	4.48	5.99
4.5	1.70	1,180	2.65	9.81	0.38	264	6.32	7.46
1.0	0.40	278	2.50	9.25	0.40	278	6.00	7.13
8.0	2.35	1,631	3.40	12.58	0.29	201	7.96	9.62
96.0	26.40	18,324	3.64	13.47	0.27	187	4.21	5.34
1.0	0.40	278	2.50	9.25	0.40	278	2.48	3.01
1.0	0.35	243	2.86	12.95	0.35	243	2.50	2.50
0.5	0.35	243	1.43	5.29	0.70	486	3.38	4.17
1.5	0.75	520	2.00	7.40	0.50	347	6.00	7.80
1.0	0.70	486	1.43	5.29	0.70	486	6.81	8.88
5.0	2.55	1,770	1.96	7.25	0.51	354	4.90	6.24

TABLE 24.--Continued

Terrain Type	Waveform Segment	n	Σx	$\bar{x}$
Lake	PAN 1-1	21	936	44.6
	-2	19	772	40.6
	-3	43	1,346	31.3
	-4	8	225	28.1
Totals		91	3,279	36.0
Dense woods (coniferous)	PAN 2-1	36	1,457	40.2
	-2	27	1,078	39.9
	-3	8	290	36.2
	PAN 3-1	9	257	28.6
Totals		80	3,082	38.5
Open woods (coniferous)	PAN 3-1	8	287	35.9
	-2	9	304	33.8
Totals		17	591	34.8
Tree row	PAN 2-1	2	122	61.0
	-2	2	89	44.5
	-3	3	63	31.5
	-4	5	148	29.6
	PAN 3-1	3	112	37.3
	-2	2	94	47.0
	-3	2	66	33.0
Totals		19	694	36.5
Road	PAN 2-1	4	225	56.2
	PAN 3-1	3	192	64.0
Totals		7	417	59.6

TABLE 24.--Extension (Continued)

Statistical Parameters								
E	L_x	L_s	$\bar{f}$	$\bar{f}_s$	$\bar{\lambda}$	$\bar{\lambda}_s$	$\overline{\lvert x-\bar{x}\rvert}$	s
8.5	2.05	1,423	4.15	15.35	0.24	167	2.46	2.74
6.0	1.80	1,249	3.33	12.30	0.30	208	2.24	3.23
13.5	4.25	2,950	3.18	11.77	0.31	215	1.22	1.50
1.5	0.75	520	2.00	7.40	0.50	347	2.41	2.76
29.5	8.85	6,142	3.33	12.32	0.30	208	1.82	2.26
12.0	3.55	2,464	3.38	12.51	0.30	208	3.23	3.73
11.5	2.65	1,839	4.34	16.06	0.23	160	3.48	4.49
1.0	0.70	486	1.43	5.29	0.70	486	4.25	5.36
1.5	0.80	555	1.88	6.96	0.53	368	2.96	3.37
26.0	7.70	5,344	3.38	12.51	0.30	208	3.39	4.11
4.0	0.80	555	5.00	18.50	0.20	139	4.66	5.46
3.0	9.90	625	3.33	12.30	0.30	208	5.53	6.76
7.0	1.70	1,180	4.12	15.24	0.24	167	5.12	6.15
1.0	0.10	69	10.00	37.00	0.10	69	1.00	1.00
1.0	0.15	104	6.67	24.68	0.15	104	2.50	2.50
1.0	0.15	104	6.67	24.68	0.15	104	3.50	3.50
1.0	0.45	312	2.22	8.21	0.45	312	2.88	3.20
1.5	0.30	208	5.00	18.50	0.20	139	2.89	3.30
1.0	0.25	174	4.00	14.80	0.25	174	3.00	3.00
1.0	0.30	208	3.33	12.30	0.30	208	2.00	2.00
7.5	1.70	1,179	4.41	16.32	0.23	160	2.66	2.81
1.0	0.30	208	3.33	12.32	0.30	208	2.65	3.92
1.0	0.40	278	2.50	9.25	0.40	278	3.33	4.00
2.0	0.70	486	2.86	10.58	0.35	243	2.94	3.95

TABLE 24.--Continued

Terrain Type	Waveform Segment	n	Σx	$\bar{x}$
Dense woods (deciduous)	PAN 1-1	6	242	40.3
	-2	9	342	38.0
	PAN 2-1	10	286	28.6
	-2	11	314	28.5
	PAN 3-1	36	1,273	35.4
	-2	29	941	32.4
	-3	15	494	32.9
Totals		116	3,892	33.6
Open woods (deciduous)	PAN 1-1	5	323	64.6
	-2	9	378	42.0
	-3	8	505	63.1
	-4	32	1,341	41.9
	-5	9	442	49.1
	PAN 2-1	14	633	45.2
	-2	11	462	42.0
	-3	13	475	38.1
	PAN 3-1	14	613	43.8
	-2	7	372	53.1
Totals		122	5,544	45.4
Swamp	PAN 1-1	6	261	43.5
	-2	15	661	44.1
	PAN 2-1	16	952	59.5
	PAN 3-1	17	988	58.1
	-2	9	318	35.3
Totals		63	3,180	50.5
Cleared right-of-way	PAN 2-1	2	135	67.5

TABLE 24.--Extension (Continued)

Statistical Parameters								
E	L_x	L_s	$\bar{f}$	$\bar{f}_s$	$\bar{\lambda}$	$\bar{\lambda}_s$	$\overline{\lvert x-\bar{x}\rvert}$	s
1.5	0.60	416	2.50	9.25	0.40	278	2.33	2.92
1.5	0.80	555	1.88	6.96	0.53	368	2.67	3.20
2.5	1.55	1,070	1.61	5.96	0.62	430	2.12	2.58
7.0	1.05	770	6.67	24.68	0.15	104	5.42	6.40
15.5	3.60	2,498	4.31	15.95	0.23	160	3.56	4.27
10.0	2.80	1,943	3.57	13.21	0.28	194	4.29	4.92
5.0	1.50	1,041	3.33	12.30	0.30	208	3.81	4.49
43.0	11.90	8,259	3.61	13.36	0.28	194	3.69	4.36
2.0	0.55	382	3.64	13.45	0.27	187	4.32	4.54
3.0	0.80	555	3.75	13.88	0.27	187	6.00	8.11
1.5	0.70	486	2.14	7.92	0.47	326	8.38	9.78
11.0	3.20	2,221	3.44	12.72	0.29	201	6.34	7.72
3.5	0.85	590	4.12	15.25	0.24	167	3.93	5.04
5.0	1.40	972	3.57	13.21	0.28	194	4.39	5.21
4.0	1.05	729	3.33	14.10	0.26	180	3.64	4.82
3.5	1.30	902	3.81	9.95	0.37	257	4.40	5.25
3.5	1.35	937	2.59	9.58	0.39	271	5.79	6.66
3.0	0.65	451	4.62	17.09	0.22	153	4.69	5.14
40.0	11.85	8,225	3.38	12.51	0.30	208	5.36	6.47
1.0	0.50	347	2.00	7.40	0.50	347	4.00	4.65
4.0	1.60	1,110	2.50	9.25	0.40	278	1.54	1.69
4.0	1.65	1,145	2.42	8.95	0.41	285	3.62	4.21
7.0	1.65	1,145	4.24	15.69	0.24	167	4.49	5.44
1.5	0.85	590	1.76	6.51	0.57	396	5.92	6.63
17.5	6.25	4,337	2.80	10.36	0.36	250	3.72	4.33
1.0	0.15	104	6.67	24.68	0.15	104	2.50	2.51

TABLE 25

TERRAIN-TYPE COMPILATIONS CORRECTED FOR RISE TIME: THERMAL INFRARED IMAGE, ALL LINES

Terrain Type	Waveform Segment	n	Σx	$\bar{x}$
Lake	IR 1-1	33	2,341	70.0
	-2	29	1,929	66.5
	-3	56	3,777	67.4
	IR 3-1	2	127	63.5
Totals		120	8,174	68.1
River	IR 1-1	4	281	70.2
	IR 2-1	4	244	61.0
	IR 3-1	3	231	77.0
Totals		11	756	68.7
Open woods (deciduous)	IR 1-1	6	400	66.7
	-2	12	813	67.8
	-3	9	459	51.0
	-4	6	277	46.2
	IR 2-1	15	545	36.3
	-2	8	321	40.1
	-3	6	188	31.3
	-4	24	1,254	52.2
	IR 3-1	9	631	70.1
Totals		95	4,888	51.5
Swamp	IR 1-1	8	208	26.0
	IR 2-1	10	331	33.1
	-2	6	178	29.7
	IR 3-1	16	525	32.8
	-2	9	240	25.6
Totals		49	1,482	30.2
Swamp hardwoods	IR 1-1	21	1,086	51.7

TABLE 25.--Extension

Statistical Parameters								
E	L_x	L_s	$\bar{f}$	$\bar{f}_s$	$\bar{\lambda}$	$\bar{\lambda}_s$	$\overline{\lvert x-\bar{x}\rvert}$	s
12.5	3.25	2,256	3.85	14.25	0.26	180	1.64	2.01
10.0	2.95	2,047	3.39	12.54	0.29	201	1.82	2.33
23.5	5.80	4,025	4.05	15.00	0.25	174	1.25	1.47
1.0	0.20	139	5.00	18.50	0.20	139	0.50	0.50
47.0	12.20	8,467	3.85	14.24	0.26	180	1.48	1.81
1.0	0.40	278	2.50	9.25	0.40	278	1.62	1.92
1.0	0.30	208	3.33	12.30	0.30	208	9.50	11.51
1.0	0.25	174	4.00	14.80	0.25	174	2.67	3.27
3.0	0.95	660	3.16	11.69	0.32	222	4.77	5.78
2.0	0.55	382	3.64	13.45	0.27	187	1.22	1.37
3.0	1.20	833	2.50	9.25	0.40	278	1.62	2.13
3.0	0.90	625	3.33	12.30	0.30	208	8.89	10.04
1.0	0.50	347	2.00	7.40	0.50	347	7.22	8.61
4.0	1.45	1,006	2.76	10.20	0.36	250	11.02	13.93
1.5	0.80	555	1.88	6.94	0.53	368	3.66	4.62
2.0	0.65	451	3.08	11.38	0.32	222	6.33	6.97
7.5	2.35	1,631	3.19	11.75	0.31	215	10.96	12.27
4.0	0.85	590	4.71	17.40	0.21	146	3.68	5.91
28.0	9.25	6,420	3.03	11.21	0.33	229	7.15	8.54
1.5	0.70	486	2.14	7.92	0.47	326	4.25	5.54
3.0	0.95	659	3.16	11.69	0.32	222	4.34	5.50
3.0	0.60	416	5.00	18.50	0.20	139	1.22	1.60
3.5	1.60	1,110	2.19	8.10	0.46	319	7.11	8.01
3.0	0.80	555	3.75	13.88	0.27	187	1.93	3.05
14.0	4.65	3,226	3.01	11.14	0.33	229	4.41	5.40
6.0	2.10	1,457	2.83	10.54	0.35	243	12.33	14.60

TABLE 25.--Continued

Terrain Type	Waveform Segment	n	Σx	$\bar{x}$
Open field	IR 1-1	7	418	59.7
	-2	16	860	53.8
	-3	9	635	70.6
	-4	20	858	42.9
	-5	9	335	37.2
	IR 2-1	10	316	31.6
	-2	10	409	40.9
	-3	5	347	69.4
	-4	18	400	22.2
	-5	2	74	37.0
	-6	7	211	30.1
	-7	8	334	41.8
	-8	14	384	26.6
	-9	3	80	26.7
	-10	3	75	25.0
	IR 3-1	15	428	28.5
	-2	13	611	47.0
	-3	14	369	26.4
	-4	15	285	19.0
	-5	13	237	18.2
	-6	21	1,243	59.2
	-7	25	660	26.4
Totals		257	9,569	37.2
Dense woods (deciduous)	IR 1-1	8	609	76.1
	-2	7	288	41.1
	-3	6	381	63.5
	-4	9	579	64.3
	IR 2-1	20	914	45.7
	-2	13	445	34.2
	IR 3-1	45	2,468	54.8
	-2	24	1,325	55.2
	-3	17	754	44.0
Totals		149	7,763	52.1

TABLE 25.--Extension (Continued)

Statistical Parameters								
E	L_x	L_s	$\bar{f}$	$\bar{f}_s$	$\bar{\lambda}$	$\bar{\lambda}_s$	$\overline{\lvert x-\bar{x}\rvert}$	s
2.5	0.70	486	3.57	13.20	0.28	194	7.47	8.68
6.0	1.65	1,145	3.64	13.45	0.27	187	7.78	9.38
1.5	0.85	590	1.76	6.51	0.57	396	1.70	2.11
8.0	1.95	1,353	4.10	15.15	0.24	167	7.07	8.07
1.5	0.80	555	1.88	6.95	0.53	368	8.69	10.39
3.5	1.00	694	3.50	12.95	0.28	194	2.60	2.90
3.0	0.95	625	3.15	11.65	0.32	222	1.94	2.62
1.0	0.45	312	2.22	8.22	0.45	312	4.48	5.04
6.0	1.70	1,180	3.53	13.06	0.28	194	3.80	4.55
1.0	0.20	139	5.00	18.50	0.20	139	2.00	2.00
3.0	0.65	451	4.62	17.09	0.22	153	3.26	3.76
3.0	0.80	555	3.75	13.87	0.27	187	8.69	9.43
3.5	1.30	902	2.69	9.95	0.37	257	7.99	9.14
1.0	0.35	243	2.86	10.58	0.35	243	1.11	1.25
1.0	0.25	174	4.00	14.80	0.25	174	2.67	2.94
5.5	1.45	1,006	3.79	13.65	0.26	181	1.89	2.73
2.5	1.30	902	1.92	7.11	0.52	361	8.77	10.09
5.5	1.45	1,006	3.79	14.02	0.26	180	5.46	7.01
5.0	1.45	1,006	3.45	12.76	0.29	201	2.93	4.03
3.5	1.25	868	2.80	10.36	0.36	250	2.28	3.19
7.0	2.05	1,423	3.41	12.62	0.29	201	7.84	9.09
8.5	2.40	1,666	3.54	13.10	0.28	194	2.74	3.69
83.0	24.95	17,281	3.30	12.21	0.30	208	5.03	6.03
3.0	0.80	555	3.75	13.88	0.27	187	2.62	3.59
1.5	0.70	486	2.14	7.92	0.47	326	4.45	5.46
1.0	0.50	347	2.00	7.40	0.50	347	2.17	2.36
3.0	0.80	625	3.75	13.88	0.27	187	2.00	2.25
5.5	1.90	1,319	2.90	10.70	0.34	236	7.67	8.99
4.5	1.25	868	3.60	13.32	0.28	194	7.44	8.86
21.0	4.40	3,054	4.78	17.69	0.21	146	12.10	14.80
6.5	2.45	1,700	2.65	9.80	0.38	264	11.42	13.77
5.0	1.65	1,145	3.03	11.20	0.33	229	10.57	12.12
51.0	14.45	10,099	3.53	13.06	0.28	194	8.94	10.73

TABLE 25.--Continued

Terrain Type	Waveform Segment	n	$\sum x$	$\bar{x}$
Dense woods (coniferous)	IR 2-1	4	308	77.0
	-2	4	320	80.0
	-3	31	2,087	67.3
	-4	16	1,032	64.5
	-5	13	761	58.5
	IR 3-1	12	529	44.0
Totals		80	5,037	63.0
Open woods (coniferous)	IR 3-1	11	373	33.9
Road	IR 2-1	3	121	40.3
	-2	4	274	68.5
	-3	4	251	62.8
	-4	3	192	64.0
	-5	2	107	53.5
	IR 3-1	2	113	56.5
	-2	4	269	67.2
Totals		22	1,327	60.3

TABLE 25.--Extension (Continued)

Statistical Parameters								
E	L_x	L_s	$\bar{f}$	$\bar{f}_s$	$\bar{\lambda}$	$\bar{\lambda}_s$	$\overline{\lvert x-\bar{x}\rvert}$	s
1.0	0.40	278	2.50	9.25	0.40	278	3.50	4.30
1.0	0.45	312	2.22	8.22	0.45	312	2.00	2.45
9.5	3.15	2,186	3.02	11.17	0.33	229	2.11	2.90
5.0	1.50	1,041	3.33	12.32	0.30	208	2.31	2.87
5.0	1.30	902	3.85	14.24	0.26	180	2.95	3.90
3.5	1.20	833	2.92	10.80	0.34	236	3.40	4.75
25.0	8.00	5,552	3.12	11.54	0.32	222	2.54	3.38
4.0	1.00	694	4.00	14.80	0.25	174	3.52	4.08
1.0	0.25	174	4.00	14.70	0.25	174	1.56	1.70
2.0	0.35	243	5.71	21.13	0.18	125	3.75	4.39
1.0	0.35	243	2.86	10.58	0.35	243	1.38	1.64
1.0	0.30	208	3.33	12.32	0.30	208	2.67	2.83
1.0	0.25	174	4.00	14.70	0.25	174	3.50	3.50
1.0	0.20	139	5.00	18.50	0.20	139	5.50	5.50
1.0	0.35	243	2.86	10.58	0.35	243	2.25	3.72
8.0	2.05	1,423	3.90	14.43	0.26	180	2.74	3.21

SELECTED BIBLIOGRAPHY

Books

American Society of Photogrammetry. Manual of Photographic Interpretation. Menasha, Wis.: George Banta Co., Inc., 1960.

Conn, G. K. T., and D. G. Avery. Infrared Methods. New York: Academic Press, 1960.

Eastman Kodak Company. Infrared and Ultraviolet Photography. Advanced Data Book M-3. Rochester, N. Y.: Eastman Kodak Company, 1963.

_____. Kodak Wratten Filters for Scientific and Technical Use. Scientific and Technical Data Book B-3, 22nd ed. Rochester, N. Y.: Eastman Kodak Company, 1965.

Hackforth, H. L. Infrared Radiation. New York: McGraw-Hill Book Co., Inc., 1960.

Holter, M. R., et al. Fundamentals of Infrared Technology. New York: The Macmillan Co., 1962.

Jamieson, John A., Raymond H. McFee, Gilbert N. Plass, Robert H. Grube, and Robert G. Richards. Infrared Physics and Engineering. New York: McGraw-Hill Book Co., Inc., 1963.

Kruse, P. W., L. D. McGlauchlin, and R. B. McQuistan. Elements of Infrared Technology. New York: John Wiley and Sons, 1962.

Lattman, L. H., and R. G. Ray. Aerial Photographs in Field Geology. New York: Holt, Rinehart, and Winston, 1965.

Simon, Ivan. Infrared Radiation. Princeton: D. Van Nostrand Co., Inc., 1966.

Strahler, A. N. The Earth Sciences. New York: Harper and Row, 1963.

Reports

Alexeenko, E. J. Dirt Roads as an Indicator in the Aerial Photo Interpretation of Soils and Terrain. Translated from the Russian. Washington: U.S. Army Engineers Research and Development Laboratories, 1966.

Altschaeffl, A. G. Effect of Soil Moisture and Other Natural Variables on Aerial Photo Gray Tones. Unpublished Master's thesis, Purdue University, 1955.

Avery, Gene. Forester's Guide to Aerial Photo Interpretation. Occasional Paper No. 156, Southeastern Forest Experiment Station, U.S. Department of Agriculture, 1960.

_____. Identifying Southern Forest Types on Aerial Photographs. Station Paper No. 112, Southeastern Forest Experiment Station, U.S. Department of Agriculture, 1960.

Baer, Ferdinand, and William Kamm. Numerical Analysis of Tiros Radiation Observations. Technical Paper No. 67, Department of Atmospheric Science, Colorado State University, 1965.

Bandeen, W. R., H. Halev, and I. Strange. Radiation Climatology in the Visible and Infrared from Tiros Meteorological Satellites. Technical Note D-2534, National Aeronautics and Space Administration, 1965.

Bell, E. E., et al. Infrared Techniques and Measurements. Final Engineering Report, Contract AF 33(96160)-3312, Ohio State University Research Foundation, 1957.

Brown, P. E., and A. M. O'Neal. The Color of Soils in

Relation to Organic Matter Content. Research Bulletin No. 75, Iowa Agricultural Experiment Station, 1923.

Cook, John C. Research on the Electromagnetic Measurement of Ice Properties. Report No. TR-57-219, U.S. Air Force Cambridge Research Laboratories.

Cornell Aeronautical Laboratory. A Scientific Investigation into Photographic Reconnaissance from Space Vehicles. Final Report, May 10, 1961.

Cronin, J. F. Terrestrial Features of the United States as Viewed by Tiros. U.S. Air Force Cambridge Research Laboratories and Aracon Geophysics Co., 1963.

Davies, Merton E. Inspection by Small Satellites. Santa Monica, Calif.: The Rand Corporation, 1966.

Eastman Kodak Company. The Kodak Aero-Neg Color System. Pamphlet No. M-4. Rochester, N. Y.: Eastman Kodak Company, 1966.

_____. Kodak High-Speed Infrared Film. Sales Service Pamphlet No. M-9. Rochester, N. Y.: Eastman Kodak Company, 1962.

Erickson, C. O., and L. F. Hubert. Identification of Cloudforms from TIROS I Pictures. Meteorological Satellite Laboratory, Report No. 7. Washington: U.S. Weather Bureau, 1961.

Fredrickson, W. R., and N. Ginsburg. Infrared Spectral Emissivity of Terrain. Interim Report No. 1, Contract AF 33(616)-5034. Syracuse, N. Y.: Department of Physics, Syracuse University, 1957.

Fujita, T. A. A Technique for Precise Analysis of Satellite Data. Volume I: Photogrammetry. Meteorological Satellite Laboratory, Report No. 14. Washington: U.S. Weather Bureau, 1965.

Garrison, W. C. Demands for Small-Area Data: Five Papers in Remote Sensing and Urban Information Systems. Technical Report No. 1, NR 389-143. Washington: Office of Naval Research, 1965.

Greaves, J. R., R. Wexler, and C. J. Bowley. The Feasibility of Sea Surface Temperature Determination Using Satellite Infrared Data. Final Report, Contract NASW-1157. Aracon Geophysics Co., 1965.

Holter, Marion R., and Fabian C. Polcyn. Comparative Multispectral Sensing. Report No. 2900-484-R. Ann Arbor: Institute of Science and Technology, University of Michigan, 1965.

Kern, Clifford D. Evaluation of Infrared Emission of Clouds and Ground as Measured by Weather Satellites. Environmental Research Paper No. 155, U.S. Air Force Cambridge Research Laboratories, 1965.

Latham, James P. The Distance Relations and Some Other Characteristics of Cropland Areas in Pennsylvania; An Experiment in Methodology. Technical Report No. 4, NR 389-055. Washington: Office of Naval Research, 1958.

_____. Electronic Measurement and Analysis of Geographic Phenomena. Final Report, NR 387-023. Washington: Office of Naval Research, 1964.

_____. Methodology for Instrumented Geographic Analysis. Technical Report No. 2, NR 387-023. Washington: Office of Naval Research, 1962.

_____. Possible Applications of Electronic Scanning and Computer Devices to the Analysis of Geographic Phenomena. Technical Report No. 1, NR 387-023. Washington: Office of Naval Research, 1959.

_____. A Study of the Application of Electronic Scanning and Computer Devices to the Analysis of Geographic Phenomena. Final Report, NR 387-023. Washington: Office of Naval Research, 1959.

Latham, James P., and Richard E. Witmer. Comparative Waveform Analysis of Multisensor Imagery. Technical Report No. 3, NR 387-034. Washington: Office of Naval Research, 1967. (To be published in Photogrammetric Engineering, July, 1967.)

Limperis, T., and D. George. Electromagnetic Field Signatures in the Optical Spectrum. Ann Arbor: Willow Run Laboratories, Institute of Science and Technology, University of Michigan (no date).

Ludlum, R. Ground-Truth Research for an Airborne Multisensor Survey Program. Texas Instruments, Inc., 1966.

Ludlum, R., and J. R. Van Lopik. A Remote Sensing Survey of Areas in Central Coastal Louisiana (Part I -- Discussion). Texas Instruments, Inc., 1966.

Marschner, F. J. Land Use and Its Patterns in the United States. Agricultural Handbook No. 153. Washington: U.S. Department of Agriculture, 1959.

Marshall, Ernest W. Air Photo Interpretation of Great Lakes Ice Features. Special Report No. 25. Ann Arbor: Great Lakes Research Division, Institute of Science and Technology, University of Michigan, 1966.

Mathers, Boyd L. Relative Effectiveness of Different Viewing Devices for Photo Interpretation. Technical Research Note 179. Washington: U.S. Army Personnel Research Office, 1966.

Merifield, P. M., and J. Rammelkamp. Terrain in Tiros Pictures. Lockheed-California Co., 1964.

Moxham, R. M., D. R. Crandell, and W. Marlett. Thermal Features at Mount Rainier, Washington as Revealed by Infrared Surveys. Professional Paper 525d. Washington: U.S. Geological Survey, 1965.

National Aeronautics and Space Administration. Geographic Data from Space. Proceedings of the Conference on the Use of Orbiting Spacecraft in Geographic Research, Houston: Manned Spacecraft Center, January 28-30, 1965.

Olson, Charles E., Jr., et al. An Analysis of Measurements of Light Reflectance from Tree Foliage Made during 1960 and 1961. Agricultural Experiment Station, University of Illinois, 1964.

Parker, D., D. Fisher, C. Miller, and J. Morgan. Remote Sensing of Environment (Final Report). Report No. 4864-6-F. Ann Arbor: Institute of Science and Technology, University of Michigan, 1963.

Saari, J. M., R. W. Shorthill, and T. K. Deaton. Infrared and Visible Images of the Eclipsed Moon of December 19, 1964. U.S. Air Force Cambridge Research Laboratories, 1966.

Swet, C. J. Line Scan Television for Earth Observation Satellites. Baltimore: Applied Physics Laboratory, The Johns Hopkins University, 1966.

U.S. Air Force. Tactical Air Reconnaissance. Manual 55-6. Washington: U.S. Air Force, August, 1964.

U.S. Army. Basic and Advanced Infrared Technology. Redstone Arsenal, Ala.: U.S. Army, April, 1965.

_____. Electronics Applied in Aerial Surveying. Fort Belvoir, Va.: U.S. Army, 1965. (Translated from Chinese. Author: Kuo, Wei-hsing.)

_____. Transients and Waveforms. Department of the Army Technical Manual 11-669. Washington: U.S. Army, November, 1951.

U.S. Naval Photographic Interpretation Center. Photographic Interpretation Keys: Military Geology. U.S. Naval Photographic Intelligence Series, November, 1956.

_____. Photographic Interpretation Manual: Photographic Metrics. U.S. Naval Photographic Intelligence Series, April, 1955.

Willow Run Laboratories. Peaceful Uses of Earth-Observation Spacecraft. Volume I: Introduction and Summary. Volume II: Survey of Applications and Benefits. Volume III: Sensor Requirements. Ann Arbor: Institute of Science and Technology, University of Michigan, 1966.

Wilson, R. A. The Evaluation of an Airborne Infrared Mapper as a Tool for Detecting and Measuring Fires. Research

Paper INT-25. Intermountain Forest and Range Experiment Station, 1966.

Articles and Periodicals

Abraham, V. "Relative Geometric Strength of Frame, Strip, and Panoramic Cameras," Photogrammetric Engineering, December, 1961, pp. 755-766.

Adams, F. L. "The Design of Meteorological Sensors," in Proceedings of the Second Symposium on Remote Sensing of Environment. Ann Arbor: University of Michigan, 1963, pp. 435-452.

Alexander, Robert H. "Geographic Data from Space," Professional Geographer, November, 1964, pp. 1-5.

Astheimer, R. W. "An Infrared Radiation Air Thermometer," in Proceedings of the Second Symposium on Remote Sensing of Environment. Ann Arbor: University of Michigan, 1963, pp. 375-402.

Avery, Gene, and Cirilo B. Serna. "Photo Interpretation Keys for Identifying Vegetation," Proceedings of the Society of American Foresters, 1965, p. 159.

Badgley, Peter C. "The Applications of Remote Sensors in Planetary Exploration," in Proceedings of the Third Symposium on Remote Sensing of Environment. Ann Arbor: University of Michigan, 1965, pp. 9-28.

Badgley, Peter C., and W. L. Vest. "Orbital Remote Sensing and Natural Resources," Photogrammetric Engineering, September, 1966, pp. 780-790.

Baily, Everett M., and William R. Parish. "Portable Low Cost Detector for Latent Forest Fires," in Proceedings of the Third Symposium on Remote Sensing of Environment. Ann Arbor: University of Michigan, 1965, pp. 649-666.

Ballard, S., and W. Wolfe. "Recent Developments in Infrared Technology," Applied Optics, September, 1962.

Bandeen, W. R., et al. "Infrared and Reflected Solar Radiation Measurements from the TIROS II Meteorological Satellite," Journal of Geophysical Research, October, 1961, pp. 3169-3185.

Bang, B. A. "High Sensitivity Television as an Aid to Low Level Photographic Recording," Journal of the Society of Motion Picture and Television Engineers, September, 1961.

Barnes, R. B. "Thermography of the Human Body," Science, Volume 140 (1963), pp. 870-877.

Barr, E. Scott. "Historical Survey of the Early Development of the Infrared Spectral Region," American Journal of Physics, Volume 28, No. 42 (1960).

Barringer, A. R. "The Use of Multi-Parameter Remote Sensors as an Important New Tool for Mineral and Water Resource Evaluation," in Proceedings of the Fourth Symposium on Remote Sensing of Environment. Ann Arbor: University of Michigan, 1966, pp. 313-326.

Bell, E. E., and I. L. Eisner. "Infrared Radiation from the White Sands at White Sands National Monument, New Mexico," Journal of the Optical Society of America, Volume 46 (1956), pp. 303-304.

Beller, William S. "IR Photos Yield Data on Natural Resources," Technology Week, August 15, 1966, pp. 24-30.

Beuttner, Konrad J. "The Consequences of Terrestrial Surface Infrared Emissivity," in Proceedings of the Third Symposium on Remote Sensing of Environment. Ann Arbor: University of Michigan, 1965, pp. 549-562.

Biberman, L. "Problems in Near Real Time Reconnaissance," in Proceedings of the Fourth Symposium on Remote Sensing of Environment. Ann Arbor: University of Michigan, 1966, pp. 101-110.

Bird, J. B., and A. Morrison. "Space Photography and Its Geographical Applications," Geographical Review, October, 1964, pp. 464-486.

Brody, R. H., and J. R. Ermlich. "Fourier Analysis of Aerial Photographs," in Proceedings of the Fourth Symposium on Remote Sensing of Environment. Ann Arbor: University of Michigan, 1966, pp. 375-392.

Cantrell, J. L. "Infrared Geology," Photogrammetric Engineering, November, 1964, pp. 916-922.

Carneggie, David M., and Donald T. Lauer. "Uses of Multiband Remote Sensing in Forest and Range Inventory," Photogrammetria, August, 1966, pp. 115-141.

Carr, D. D., and R. F. Blakely. "Temperature Variation at a Depth of 30 Cm. in Clay Till and Outwash Sand and Gravel," in Proceedings of the Fourth Symposium on Remote Sensing of Environment. Ann Arbor: University of Michigan, 1966, pp. 203-214.

Chalfin, G. T., and W. B. Ricketts. "3.2 Mm Thermal Imaging Experiments," in Proceedings of the Fourth Symposium on Remote Sensing of Environment. Ann Arbor: University of Michigan, 1966, pp. 859-865.

Colwell, Robert N. "Aerial Photographs Show Range Conditions," California Agriculture, December, 1961, pp. 12-13.

_____. "Aerial Photography -- A Valuable Sensor for the Scientist," American Scientist, March, 1964.

_____. "Aerial Photography of the Earth's Surface; Its Procurement and Use," Applied Optics, June, 1966, pp. 883-892.

_____. "Multiband Sensing," in Proceedings of the First Symposium on Remote Sensing of Environment. Ann Arbor: University of Michigan, 1962, pp. 69-70.

_____. "Platforms for Testing Multi-Sensor Equipment," in Proceedings of the Second Symposium on Remote Sensing of Environment. Ann Arbor: University of Michigan, 1963, pp. 7-49.

_____. "Some Practical Applications of Multispectral Reconnaissance," American Scientist, March, 1961.

Colwell, Robert N. "A Systematic Analysis of Some Factors Affecting Photographic Interpretation," Photogrammetric Engineering, May, 1954, pp. 433-453.

_____. "The Taking of Helicopter Photography for Use in Photogrammetric Research and Training," Photogrammetric Engineering, September, 1956, pp. 613-621.

_____. "Uses and Limitations of Multispectral Remote Sensing," in Proceedings of the Fourth Symposium on Remote Sensing of Environment. Ann Arbor: University of Michigan, 1966, pp. 71-100.

Colwell, Robert N., et al. "Basic Matter and Energy Relationships Involved in Remote Reconnaissance," Photogrammetric Engineering, September, 1963.

Colwell, Robert N., and D. C. Olson. "Thermal Infrared Imagery and Its Use in Vegetation Analysis by Remote Aerial Reconnaissance," in Proceedings of the Third Symposium on Remote Sensing of Environment. Ann Arbor: University of Michigan, 1965, pp. 607-622.

Cook, R. N. "Preliminary Findings on a New Method of Measurement of Photographic Resolving Power," in Proceedings of the Second Symposium on Remote Sensing of Environment. Ann Arbor: University of Michigan, 1963, pp. 139-144.

Cooper, Charles F. "Potential Applications of Remote Sensing to Ecological Research," in Proceedings of the Third Symposium on Remote Sensing of Environment. Ann Arbor: University of Michigan, 1965, pp. 601-606.

Coulson, K. L., G. M. Bouricus, and E. L. Gray. "Optical Reflection Properties of Natural Surfaces," Journal of Geophysical Research, September 15, 1965, pp. 4601-4611.

Crawford, N. C., and R. W. Peplies. "Remote Sensor Returns as Historical Documents," in Proceedings of the Fourth Symposium on Remote Sensing of Environment. Ann Arbor: University of Michigan, 1966, pp. 599-604.

Davis, Charles M. "Geographic Application Program for Data from Remote Sensors in Aircraft and Spacecraft," Professional Geographer, September, 1966, p. 318.

Derenyi, Eugene E., and Gottfried Konecny. "Geometry of Infrared Imagery," Canadian Surveyor, September, 1964, pp. 279-290.

_____. "Infrared Scan Geometry," Photogrammetric Engineering, September, 1966, pp. 773-778.

DeWaard, R., and E. M. Wormser. "Description and Properties of Various Thermal Detectors," Proceedings of the Institute of Radio Engineers, Volume 47, No. 1508 (1959).

El-Ashby, M. R., and H. R. Wanless. "Shoreline Features and Their Changes," Photogrammetric Engineering, February, 1967, pp. 184-189.

Elms, D. G. "Mapping with a Strip Camera," Photogrammetric Engineering, September, 1964, pp. 638-653.

England, G., and J. O. Morgan. "Quantitative Airborne Infrared Mapping," in Proceedings of the Third Symposium on Remote Sensing of Environment. Ann Arbor: University of Michigan, 1965, pp. 681-690.

Estes, John E. "Some Applications of Aerial Infrared Imagery," Annals of the Association of American Geographers, December, 1966, pp. 673-682.

_____. "Some Geographic Applications of Aerial Infrared Imagery," in Proceedings of the Fourth Symposium on Remote Sensing of Environment. Ann Arbor: University of Michigan, 1966, pp. 173-182.

Feder, A. M. "Programs in Remote Sensing of Terrain," in Proceedings of the Second Symposium on Remote Sensing of Environment. Ann Arbor: University of Michigan, 1963, pp. 51-63.

Fischer, W. A. "Geologic Applications of Remote Sensors," in Proceedings of the Fourth Symposium on Remote Sensing of Environment. Ann Arbor: University of Michigan, 1966, pp. 13-20.

Fischer, W. A., et al. "Infrared Surveys of Hawaiian Volcanoes," Science, Volume 146, No. 6 (1964), pp. 733-742.

Fritz, S. "The Variable Appearance of the Earth from Satellites," Monthly Weather Review, October-December, 1963, pp. 613-620.

Frost, Robert E. "Aerial Photography; A Reappraisal of the Technology," in Proceedings of the First Symposium on Remote Sensing of Environment. Ann Arbor: University of Michigan, 1962, pp. 61-68.

Fujita, T. "Evaluation of Errors in the Graphical Rectification of Satellite Photographs," Journal of Geophysical Research, Volume 70, No. 24 (1965), pp. 5997-6007.

Fujita, T., and W. Bandeen. "Resolution of the Nimbus High Resolution Infrared Radiometer," Journal of Applied Meteorology, Volume 4, No. 4 (1965), pp. 492-503.

Gates, D. M. "The Energy Environment in Which We Live," American Scientist, September, 1963.

Gates, D. M., et al. "Spectral Properties of Plants," Applied Optics, April, 1965, pp. 11-20.

Gates, M. "Characteristics of Soil and Vegetated Surfaces to Reflected and Emitted Radiation," in Proceedings of the Third Symposium on Remote Sensing of Environment. Ann Arbor: University of Michigan, 1965, pp. 573-600.

Giever, P. M. "Needs for Remote Sensing Data in the Field of Air and Water Pollution Control," in Proceedings of the Fourth Symposium on Remote Sensing of Environment. Ann Arbor: University of Michigan, 1966, pp. 21-24.

Gimbarzevsky, Philip. "Land Inventory Interpretation," Photogrammetric Engineering, November, 1966, pp. 967-976.

Goldbert, I. L., et al. "Nimbus High Resolution Infrared Measurements," in Proceedings of the Third Symposium

on Remote Sensing of Environment. Ann Arbor: University of Michigan, 1965, pp. 141-152.

Goodman, R. E. "Photo/Field Prospecting," Photogrammetric Engineering, March, 1960, pp. 100-105.

Harpe, E., Jr. "Anthropology and Remote Sensing," in Proceedings of the Fourth Symposium on Remote Sensing of Environment. Ann Arbor: University of Michigan, 1966, pp. 727-730.

Harris, David E., and Caspar L. Woodbridge. "Terrain Mapping by Use of Infrared Radiation," Photogrammetric Engineering, January, 1964, pp. 134-139.

Hawkins, J. K., and C. J. Munsey. "Automatic Photo Reading," Photogrammetric Engineering, July, 1963, pp. 627-637.

Hirsch, S. N. "Applications of Remote Sensing to Forest Fire Detection and Suppression," in Proceedings of the Second Symposium on Remote Sensing of Environment. Ann Arbor: University of Michigan, 1963, pp. 295-308.

_____. "Preliminary Experimental Results with Infrared Line Scanners for Forest Fire Surveillance," in Proceedings of the Third Symposium on Remote Sensing of Environment. Ann Arbor: University of Michigan, 1965, pp. 623-648.

Hoffer, R. M., et al. "Vegetable, Soil, and Photographic Factors Affecting Tone in Agricultural Remote Multispectral Sensing," in Proceedings of the Fourth Symposium on Remote Sensing of Environment. Ann Arbor: University of Michigan, 1966, pp. 115-134.

Holter, M. R., and W. C. Wolfe. "Optical-Mechanical Scanning Techniques," Proceedings of the Institute of Radio Engineers, September, 1959, pp. 1540-1550.

Horwitz, L. P., and G. L. Shelton, Jr. "Pattern Recognition Using Autocorrelation," Proceedings of the Institute of Radio Engineers, January, 1961, pp. 175-185.

Hubbs, John C. "The New Pulse," Journal of the Precision Measurements Association (Instruments and Control Systems), November, 1966, pp. 109-116.

Jastrow, R., and A. G. W. Cameron. "Space: Highlights of Recent Research," Science, September 11, 1964, pp. 1129-1139.

Jensen, Herbert A., and Robert N. Colwell. "Panchromatic versus Infrared Minus-Blue Aerial Photography for Forestry Purposes in California," Photogrammetric Engineering, March, 1949, pp. 201-223.

Johnson, P. L. "A Consideration of Methodology in Photo Interpretation," in Proceedings of the Fourth Symposium on Remote Sensing of Environment. Ann Arbor: University of Michigan, 1966, pp. 719-726.

Jones, R. Clark. "Noise in Radiation Detectors," Proceedings of the Institute of Radio Engineers, Volume 47, No. 1481 (1959).

_____. "Phenomenological Description of the Response and Detecting Ability of Radiation Detectors," Proceedings of the Institute of Radio Engineers, Volume 47, No. 1495 (1959).

Kedar, Yehuda. "The Use of Aerial Photographs in Research in Physiographic Conditions and Anthropogeographic Data in Various Historic Periods," Photogrammetric Engineering, July, 1958, pp. 584-587.

Kern, C. D. "Desert Soil Temperatures and Infrared Radiation Received by TIROS III," Journal of Atmospheric Science, Volume 20 (1963), p. 175.

Ketchum, R. D., Jr., and W. I. Wittman. "Infrared Scanning the Arctic Pack Ice," in Proceedings of the Fourth Symposium on Remote Sensing of Environment. Ann Arbor: University of Michigan, 1966, pp. 636-656.

Kiefer, Ralph W. "Landform Features in the United States," Photogrammetric Engineering, February, 1967, pp. 174-182.

Kinsman, Frank E. "Some Fundamentals in Non-Contact Electro-

magnetic Sensing for Geoscience Purposes," in Proceedings of the Third Symposium on Remote Sensing of Environment. Ann Arbor: University of Michigan, 1965, pp. 495-516.

Kintzinger, P. R. "Geothermal Survey of Hot Ground near Lordsbury, New Mexico," Science, Volume 124 (1956), p. 629.

Klimm, Lester E. "Regional Description Based on Texture and Pattern of Unit Areas" (Abstract), Annals of the Association of American Geographers, September, 1956, p. 256.

Konecny, Gottfried, and Eugene E. Derenyi. "Geometrical Considerations for Mapping from Scan Imagery," in Proceedings of the Fourth Symposium on Remote Sensing of Environment. Ann Arbor: University of Michigan, 1966, pp. 327-338.

Lacate, D. S. "Wildland Inventory and Mapping," Forestry Chronicle, June, 1966, pp. 184-194.

LaFord, Charles D. "IR Mapping System Readied for Market," Technology Week, February 27, 1967, pp. 30-33.

Lancaster, Charles W., and Allen M. Feder. "The Multisensor Mission," Photogrammetric Engineering, May, 1966, pp. 484-494.

Latham, James P. "The Distance Relations of Cropland Areas in Pennsylvania" (Abstract), Annals of the Association of American Geographers, September, 1958, p. 277.

_____. "Geographic Analysis and Remote Sensing Capability," in Proceedings of the Second Symposium on Remote Sensing of Environment. Ann Arbor: University of Michigan, 1963, pp. 65-79.

_____. "Remote Sensing of Environment," Geographical Review, April, 1966, pp. 288-291.

_____. "Resume of the Special Session on Remote Sensing Held at the 1965 AAAS Meeting," in Proceedings of the Fourth Symposium on Remote Sensing of Environ-

ment. Ann Arbor: University of Michigan, 1966, pp. 539-546.

Lattman, L. H. "Geologic Interpretation of Airborne Infrared Imagery," in Proceedings of the Second Symposium on Remote Sensing of Environment. Ann Arbor: University of Michigan, 1963, pp. 289-293.

Leestma, R. A. "Applications of Air and Spaceborne Sensor Imagery for the Study of Natural Resources," in Proceedings of the Fourth Symposium on Remote Sensing of Environment. Ann Arbor: University of Michigan, 1966, pp. 111-118.

Legault, R. R. "The Motivation for Multispectral Sensing," in Proceedings of the Third Symposium on Remote Sensing of Environment. Ann Arbor: University of Michigan, 1965, pp. 71-78.

Legault, R. R., and F. C. Polcyn. "Investigations of Multi-Spectral Image Interpretation," in Proceedings of the Third Symposium on Remote Sensing of Environment. Ann Arbor: University of Michigan, 1965, pp. 813-821.

Leistner, G., and P. P. Dieter. "Some Characteristics of Panoramic Cameras for Aerial Surveillance," Photographic Science and Engineering, Volume 5, No. 5, pp. 257-262.

Leonardo, Earl S. "Capabilities and Limitations of Remote Sensors," Photogrammetric Engineering, November, 1964, pp. 1005-1010.

Leuder, D. R. "Airphoto Interpretation as an Aid in Mineral Reconnaissance and Development," Photogrammetric Engineering, December, 1953, pp. 819-830.

Liang, Ta. "Airphoto Interpretation of Engineering Soils in Tropical Environments," in Proceedings of the Third Symposium on Remote Sensing of Environment. Ann Arbor: University of Michigan, 1965, pp. 531-536.

Limperis, T. "Target and Background Signature Study," in Proceedings of the Third Symposium on Remote Sens-

ing of Environment. Ann Arbor: University of Michigan, 1965, pp. 423-434.

Livingston, W. C. "Resolution Capability of the Image-Orthicon Camera Tube under Nonstandard Conditions," Journal of the Society of Motion Picture and Television Engineers, October, 1963.

Lohman, S. W., and C. J. Robinove. "Photographic Description and Appraisal of Water Resources," Photogrammetria, Volume 19, No. 3 (1964).

Lowe, D. S., and John G. N. Braithwaite. "A Spectrum Matching Technique for Enhancing Image Contrast," Applied Optics, June, 1966, pp. 893-898.

Lowe, D. S., and F. C. Polcyn. "Multispectral Data Collection Program," in Proceedings of the Third Symposium on Remote Sensing of Environment. Ann Arbor: University of Michigan, 1965, pp. 667-680.

Lyon, R. J. P., and E. A. Burns. "Analysis of Rocks and Minerals by Reflected Infrared Radiation," Economic Geology, Volume 58 (1963), p. 274.

Lyon, R. J. P., and J. W. Patterson. "Infrared Spectral Signatures -- A Field Geological Tool," in Proceedings of the Fourth Symposium on Remote Sensing of Environment. Ann Arbor: University of Michigan, 1966, pp. 215-230.

McAlister, E. D. "Infrared-Optical Techniques Applied to Oceanography Measurement of Total Heat Flow from the Sea Surface," Applied Optics, May, 1964.

McClellan, W. D., J. P. Meiners, and D. G. Orr. "Spectral Reflection Studies on Plants," in Proceedings of the Second Symposium on Remote Sensing of Environment. Ann Arbor: University of Michigan, 1963, pp. 403-414.

McLerran, James H. "Airborne Crevasse Detection," in Proceedings of the Third Symposium on Remote Sensing of Environment. Ann Arbor: University of Michigan, 1965, pp. 801-802.

McLerran, James H. "Infrared Sea Ice Reconnaissance," in Proceedings of the Third Symposium on Remote Sensing of Environment. Ann Arbor: University of Michigan, 1965, pp. 789-800.

McLerran, James H., and Joseph O. Morgan. "Thermal Mapping of Yellowstone National Park," in Proceedings of the Third Symposium on Remote Sensing of Environment. Ann Arbor: University of Michigan, 1965, pp. 517-530.

Marble, D. F., and E. N. Thomas. "Some Observations on the Utility of Multispectral Photography for Urban Research," in Proceedings of the Fourth Symposium on Remote Sensing of Environment. Ann Arbor: University of Michigan, 1966, pp. 135-144.

Marcus, Leslie F., and Robert N. Colwell. "Determining the Specifications for Special Purpose Photography," Photogrammetric Engineering, September, 1961, pp. 618-626.

Meier, M. F., R. H. Alexander, and W. J. Campbell. "Multispectral Sensing Tests at South Cascade Glacier, Washington," in Proceedings of the Fourth Symposium on Remote Sensing of Environment. Ann Arbor: University of Michigan, 1966, pp. 145-160.

Meyer, M. A. "Remote Sensing of Ice and Snow Thickness," in Proceedings of the Fourth Symposium on Remote Sensing of Environment. Ann Arbor: University of Michigan, 1966, pp. 183-192.

Meyer, M. P., and D. W. French. "Forest Disease Spread," Photogrammetric Engineering, September, 1966, pp. 812-814.

Miller, Lee D. "Location of Anomalously Hot Earth with Infrared Imagery in Yellowstone National Park," in Proceedings of the Fourth Symposium on Remote Sensing of Environment. Ann Arbor: University of Michigan, 1966, pp. 751-769.

Miller, William C. "Uses of Aerial Photographs in Archeological Field Work," American Antiquity, January, 1957, pp. 46-62.

Molineux, Carlton E. "Aerial Reconnaissance of Surface Features with the Multiband Spectral System," in Proceedings of the Third Symposium on Remote Sensing of Environment. Ann Arbor: University of Michigan, 1965, pp. 399-422.

_____. "Air Force Remote Sensing Programs," in Proceedings of the First Symposium on Remote Sensing of Environment. Ann Arbor: University of Michigan, 1962, pp. 71-74.

Morgan, Joseph. "Infrared Technology," in Proceedings of the First Symposium on Remote Sensing of Environment. Ann Arbor: University of Michigan, 1962, pp. 45-60.

Morrison, A., and B. J. Bird. "Photography of the Earth from Space and Its Non-Meteorological Applications," in Proceedings of the Third Symposium on Remote Sensing of Environment. Ann Arbor: University of Michigan, 1965, pp. 357-376.

Moxham, R. M., and A. Alcraz. "Infrared Surveys at Taal Volcano, Philippines," in Proceedings of the Fourth Symposium on Remote Sensing of Environment. Ann Arbor: University of Michigan, 1966, pp. 827-844.

Narva, M. A., and F. A. Muckler. "Visual Surveillance and Reconnaissance from Space Vehicles," Human Factors, 1963, pp. 295-315.

Neuhauser, R. G., et al. "The Design and Performance of a High-Resolution Vidicon," Journal of the Society of Motion Picture and Television Engineers, November, 1962.

Norberg, W., et al. "Preliminary Results of Radiation Measurements from the TIROS III Meteorological Satellite," Journal of Atmospheric Science, Volume 19 (1962), pp. 20-30.

Ockert, D. L. "Satellite Photography with Strip and Frame Cameras," Photogrammetric Engineering, September, 1960, pp. 562-568.

Olson, C. E., Jr. "Elements of Photographic Interpretation

Common to Several Sensors," Photogrammetric Engineering, September, 1960, pp. 651-656.

Olson, C. E., Jr. "The Energy Flow Profile in Remote Sensing," in Proceedings of the Second Symposium on Remote Sensing of Environment. Ann Arbor: University of Michigan, 1963, pp. 187-199.

_____. "Infrared Sensors and Their Potential Applications to Forestry," Papers of the Michigan Academy of Science, Arts, and Letters, Volume 50 (1965), pp. 39-47.

Olson, C. E., Jr., and R. E. Good. "Seasonal Changes in Light Reflectance from Forest Vegetation," Photogrammetric Engineering, March, 1962, pp. 107-114.

Ory, Thomas R. "Line-Scanning Reconnaissance Systems in Land Utilization and Terrain Studies," in Proceedings of the Third Symposium on Remote Sensing of Environment. Ann Arbor: University of Michigan, 1965, pp. 393-398.

Paijmans, K. "Typing of Tropical Vegetation by Aerial Photographs and Field Sampling in Northern Papua," Photogrammetria, February, 1966, pp. 1-25.

Parker, Dana. "Some Basic Considerations Related to the Problem of Remote Sensing," in Proceedings of the First Symposium on Remote Sensing of Environment. Ann Arbor: University of Michigan, 1962, pp. 7-18.

Poulin, A. O., and T. A. Harwood. "Infrared Mapping of Glacier Thermal Anomalies," Proceedings of the Symposium on Glacier Mapping, Ottawa, Ontario, Canada, September, 1965.

Poulin, A. O., and J. W. Patterson. "Infrared Imagery in the Arctic under Daylight Conditions," in Proceedings of the Fourth Symposium on Remote Sensing of Environment. Ann Arbor: University of Michigan, 1966, pp. 231-242.

Pourciau, L. L., M. Altman, and C. A. Washburn. "A High-Resolution Television System," Journal of the Society

of Motion Picture and Television Engineers, February, 1960.

Prentice, Virginia L. "Remote Sensing of Environment," Professional Geographer, January, 1965, pp. 20-21.

Proceedings of the Institute of Radio Engineers, Special Issue on Infrared Physics and Technology, September, 1959, pp. 1420-1647.

Reeves, Dache. "Aerial Photography and Archaeology," American Antiquity, Volume 2 (1936), pp. 102-107.

Robinove, C. J. "Infrared Photography and Imagery in Water Resources Research," American Water Works Association Journal, Volume 57, No. 7 (1965), pp. 834-840.

_____. "Remote-Sensor Applications in Hydrology," in Proceedings of the Fourth Symposium on Remote Sensing of Environment. Ann Arbor: University of Michigan, 1966, pp. 25-32.

Rosenfeld, Azriel. "An Approach to Automatic Photographic Interpretation," Photogrammetric Engineering, September, 1962, pp. 660-665.

_____. "Automatic Recognition of Basic Terrain Types from Aerial Photographs," Photogrammetric Engineering, March, 1962, pp. 115-132.

Saunders, P. M., and C. H. Wilkens. "Precise Airborne Radiation Thermometry," in Proceedings of the Fourth Symposium on Remote Sensing of Environment. Ann Arbor: University of Michigan, 1966, pp. 815-826.

Schneider, William J. "Water Resources in the Everglades," Photogrammetric Engineering, November, 1966, pp. 958-966.

Schulte, D. W. "The Use of Panchromatic, Infrared, and Color Aerial Photography in the Study of Plant Distribution," Photogrammetric Engineering, December, 1951, pp. 688-712.

Shay, J. R. "Some Needs for Expanding Agricultural Remote Sensing Research," in Proceedings of the Fourth

Symposium on Remote Sensing of Environment. Ann Arbor: University of Michigan, 1966, pp. 33-36.

Sherman, J. C. "Accumulation of Geographic Data through Remote Sensing Techniques," in Proceedings of the Second Symposium on Remote Sensing of Environment. Ann Arbor: University of Michigan, 1963, pp. 427-430.

Simonett, D. S. "Present and Future Needs of Remote Sensing in Geography," in Proceedings of the Fourth Symposium on Remote Sensing of Environment. Ann Arbor: University of Michigan, 1966, pp. 37-48.

Steiner, D., and H. Haefner. "Tone Distortion for Automated Interpretation," Photogrammetric Engineering, March, 1965, pp. 269-280.

Stone, Kirk H. "A Guide to the Interpretation and Analysis of Aerial Photos," Annals of the Association of American Geographers, September, 1964, pp. 318-328.

Strandberg, Carl H. "Water Quality Analysis," Photogrammetric Engineering, March, 1966, pp. 234-248.

Strangeway, D. W., and R. C. Holmer. "Infrared Geology," in Proceedings of the Third Symposium on Remote Sensing of Environment. Ann Arbor: University of Michigan, 1965, pp. 293-320.

Suits, G. H. "Declassification of Infrared Devices," Photogrammetric Engineering, November, 1966, pp. 988-992.

_____. "The Nature of Infrared Radiation and Ways to Photograph It," Photogrammetric Engineering, December, 1960, pp. 763-772.

Tarkington, R. G., and A. L. Sorem. "Color and False-Color Films for Aerial Photography," Photogrammetric Engineering, January, 1963, pp. 88-95.

Teleki, Geza. "Aerial Photography and Sea-Ice Forecasting," Naval Research Reviews, March, 1962, pp. 1-8.

Tewinkel, G. C. "Water Depths from Aerial Photographs," Photogrammetric Engineering, November, 1963, pp. 1037-1042.

Theurer, Charles. "Color and Infrared Experimental Photography for Coastal Mapping," Photogrammetric Engineering, September, 1959, p. 568.

Thoren, Ragner. "Photointerpretation in Military Intelligence," Photogrammetric Engineering, April, 1952, pp. 428-451.

Udall, S. L. "Resource Understanding -- A Challenge to Aerial Methods," Photogrammetric Engineering, January, 1965, pp. 63-75.

Van Lopik, J. R., and L. A. Yarborough. "Comments on Remote Sensing Needs in Geoscience Engineering and Explorations," in Proceedings of the Fourth Symposium on Remote Sensing of Environment. Ann Arbor: University of Michigan, 1966, pp. 49-54.

Wark, D. Q., G. Yamamoto, and J. H. Lienesch. "Methods of Estimating Infrared Flux and Surface Temperature from Meteorological Satellites," Journal of Atmospheric Science, September, 1962, pp. 369-384.

Wickens, G. C. "The Practical Application of Aerial Photography for Ecological Surveys in the Savannah Regions of Africa," Photogrammetria, August, 1966, pp. 33-41.

Wilson, R. C. "Forestry Applications of Remote Sensing," in Proceedings of the Fourth Symposium on Remote Sensing of Environment. Ann Arbor: University of Michigan, 1966, pp. 63-70.

Winkler, E. M. "Relationship of Airphoto Tone Control and Moisture Content in Glacial Soils," in Proceedings of the Second Symposium on Remote Sensing of Environment. Ann Arbor: University of Michigan, 1962, pp. 107-118.

Wolvin, John H. "Multi-Channel Photo Spectrum Recording," in Proceedings of the Second Symposium on Remote Sensing of Environment. Ann Arbor: University of Michigan, 1963, pp. 81-88.

Papers

Atkinson, John H. "Optimizing Photography through the Atmosphere," paper presented at 1966 A.S.P. Semi-Annual Convention, Los Angeles, California, September 27-30, 1966.

Heller, R. C., G. E. Doverspike, and R. C. Aldrich. "Identification of Tree Species on Large-Scale Panchromatic and Color Photographs," paper presented at 1963 Annual Meeting of American Society of Photogrammetry, Washington, D. C., March 25-28, 1963.

Holter, M. R. "Infrared and Multispectral Sensors," paper presented at the 61st Annual Meeting of the A.A.G., Columbus, Ohio, April 18-22, 1965.

_____. "Sensing Instruments," paper presented at the Conference on Planetology and Space Mission Planning, New York, N. Y., November, 1965.

Latham, James P. "Machine Evaluation of Images for Regionalization Problems," paper presented to the Commission on the Interpretation of Aerial Photographs, International Geographical Union, Ottawa, Canada, March 16, 1967.

_____. "Role of Instrumentation in Geographic Research," paper presented to the Annual Meetings of the American Association for the Advancement of Science, Philadelphia, Pennsylvania, December 29, 1962.

Numbower, Leonard E. "Extraction of Socio-Economic Information from Aerial Photographs," paper presented at 1966 A.S.P. Semi-Annual Convention, Los Angeles, California, September 27-30, 1966.

Weber, Philip A. "Photogrammetric Research Work on the Gulf Stream," paper presented at 1966 A.S.P. Semi-Annual Convention in Los Angeles, California, September 27-30, 1966.

Miscellaneous

Brunnschweiler, Dieter. Physiographic Elements of the Dexter Test Area Relevant to the Interpretation of Remote Sensing Records. Unpublished report, NSF Summer Conference on Remote Sensing of Environment, University of Michigan, June, 1966.

University of Michigan, School of Natural Resources. Stinchfield Woods (Map). Ann Arbor: University of Michigan, 1961. (Scale: 1:11,520.)

BIOGRAPHICAL SKETCH

Richard Everett Witmer was born in Swarthmore, Pennsylvania, on July 3, 1942. He moved to Miami, Florida, in 1944, where he received his elementary and secondary education. He entered the University of Florida in September, 1958, where he received the degree Bachelor of Science with a major in physics in 1962. Shortly thereafter, he entered the Graduate School of the University of Florida in the Department of Geography and pursued graduate study toward the degree Master of Science, which was awarded in December, 1964. During 1964 and 1965, he continued graduate studies in the Departments of Geography and Geology at the University of Colorado, and returned to the University of Florida in 1965 to continue studying for the degree Doctor of Philosophy. In June, 1965, he became Instructor of Geography at Florida Atlantic University and Research Assistant for an Office of Naval Research contract. In July, 1967, he became Research Assistant Professor of Geography and Research Associate for a National Aeronautics and Space Administration/Geological Survey research contract.

The author is a member of the Association of American

Geographers and its Southeastern Division, the Florida Society of Geographers, the American Society of Photogrammetry, and the American Association for the Advancement of Science.

This dissertation was prepared under the direction of the chairman of the candidate's supervisory committee and has been approved by all members of that committee. It was submitted to the Dean of the College of Arts and Sciences and to the Graduate Council, and was approved as partial fulfillment of the requirements for the degree of Doctor of Philosophy.

December 19, 1967

E. Ruffin Jones

Dean, College of Arts and Sciences

Dean, Graduate School

SUPERVISORY COMMITTEE:

Clark T. Cross

Chairman

James R. Anderson

O.A. Edwards